Journal of Building Engineering 122 (2026) 115721

Contents lists available at ScienceDirect

Journal of Building Engineering

journal homepage: www.elsevier.com/locate/jobe

Full length article

Generalized probabilistic models for performance assessment of bio-based insulation materials in sustainable constructions

Fengyang Ye [a], Hanlin Wei [c,e], Junsong Wang [b], Yan Xiao [d], Giuseppe Quaranta [e], Paolo Gardoni [d], Cristoforo Demartino [f,d,*]

[a] Department of Civil Engineering, The University of Hong Kong, Pokfulam, Hong Kong, China
[b] Department of Building Environment and Energy Engineering, The Hong Kong Polytechnic University, 999077, Hong Kong, China
[c] College of Civil Engineering and Architecture, Zhejiang University, Hangzhou, 310058 Zhejiang, PR China
[d] Department of Civil and Environmental Engineering, University of Illinois at Urbana-Champaign, Urbana, IL 61801, USA
[e] Department of Structural and Geotechnical Engineering, Sapienza University of Rome, Via Eudossiana 18, 00184 Rome, Italy
[f] Department of Architecture, Roma Tre University, Largo G. B. Marzi 10, 00153 Rome, Italy

ARTICLE INFO

Dataset link: 10.5281/zenodo.18061591

Keywords:
Bio-based materials
Building insulation
Thermal performance
Sound absorption
Carbon footprint
Probabilistic model
Bayesian analysis
Sustainable construction

ABSTRACT

The widespread adoption of sustainable, bio-based insulation is hindered by the inherent variability of its properties, making reliable performance prediction a significant challenge for engineers. To address this problem, this study develops a robust probabilistic framework to predict performance while explicitly accounting for this uncertainty. The methodology is based on a comprehensive literature review of 266 studies to establish a performance database for thermal conductivity (λ), Noise Reduction Coefficient (NRC), and carbon footprint (CF). Bayesian statistical methods were then applied to derive generalized predictive models from this data. The findings reveal that λ correlates non-linearly with mass density (ρ), while NRC is a nonlinear function of both ρ and thickness (t). The carbon footprint is characterized using material-specific uniform and normal distributions, confirming the net carbon sequestration potential of key bio-based options. The main conclusion is that performance can be reliably predicted when variability is statistically quantified. The key contribution of this work is a practical framework that enables designers to make informed material selections, accounting for performance variability and environmental impact. The novelty lies in the creation of generalized, data-driven models applicable across a wide range of bio-based materials, providing a valuable tool to streamline the design of sustainable buildings and support the transition to a low-carbon built environment.

1. Introduction

The global construction sector is a major contributor to carbon emissions, stemming from both the operational energy demands of buildings and the energy-intensive production and transportation of construction materials [1,2]. These emissions contribute significantly to climate change and its associated detrimental impacts [3]. Consequently, achieving carbon reduction targets and advancing sustainable development goals necessitates transformative changes within the building and construction industry. Key strategies include adopting low-carbon materials, optimizing building designs for energy efficiency, and integrating renewable

* Corresponding author at: Department of Architecture, Roma Tre University, Largo G. B. Marzi 10, 00153 Rome, Italy.
E-mail addresses: fengyangye@connect.hku.hk (F. Ye), hanlin.23@intl.zju.edu.cn (H. Wei), jun-song.wang@connect.polyu.hk (J. Wang), yanxiao@intl.zju.edu.cn (Y. Xiao), giuseppe.quaranta@uniroma1.it (G. Quaranta), gardoni@illinois.edu (P. Gardoni), cristoforo.demartino@me.com (C. Demartino).

https://doi.org/10.1016/j.jobe.2026.115721
Received 27 April 2025; Received in revised form 22 February 2026; Accepted 24 February 2026
Available online 2 March 2026

Nomenclature and abbreviations

Symbols

λ	Thermal conductivity [W/(m K)] (Eq. (1)).
Q	Heat transfer rate [W] (Eq. (1)).
A	Area normal to heat flow [m^2] (Eq. (1)).
ΔT	Temperature difference across the thermal plates [K] (Eq. (1)).
R_t	Total thermal resistance of the assembly excluding surface resistances [m^2 K/W] (Eq. (2)).
$R_{t,u}$	Upper-bound (parallel-path) thermal resistance [m^2 K/W] (Eq. (3)).
$R_{t,l}$	Lower-bound (series-path) thermal resistance [m^2 K/W] (Eq. (3)).
$R_{m,j}$	Thermal resistance of layer j in section m [m^2 K/W] (Eq. (3)).
f_m	Area fraction of section m [–] (Eq. (3)).
U	Thermal transmittance (U-value) [W/(m^2 K)] (Eq. (4)).
R_{si}, R_{se}	Internal/external surface thermal resistances [m^2 K/W] (Eq. (4)).
C	Envelope thermal conductance (sum of $U_i A_i$) [W/K] (Eq. (5)).
N	Number of envelope components/surfaces considered [–] (Eq. (5)).
A_i	Area of component/surface i [m^2] (Eq. (5)).
U_i	Thermal transmittance of component i [W/(m^2 K)] (Eq. (5)).
NRC	Noise Reduction Coefficient [–] (Eq. (6)).
α_{250}, α_{500}, α_{1000}, α_{2000}	Absorption coefficients at octave-band center frequencies [–] (Eq. (6)).
α_ω	Sound absorption coefficient at frequency ω [–] (Eq. (6)).
T_{60}	Reverberation time (60 dB decay) [s] (Eq. (7)).
V	Room volume [m^3] (Eq. (7)).
A_{total}	Total absorption area (Sabine) [m^2] (Eq. (7)).
CF	Carbon footprint [kg $CO_{2,eq}$/kg] (functional unit as reported, typically cradle-to-gate/site for each material) (Eq. (8)).
CF_t	Total carbon footprint [kg $CO_{2,eq}$] (Eq. (9)).
ρ	Bulk density [kg/m^3] (Eq. (9)).
$CF_{Building}$	Carbon footprint of building [kg $CO_{2,eq}$/m^2] (Eq. (10)).
A_{Building}	Area of the building [m^2] (Eq. (10)).
ε	Model residual term, $\varepsilon \sim \mathcal{N}(0, \sigma^2)$ (Eq. (11)).
$\mathbf{x}$	Vector of predictors (e.g., ρ, t, T) (Eqs. (11), (12)).
$\mathbf{\Theta}$	Vector of model parameters (Eqs. (11), (12)).
$h_i(\mathbf{x})$	Explanatory functions [–] (Eqs. (12), (13)).
σ_t	Residual standard deviation for $\ln(\lambda)$ model [–] (Eq. (14)).
σ_s	Residual standard deviation for logit(NRC) model [–] (Eq. (15)).
$\theta_{t,\cdot}$	Thermal model coefficients (Eq. (16)).
$\theta_{s,\cdot}$	Acoustic model coefficients (Eq. (17)).
$CF \sim \mathcal{U}(CF_{min}, CF_{max})$	Uniform distribution formula (Eq. (18)).
CF_{min}, CF_{max}	Minimum/maximum carbon footprint of a specific material [kg $CO_{2,eq}$] (Eq. (18)).
$CF \sim \mathcal{N}(\mu_c, \sigma_c^2)$	Normal distribution formula (Eq. (19)).
μ_c, σ_c	Mean and standard deviation of material-class CF distribution (Eq. (19)).
t	Thickness [m] (or [mm] where explicitly stated).
T	Temperature [°C] (test/conditioning temperature for material property evaluation).

Abbreviations

CO_2	Carbon dioxide.
CoV	Coefficient of variation.
GWP	Global Warming Potential.
HDI	Highest Density Interval.
ISO	International Organization for Standardization.
LCA	Life Cycle Assessment.
MCMC	Markov Chain Monte Carlo.
PLA	Polylactic Acid.

PVA	Polyvinyl Acetate.
PCM	Phase-change-material.
PRISMA	Preferred Reporting Items for Systematic Reviews and Meta-Analyses.

Material and system classes

Bio-based insulation	Plant-derived insulation products (loose-fill, mats, boards/panels, lightweight bio-aggregate composites) within the scope of Fig. 1.
Conventional insulation	Reference materials such as rock wool and glass wool (used for contextual comparison).
Loose-fill	Unbound fibrous/granular insulation placed by blowing or pouring.
Panel/board	Compacted insulation products formed as mats, boards, or panels (typically with binders).
Plant-based categories	Wood, bamboo, hemp, straw, sunflower, sugarcane bagasse, crop husk, palm residues, kenaf, fruit residues (primary classes used for Bayesian calibration).

energy sources [4–6]. Globally, the Paris Agreement encourages the sector to reduce greenhouse gas emissions through sustainable building practices and improved energy efficiency [7], and it establishes the global framework for limiting temperature rise while calling for economy-wide mitigation pathways consistent with long-term climate goals [8]. China, for example, has committed to achieving peak carbon emissions by 2030 and carbon neutrality by 2060 [9]. In the European Union, the European Climate Law makes climate neutrality by 2050 legally binding and sets an intermediate 2030 target, while in the United States, a long-term strategy targets net-zero greenhouse gas emissions by 2050 [10,11]. Beyond structural components [12], building insulation materials play a critical role, capable of reducing operational energy consumption by at least 20% [13] and thereby lowering greenhouse gas emissions [14,15]. Reflecting its importance, the global market for building thermal insulation is substantial, valued at nearly USD 30 billion in 2020 and projected to exceed USD 38 billion by 2026 [16].

Bio-based materials [17], particularly those derived from plants, represent a compelling solution to decarbonize the building sector [18,19]. Materials such as timber, bamboo, and hemp inherently exhibit lower embodied energy compared to many conventional alternatives and actively sequester atmospheric carbon dioxide during their growth [20–22]. Incorporating these plant-based materials into construction projects not only decreases the initial carbon footprint of buildings but can also enable structures to function as long-term carbon sinks, contributing towards net-negative emissions [23–25]. Furthermore, their renewability and biodegradability aligns seamlessly with the principles of the circular economy and the broader goals of sustainable development. Therefore, widespread adoption of bio-based materials can significantly advance the decarbonization goals while simultaneously promoting environmental sustainability, fostering innovation in construction techniques, and enhancing the resilience of our built environment [17,26].

The growing interest and recent advancements in bio-based insulation materials have driven significant progress in thermal insulation technology, offering environmentally sound alternatives to conventional options [27]. Despite their effectiveness, conventional insulation materials such as glass wool and polymeric foams (e.g., polyurethane and phenolic foam) are associated with high embodied energy and significant environmental impacts throughout their lifecycle [28,29]. In contrast, bio-based alternatives such as hempcrete, cork panels, and straw bales utilize their natural porous structures to provide effective thermal resistance [27,30,31]. As renewable resources, these materials boast considerably lower embodied energy than their synthetic counterparts. Their use in building envelopes can substantially reduce the dependence on mechanical heating and cooling systems, leading to a decrease in operational energy consumption and associated carbon emissions. In addition, bio-based insulation often contributes positively to indoor environmental quality and overall building energy efficiency [32]. This shift towards bio-based thermal insulation marks a critical move towards more sustainable building practices, emphasizing resource efficiency and energy conservation.

Similarly, the use of bio-based materials has enhanced the solutions for managing building acoustics sustainably [33]. Traditional sound-absorbing materials such as synthetic foams and mineral wool often have a high embodied energy and potential health or environmental concerns related to their chemical composition and manufacturing processes [28,29]. Bio-based materials, including processed straw, certain grasses, and kenaf fibers, exhibit excellent sound absorption characteristics due to their inherent fibrous and porous structures [34–36]. These natural materials effectively dissipate sound energy, thereby improving acoustic comfort and mitigating noise pollution within buildings [37]. Moreover, they generally contribute to better indoor air quality by minimizing the emission of volatile organic compounds often associated with synthetic products [38]. As renewable resources, their use directly supports sustainable development goals by lowering the environmental footprint of construction [23]. The adoption of bio-based sound absorbers signifies a move towards more environmentally responsible and health-conscious building design without compromising acoustic performance.

Despite the promising potential demonstrated in numerous experimental studies, the widespread practical application of bio-based materials for thermal insulation, sound absorption, and carbon storage faces hurdles [39]. A primary challenge lies in the inherent variability of their properties. Unlike highly controlled synthetic materials, the characteristics of bio-based materials can fluctuate significantly based on factors like the specific source plant, growth conditions, harvesting time, and processing methods [40]. This natural variability can lead to inconsistencies in performance under different environmental conditions, making standardization and reliable prediction difficult within established engineering workflows. Consequently, there is a critical need for robust models that can accurately evaluate thermal and acoustic performance, alongside the carbon footprint, while explicitly accounting for this inherent variability. Establishing such models would bridge the gap between research and practice, thereby enhancing the reliability and adoption of these sustainable materials.

This study introduces a novel and consistent probabilistic framework designed to predict the thermal, acoustic, and environmental performance of bio-based building insulation materials using analytically derived models. To establish this framework, we first conducted one of the most extensive literature reviews to date, synthesizing data on thermal conductivity (λ), Noise Reduction Coefficient (NRC), and carbon footprint (CF) from 266 distinct studies covering a wide range of bio-based materials. Employing Bayesian statistical methods, we then developed predictive generalized probabilistic models that capture the relationships between material properties and performance metrics while accounting for inherent uncertainties. Specifically, our models correlate λ with mass density (ρ) and NRC with both ρ and material thickness (t), revealing significant nonlinear dependencies. Furthermore, we established normal distribution models to characterize the material-specific carbon footprint (CF). These models are generalized, as they apply regardless of the specific natural resources and/or production processes involved in obtaining the final bio-based building insulation material. This makes them a valuable tool for developing large-scale sustainable policies as well as for designing efficient solutions at the individual building level. This probabilistic approach complements product-specific data sheets and applies to both loose-fill and compacted bio-based insulation materials. It is particularly valuable during early design stages, where designers must efficiently screen material options and density ranges before final product selection, reducing the need for time-consuming iterative calculations based on multiple deterministic inputs. Through the analysis of three practical case studies (viz., an insulation wall, a sound-absorbing ceiling, and a prefabricated temporary house), we demonstrate the practical utility and feasibility of our probabilistic models. These models offer a powerful tool for designers, enabling a more informed selection of bio-based materials and streamlining the implementation of sustainable building solutions by explicitly considering performance variability and environmental impact.

Following this introduction, the manuscript is structured as follows. Section 2 details the collection of data from an extensive review of the literature and the Bayesian statistical framework used to develop probabilistic models. Section 3 presents the probabilistic models derived for thermal conductivity, Noise Reduction Coefficient, and carbon footprint, together with validation against the compiled data. Section 4 presents the practical utility of these models through illustrative case studies of building elements and a complete prefabricated house, demonstrating their application in performance evaluation. Finally, the findings are discussed in Section 5 and summarized in Section 6, where Section 6.1 provides recommendations and Section 6.2 proposes future directions. Additional data and case study details are provided in Appendices A and B.

2. Methods

This section outlines the methodology employed in this study. It details the literature search strategy used to compile the performance databases for bio-based materials and describes the Bayesian statistical approach used to derive the probabilistic predictive models for thermal conductivity, Noise Reduction Coefficient, and carbon footprint, as well as the definition of these performance metrics.

2.1. Bio-based materials and their carbon removal potential

In this study, the term bio-based insulation materials is defined in Fig. 1, which summarizes the plant-to-product pathway considered in compiling the performance databases. As illustrated in Fig. 1, the scope is intentionally restricted to insulation products derived from the *plant-based* renewable feedstocks shown in the "Bio-based resources" bubble (wood, bamboo, hemp, straw, sunflower, sugarcane bagasse, crop husk, palm residues, kenaf, and fruit residues), processed through the depicted preparation and forming steps (e.g., harvesting, blending, drying, mixing, and molding) and using the adhesive families shown (natural/organic, polymers, and inorganic binders) [18,41].

Consistent with this definition, animal-based and marine-based biomaterials are excluded from the database to maintain a coherent plant-based material class and to avoid introducing fundamentally different biological structures, moisture-related behaviors, and processing routes that would require separate modeling assumptions. In addition, composites incorporating metallic or plastic structural components are excluded to focus on the intrinsic performance of plant-derived insulation products within the manufacturing logic represented in Fig. 1. Accordingly, the database comprises plant-based fiberboard products (e.g., straw, wood, bamboo, hemp, jute, grass, and date palm fiberboards), plant-based aggregate composites (e.g., hemp shiv boards, rice husk composites, bamboo or wood particle/powder composites, and fruit-residual-based composites), as well as plant-derived structural and insulation panels (e.g., wood and bamboo panels), provided that their principal constituent material is plant biomass.

The ten plant-based categories highlighted in Fig. 1 were selected because they are globally available and constitute the dominant share of thermal-conductivity and sound-absorption data identified in the systematic review, enabling statistically representative Bayesian calibration. For completeness, other plant-based fibers (e.g., flax) were also screened; however, inclusion in each performance database is conditioned on data availability and methodological comparability for that specific metric. Consequently, some supplementary plant-based materials may appear in one database (e.g., acoustic NRC) but not in another (e.g., thermal conductivity) when the corresponding literature does not meet the same inclusion criteria.

The life cycle carbon implications of building materials vary significantly. Conventional cementitious and mineral materials typically involve energy-intensive processing, leading to substantial upfront carbon emissions [42]. While they can absorb some CO_2 through carbonation, their overall carbon footprint is often positive. In contrast, plant-derived bio-based materials leverage photosynthesis during growth to actively remove CO_2 from the atmosphere, converting it into biomass before manufacturing.

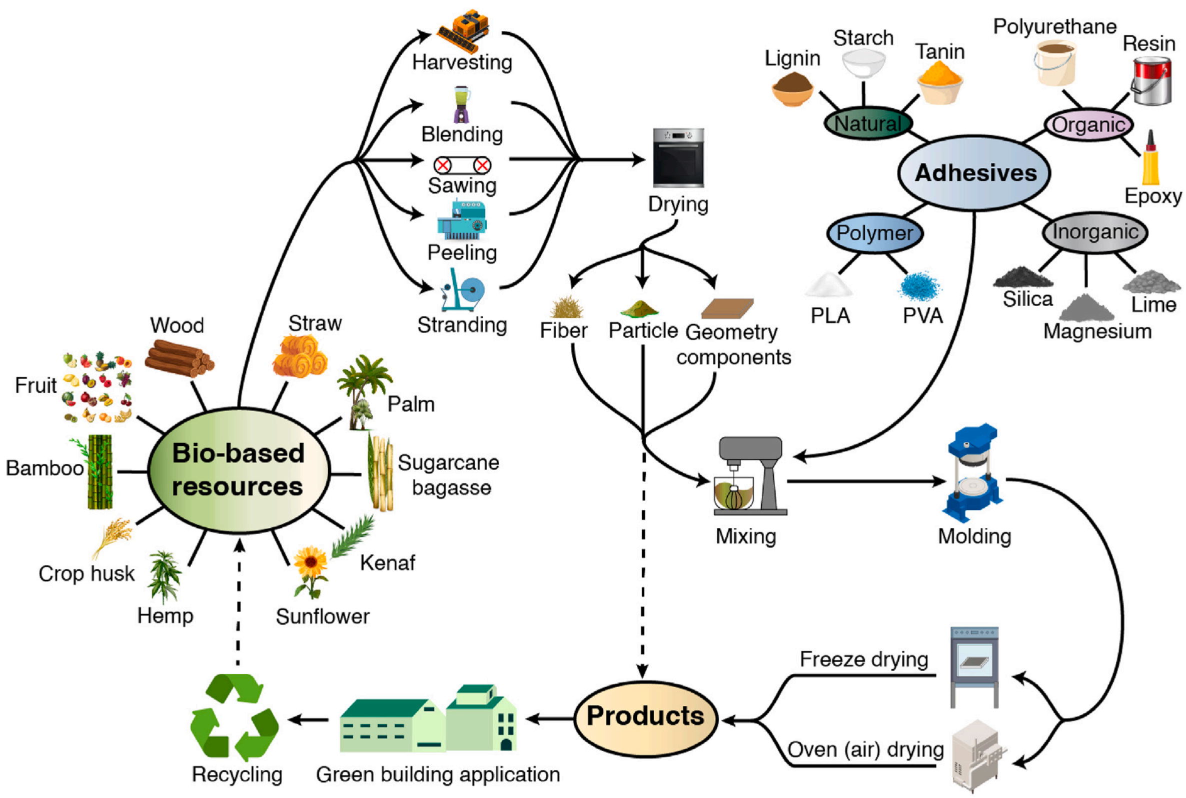

Fig. 1. Bio-based resources utilization for green building insulation and operational scope definition used in this study.

Although processing steps release some carbon, this is often offset by initial sequestration. Once in buildings, bio-based products such as wood, bamboo, hemp, straw, and cork act as carbon storage reservoirs [23,24,43]. Their end-of-life management, from incineration to reuse or recycling, determines the final carbon outcome. Depending on the life cycle path, bio-based materials can achieve significantly reduced, neutral, or even net-negative carbon footprints [44]. Fig. 2 contrasts these carbon dynamics.

2.2. Search strategy

A comprehensive literature search was conducted using Google Scholar to collect data on the thermal, acoustic, and carbon footprint properties of bio-based building materials. The search employed combinations of keywords such as ‘bio-based material’, ‘insulation’, ‘thermal conductivity’, ‘sound absorption’, ‘Noise Reduction Coefficient’, ‘carbon footprint’, ‘life cycle assessment’, complemented by specific material names (e.g., ‘hempcrete’, ‘straw bale’, ‘bamboo panel’). No publication year restrictions were applied and only documents published in English were included. This initial search yielded 831 potentially relevant studies.

The scope was refined to focus on 10 major bio-based material categories (wood, bamboo, hemp, straw, sunflower, sugarcane bagasse, crop husk, palm, kenaf, and fruit) and other less common but relevant bio-based materials (e.g., cork, coir, grass, reed). Studies were included in the thermal-performance database only if the investigated product was explicitly intended for, or commonly used as, an insulating layer, such as loose-fill materials, fibrous mats, insulation boards or panels, and lightweight bio-aggregate insulation composites. Conversely, material groups and studies reporting values non-representative of insulation applications were excluded, specifically those primarily designed for structural, decorative, or multifunctional purposes such as PCM systems, cladding, and dense structural products.

Studies primarily focusing on composites with significant non-bio-based components (e.g., plastics, metals) were excluded. After screening for relevance and data availability, a final database of 266 studies was compiled. Performance data (thermal conductivity, sound absorption coefficients/NRC, carbon footprint values) along with relevant parameters (density, temperature, thickness) were extracted from text, tables, and graphs (using WebPlotDigitizer, https://automeris.io/WebPlotDigitizer/, where necessary). The systematic search and screening process, detailed in the PRISMA flow diagram in Fig. C.15, resulted in three distinct databases compiled from a total of 266 studies, detailed in the Appendix:

- Thermal performance database (Table A.8, 96 studies): Contains thermal conductivity (λ), density (ρ), and test temperature (T).

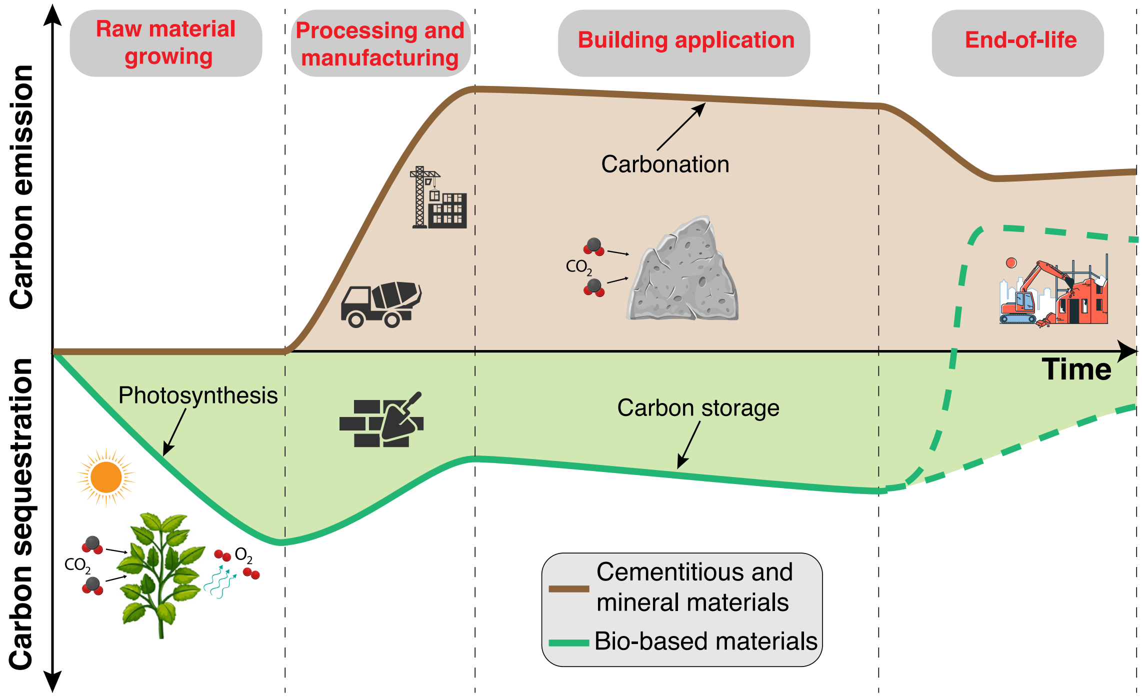

Fig. 2. Carbon sequestration dynamics across material lifecycles. Comparison of carbon emissions and sequestration for cementitious/mineral materials (brown line) versus bio-based materials (green line).
Source: Adapted from Arehart et al. [44].

- Acoustic performance database (Table A.9, 86 studies): Contains Noise Reduction Coefficient (NRC) or frequency-dependent absorption coefficients, density (ρ), and material thickness (t).
- Carbon footprint database (Table A.10, 84 studies): Contains carbon footprint (CF) values (typically cradle-to-gate) and, where available, density (ρ).

2.3. Definition of performance metrics

2.3.1. Thermal insulation performances

Thermal conductivity (λ) quantifies a material's ability to conduct heat and is defined as:

$$\lambda = \frac{Q \cdot t}{A \cdot \Delta T}, \tag{1}$$

where Q is the rate of heat transfer (W), t is the material thickness (m), A is the cross-sectional area perpendicular to heat flow (m^2), and ΔT is the temperature difference across the thickness t (K). Lower λ indicates better insulation.

For multi-layered building elements like walls, the overall thermal resistance (R_t) is calculated according to ISO 6946 [45], often using an area-weighted average method considering different sections (e.g., insulation cavity vs. stud). A simplified approach averages the upper ($R_{t,u}$) and lower ($R_{t,l}$) bounds of thermal resistance:

$$R_t = \frac{R_{t,u} + R_{t,l}}{2}. \tag{2}$$

$R_{t,u}$ (parallel path, assuming isothermal surfaces) and $R_{t,l}$ (series path, assuming one-dimensional flow) are calculated as:

$$R_{t,u} = \left[\sum_m \frac{f_m}{(\sum_j R_{m,j})}\right]^{-1}, \quad R_{t,l} = \sum_j \left(\sum_m \frac{f_m}{R_{m,j}}\right)^{-1}, \tag{3}$$

where m indexes the parallel sections (e.g., cavity, stud), j indexes the layers within a section, f_m is the fractional area of section m, and $R_{m,j}$ is the thermal resistance of layer j in section m, given by $R_{m,j} = t_{m,j}/\lambda_{m,j}$. Standard surface resistances (R_{si} for interior, R_{se} for exterior) are added to the material resistances ($R_{si} = 0.13\,\mathrm{m^2\,K/W}$, $R_{se} = 0.04\,\mathrm{m^2\,K/W}$) [45]. The overall thermal transmittance (U-value) is the reciprocal of the total thermal resistance:

$$U = 1/(R_{si} + R_t + R_{se}). \tag{4}$$

Table 1
Maximum permissible thermal transmittance (U_{max}) and typical temperature ranges for Chinese thermal regions (GB/50176 [46]).

Thermal region	Acronym	Temperature range [°C]	U_{max} [W/(m^2 K)]
Severe Cold Area	SCA	$-60 \leq T \leq 40$	≤ 0.4
Cold Area	CA	$-40 \leq T \leq 40$	≤ 0.5
Hot Summer and Cold Winter Area	HCA	$-20 \leq T \leq 40$	≤ 0.6
Warm Area	WA	$-10 \leq T \leq 40$	≤ 0.8
Hot Summer and Warm Winter Area	HWA	$0 \leq T \leq 40$	≤ 1.0

Table 2
Approximate sound absorption classes based on Noise Reduction Coefficient (NRC), adapted from the principles of ISO 11654:1997 [47]. (Note: The standard defines classes based on weighted absorption coefficient α_w, not directly on NRC, but NRC ranges are often used as a simplified guide).

Sound absorption Class	Typical NRC Range
I (or A)	$NRC \geq 0.90$ (Highly Absorptive)
II (or B)	$0.80 \leq NRC < 0.90$
III (or C)	$0.60 \leq NRC < 0.80$
IV (or D)	$0.30 \leq NRC < 0.60$
V (or E)	$0.15 \leq NRC < 0.30$
Unclassified	$NRC < 0.15$ (Reflective)

National standards often specify maximum permissible U-values based on climate zone. For context, Table 1 shows the requirements for different thermal regions in China according to GB/50176 [46].

The total thermal conductance (C) of a building or room envelope, representing the overall rate of heat loss excluding infiltration, is calculated by adding the $U \cdot A$ products for all external envelope components (walls, roof, floor, windows, doors):

$$C = \sum_{i=1}^{N} U_i \cdot A_i, \tag{5}$$

where N is the number of distinct envelope components and U_i and A_i are the thermal transmittance and area of the ith component, respectively.

2.3.2. Sound absorption performances

This study focuses exclusively on sound absorption performance, as quantified by the Noise Reduction Coefficient (NRC), which characterizes in-room acoustic conditioning (echo and reverberation control). Sound transmission (sound insulation) metrics (e.g., transmission loss, STC/R_w) are not considered because they are strongly assembly- and detailing-dependent (mass–spring–mass effects, airtightness, flanking paths) and cannot be generalized as a material-only probabilistic model from heterogeneous literature sources.

NRC is defined in standards like ISO 11654:1997 [47] as the arithmetic average of the sound absorption coefficients (α) measured at four standard octave band center frequencies: 250 Hz, 500 Hz, 1000 Hz and 2000 Hz.

$$NRC = \frac{\alpha_{250} + \alpha_{500} + \alpha_{1000} + \alpha_{2000}}{4}. \tag{6}$$

The sound absorption coefficient α_ω at a given frequency ω represents the fraction of incident sound energy absorbed by the material (ranging from 0 for perfect reflection to 1 for perfect absorption). NRC provides a single-number rating for general sound absorption across the speech frequency range. Higher NRC values indicate better absorption. ISO 11654:1997 also defines the sound absorption classes based on the weighted absorption coefficient α_w, and NRC values are often correlated to these classes for simplification, as shown in Table 2. Materials with $NRC \geq 0.20$ are generally considered useful for acoustic treatment.

The reverberation time (T_{60}) of a room, defined as the time required for the sound pressure level to decay by 60 dB after the sound source stops, is a key indicator of room acoustics. For moderately live rooms, it can be estimated using Sabine's formula [48]:

$$T_{60} = 0.161 \cdot \frac{V}{\sum_{i=1}^{N} \alpha_i \cdot A_i} = 0.161 \cdot \frac{V}{A_{total}}, \tag{7}$$

where V is the room volume (m^3), α_i is the sound absorption coefficient of the ith surface, A_i is the area of the ith surface (m^2), N is the number of distinct surfaces and $A_{total} = \sum \alpha_i A_i$ is the total absorption area of the room (in Sabins or metric Sabins). The constant 0.161 has units of s/m. For simplified calculations involving NRC, one might approximate the total absorption using $A_{total} \approx \sum NRC_i \cdot A_i$, although this is less accurate than using frequency-dependent values α.

2.3.3. Carbon footprint

Based on the life cycle assessment (LCA) system boundary shown in Fig. 3 (modules A1–A5, B1–B7, C1–C4), the carbon footprint (CF) of a material is defined as the net greenhouse gas (GHG) emissions accumulated over its life cycle, Normalized to a functional

Product stage			Construction process stage		Use stage							End of life stage			
Raw material supply	Transport	Manufacturing	Transport	Assembly	Use	Maintainance	Repair	Replacement	Refurbishment	Energy consumption	Water consumption	Demolition	Transport	Waste processing	Disposal
A1	A2	A3	A4	A5	B1	B2	B3	B4	B5	B6	B7	C1	C2	C3	C4

Fig. 3. Description of different stages of the life cycle assessment (LCA) according to EN 15978:2011 [51].

unit and expressed in kg $CO_{2,eq}$ [49]. For bio-based materials, the CF formulation explicitly captures emissions across the production, use, and end-of-life stages, as well as the effect of biogenic carbon sequestration. Specifically:

- Product stage (A1–A3) and construction stage (A4–A5) account for upstream emissions from raw material extraction, agricultural inputs such as fertilizers and pesticides (E_p), energy consumption for cultivation, processing, and manufacturing (E_e), and transportation (E_t).
- Use stage (B1–B7) includes emissions associated with maintenance, repair, replacement, refurbishment, and operational energy or water use during the service life of the material (E_B).
- End-of-life stage (C1–C4) covers emissions from deconstruction or demolition, transport of waste, waste processing, and final disposal (E_C).
- Biogenic carbon sequestration, C_s, represents the atmospheric CO_2 absorbed during biomass growth and stored in the bio-based material, offsetting part of the life-cycle emissions.

Accordingly, when the full life cycle is considered, the carbon footprint of a bio-based material can be expressed in a generalized form as [18,50]:

$$CF = E_p + E_e + E_t + E_B + E_C - C_s. \tag{8}$$

It is worth noting that most existing studies on bio-based materials limit their assessment to the cradle-to-gate or cradle-to-site boundary (A1–A5), primarily due to uncertainties in service-life assumptions and end-of-life scenarios. While this approach facilitates comparison across materials, it may underestimate the total life-cycle impacts or overlook potential benefits and burdens arising during the use and end-of-life stages.

The total carbon footprint contribution (CF_t) of the insulation system within a larger assembly (like the prefabricated house) can be calculated by summing the CF contributions of each material component based on its volume (V), density (ρ), and material-specific CF:

$$CF_t = \sum_{i=1}^{N_m} V_i \cdot \rho_i \cdot CF_i + V_b \cdot \rho_b \cdot CF_b. \tag{9}$$

Here, the sum runs over N_m non-bio-based materials in the system (e.g., steel sheets, fixings), and the last term represents the contribution from the bio-based insulation material (V_b, ρ_b, CF_b).

To better visualize the carbon footprint at the building level, the carbon footprint of the building ($CF_{Building}$) is calculated using the specific building area ($A_{Building}$) as follows:

$$CF_{Building} = \frac{CF_t}{A_{Building}}. \tag{10}$$

2.4. Derivation of the probabilistic predictive models

We employed a Bayesian framework to develop probabilistic models for thermal conductivity (λ) and NRC. This approach enables robust parameter estimation, quantification of uncertainty, and incorporation of prior knowledge, although we employed non-informative priors in this study [52–54]. The general model structure is:

$$\text{Likelihood:} \quad T[C(\mathbf{\Theta}, \mathbf{x})] = \varphi(\mathbf{\Theta}_m, \mathbf{x}) + \varepsilon \quad \text{with } \varepsilon \sim \mathcal{N}(0, \sigma^2), \tag{11}$$

where C is the response variable (λ or NRC), $\mathbf{x}$ is the vector of predictor variables (e.g., ρ, t), $\mathbf{\Theta}$ is the vector of all model parameters ($\mathbf{\Theta}_m$ and σ), $T[\cdot]$ is a variance-stabilizing transformation (logarithm for λ, logit for NRC) to better meet model assumptions (linearity,

Table 3
Candidate explanatory functions $h'_{ti}(\mathbf{x}_t)$ and their database statistics used for the initial thermal conductivity model selection.

ID	Variables	Minimum	Maximum	Mean	STD	CoV
$h'_{t1}(\mathbf{x}_t)$	1	–	–	–	–	–
$h'_{t2}(\mathbf{x}_t)$	T	7.200	70.000	22.122	10.082	0.456
$h'_{t3}(\mathbf{x}_t)$	T^2	51.840	4900.000	591.038	647.300	1.095
$h'_{t4}(\mathbf{x}_t)$	ρ	16.000	1108.770	398.737	249.136	0.625
$h'_{t5}(\mathbf{x}_t)$	$\log(\rho)$	2.773	7.011	5.728	0.812	0.142
$h'_{t6}(\mathbf{x}_t)$	ρ^2	256.000	1.229×10^6	2.211×10^5	2.387×10^5	1.080
$h'_{t7}(\mathbf{x}_t)$	ρ^3	4096.000	1.363×10^9	1.455×10^8	2.136×10^8	1.468

Normality, homoscedasticity of residuals). The term $\varphi(\boldsymbol{\Theta}_m, \mathbf{x})$ represents the deterministic part of the model, formulated as a linear combination of n explanatory functions $h_i(\mathbf{x})$:

$$\varphi(\boldsymbol{\Theta}_m, \mathbf{x}) = \boldsymbol{\Theta}_m^T \cdot \mathbf{h}(\mathbf{x}) = \sum_{i=1}^{n} \Theta_{mi} h_i(\mathbf{x}). \tag{12}$$

The explanatory functions $h_i(\mathbf{x})$ are derived from measurable physical variables $\mathbf{x}$ (e.g., $h(\mathbf{x}) = \rho$, $h(\mathbf{x}) = \rho^3$, $h(\mathbf{x}) = t$) and are standardized for numerical stability during calibration:

$$h_i(\mathbf{x}) = \frac{h'_i(\mathbf{x}) - \mathrm{E}[h'_i(\mathbf{x})]}{\mathrm{SD}[h'_i(\mathbf{x})]}, \tag{13}$$

where $h'_i(\mathbf{x})$ is the original variable, and $\mathrm{E}[\cdot]$ and $\mathrm{SD}[\cdot]$ are its mean and standard deviation over the dataset. ε is the Normally distributed error term with standard deviation σ, capturing unexplained variability. We used non-informative priors $p(\boldsymbol{\Theta}) \propto 1/\sigma$ [52]. The error term ε is crucial in this framework, as it captures the combined effects of inherent randomness and unmodeled sources of variability, including differences in experimental conditions (e.g., moisture content, test standards) across the heterogeneous studies compiled in our database.

Model calibration was performed using Markov Chain Monte Carlo (MCMC) simulations implemented in PyMC [55]. We ran four parallel chains, each with 5000 samples drawn after a 1000-iteration tuning phase, targeting a high acceptance rate (0.97) to ensure adequate exploration of the posterior parameter space. This process yields posterior probability distributions for all parameters $(\boldsymbol{\Theta}_m, \sigma)$, quantifying their likely values and associated uncertainties.

To achieve models that are both accurate (low σ) and parsimonious (small number of terms n), we employed a stepwise deletion procedure based on the coefficient of variation (CoV) of the parameter estimates [52]. Starting with a full model including all candidate explanatory functions, the term whose coefficient Θ_i had the highest CoV was removed at each step. The model was then recalibrated. This process continued until removal of the next term would cause an unacceptable increase (e.g., > 10%) in the model error σ, balancing model complexity against predictive accuracy.

2.5. Model selection for thermal insulation performances

For the thermal conductivity (λ) model, the natural logarithm was used as the variance stabilizing transformation ($T[\cdot] = \ln(\cdot)$). The model form is:

$$\lambda(\boldsymbol{\Theta}_t, \mathbf{x}_t) = \exp\left[\sum_{i=1}^{n_t} \Theta_{ti} \cdot \frac{h'_{ti}(\mathbf{x}_t) - \mathrm{E}[h'_{ti}(\mathbf{x}_t)]}{\mathrm{SD}[h'_{ti}(\mathbf{x}_t)]} + \varepsilon\right] \quad \text{with } \varepsilon \sim \mathcal{N}(0, \sigma_t^2). \tag{14}$$

The candidate explanatory functions $h'_{ti}(\mathbf{x}_t)$ considered initially included constant (intercept), T, T^2, ρ, $\log(\rho)$, ρ^2, and ρ^3. Their statistics over the database are provided in Table 3.

Fig. 4 illustrates the stepwise deletion process for the thermal model. The terms associated with the parameters having the highest CoV were removed sequentially. The term h'_{t3} (T^2) was first removed ($\mathrm{CoV}_{\Theta_{t3}} = 6.204$). The process continued, removing terms such as h'_{t2} (T) and h'_{t6} (ρ^2). Elimination stopped after removing h'_{t5} ($\log(\rho)$) at Step 4, as removing the next term (h'_{t7}, ρ^3) would have increased σ_t by more than the predefined 10% threshold relative to the previous step's optimal σ_t. This procedure yielded the final parsimonious model presented in Eq. (16), which includes only the intercept, linear density (ρ), and cubic density (ρ^3) terms, providing a good balance between accuracy and simplicity.

2.6. Model selection for sound absorption performances

For the Noise Reduction Coefficient (NRC) model, the logistic transformation ($T[\cdot] = \mathrm{logit}(\cdot) = \ln(\cdot/(1-\cdot))$) was applied. The model takes the form:

$$NRC(\boldsymbol{\Theta}_s, \mathbf{x}_s) = \mathrm{logit}^{-1}\left[\sum_{i=1}^{n_s} \Theta_{si} \cdot \frac{h'_{si}(\mathbf{x}_s) - \mathrm{E}[h'_{si}(\mathbf{x}_s)]}{\mathrm{SD}[h'_{si}(\mathbf{x}_s)]} + \varepsilon\right] \quad \text{with } \varepsilon \sim \mathcal{N}(0, \sigma_s^2). \tag{15}$$

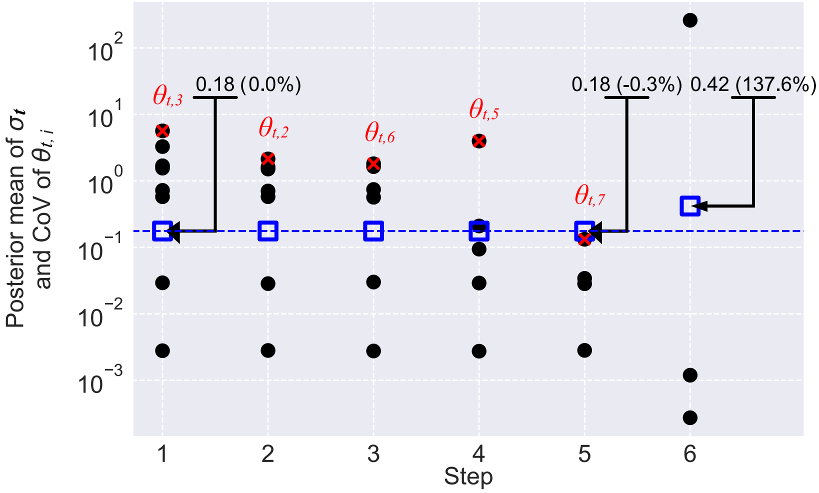

Fig. 4. Stepwise deletion process for the thermal conductivity model. Shows posterior mean σ_t (squares) and parameter CoVs (dots) at each step. Dots with crosses indicate parameters dropped. The blue dashed line marks the initial σ_t. The process stops when removing the next highest CoV term significantly increases σ_t. Values of σ_t for the last two steps are shown.

Table 4
Candidate explanatory functions $h'_{si}(\mathbf{x}_s)$ and their database statistics for the initial NRC model selection.

ID	Variables	Minimum	Maximum	Mean	STD	CoV
$h'_{s1}(\mathbf{x}_s)$	1	–	–	–	–	–
$h'_{s2}(\mathbf{x}_s)$	t	5.000	100.000	31.138	20.121	0.646
$h'_{s3}(\mathbf{x}_s)$	$\log(t)$	1.609	4.605	3.236	0.653	0.202
$h'_{s4}(\mathbf{x}_s)$	t^2	25.000	10 000	1374.413	1873.017	1.363
$h'_{s5}(\mathbf{x}_s)$	t^3	125.000	1×10^6	7.862×10^4	1.702×10^5	2.165
$h'_{s6}(\mathbf{x}_s)$	ρ	8.300	1850.000	302.617	246.568	0.815
$h'_{s7}(\mathbf{x}_s)$	ρ^2	68.890	3.423×10^6	1.524×10^5	3.024×10^5	1.984

Candidate explanatory functions $h'_{si}(\mathbf{x}_s)$ initially included terms related to thickness (t, $\log(t)$, t^2, t^3) and density (ρ, ρ^2), plus an intercept. Their database statistics are in Table 4.

Fig. 5 shows the stepwise deletion results for the NRC model. The term h'_{s7} (ρ^2) was first removed ($\text{CoV}_{\Theta_{s7}} = 1.507$). The process continued, eliminating terms like h'_{s5} (t^3) and h'_{s3} ($\log(t)$). Elimination stopped after removing h'_{s4} (t^2) at Step 4, as removing the next term (h'_{s6}, ρ) would have increased σ_s beyond the acceptable threshold. The final selected model, Eq. (17), includes only the intercept, a linear term for thickness (t), and a linear term for density (ρ), offering a parsimonious yet effective representation of NRC dependence on these key variables.

3. Results

3.1. Probabilistic model for thermal insulation performances

To quantitatively assess thermal performance while accounting for inherent variability, we developed a generalized probabilistic model describing the relationship between thermal conductivity (λ) and mass density (ρ) for bio-based insulation materials, covering a density range of 16–1022kg/m^3. Following a systematic model selection process detailed in the Methods section (Section 2.5), we established a relationship based primarily on ρ. The resulting model, incorporating density and its cubic term to capture non-linearity, takes the form:

$$\lambda = \exp\left(\theta_{t,1} + \theta_{t,4} \cdot \frac{\rho - 398.737}{249.136} + \theta_{t,7} \cdot \frac{\rho^3 - 1.455 \times 10^8}{2.136 \times 10^8} + \varepsilon\right) \quad \text{with } \varepsilon \sim \mathcal{N}(0, \sigma_t^2). \tag{16}$$

Here, $\theta_{t,1}$, $\theta_{t,4}$, and $\theta_{t,7}$ are the model coefficients determined through Bayesian calibration (Section 2.4), and ε is a normally distributed error term with zero mean and variance σ_t^2, representing residual variability. The database underpinning this calibration, comprising numerous experimental results, is detailed in the Appendix (Table A.8).

The posterior distributions of the model parameters, derived from the Bayesian analysis, are summarized in Table 5. The high precision (low standard deviation) of the estimates, particularly for the density-related terms $\theta_{t,4}$ and $\theta_{t,7}$, confirms the model's robustness and underscores the significant, non-linear influence of density on thermal conductivity. Notably, temperature (T) was excluded during the stepwise selection process, suggesting its relatively minor direct influence on λ within the typical range of

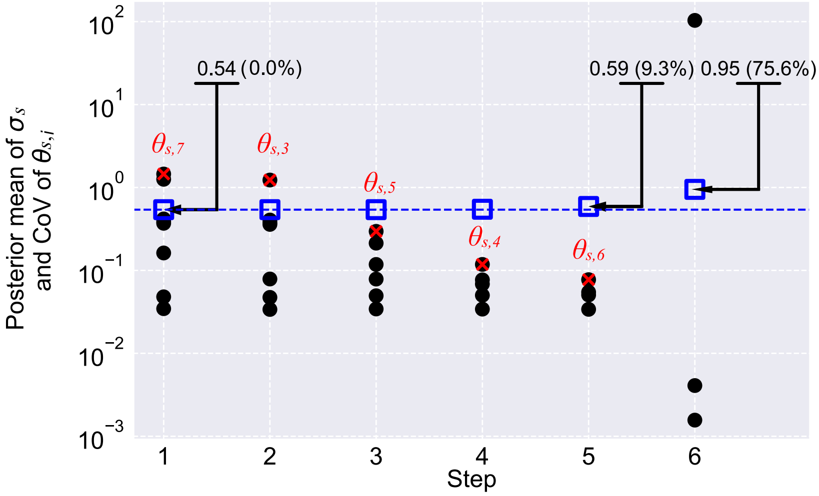

Fig. 5. Stepwise deletion process for the sound absorption (NRC) model. Shows posterior mean σ_s (squares) and parameter CoVs (dots) at each step. Dots with crosses indicate parameters dropped. The blue dashed line marks the initial σ_s. The process stops when removing the next highest CoV term significantly increases σ_s. Values of σ_s for the last two steps are shown.

Table 5
Posterior distribution parameters for the thermal conductivity model (Eq. (16)). Summarizes mean, standard deviation, and 3%–97% Highest Density Interval (HDI) for coefficients $\theta_{t,1}$, $\theta_{t,4}$, $\theta_{t,7}$ and error term standard deviation σ_t.

Parameters	Mean	Standard deviation	HDI 3%	HDI 97%	Correlation Coefficient			
					$\theta_{t,1}$	$\theta_{t,4}$	$\theta_{t,7}$	σ_t
$\theta_{t,1}$	−2.571	7.091×10^{-3}	−2.584	−2.558	1.000	−0.025	0.018	0.051
$\theta_{t,4}$	0.488	1.628×10^{-2}	0.457	0.517	−0.025	1.000	−0.897	0.003
$\theta_{t,7}$	−0.124	1.633×10^{-2}	−0.152	−0.091	0.018	−0.897	1.000	0.001
σ_t	0.175	5.043×10^{-3}	0.166	0.185	0.051	0.003	0.001	1.000

building applications, consistent with previous findings [32]. The model selection outcome confirms that λ generally increases with ρ, a trend observed experimentally for materials like cellulose fibers [56] and straw [57], though exceptions exist [58]. While earlier studies often assumed a linear relationship, our probabilistic approach, informed by a broad dataset, provides unbiased support for the non-linear dependence suggested by more recent overviews [59], captured here by the inclusion of the ρ^3 term.

Fig. 6 provides a visual assessment of the model's predictive capability against experimental data across diverse bio-based materials. Fig. 6(a) plots measured λ versus ρ, color-coded by temperature, illustrating the general trend captured by the model alongside the inherent scatter and material-specific variations. The comparison with conventional insulators (rock wool, glass wool) indicates that bio-based materials can offer competitive thermal performance, particularly at lower densities. Fig. 6(b) directly compares predicted λ values (using the mean posterior parameters) against measured values. The concentration of data points around the 1:1 line (ideal prediction) and within the $\pm\sigma_t$ bounds demonstrates the model's overall accuracy. A slight decrease in accuracy is observable at higher densities, potentially due to increased heterogeneity or different heat transfer mechanisms becoming dominant in denser materials.

3.2. Probabilistic model for sound absorption performances

To characterize the acoustic performance, we developed a generalized probabilistic model for the Noise Reduction Coefficient (NRC). Based on the model selection process (Section 2.6), the NRC is modeled as a function of material thickness (t) and density (ρ). We utilize a logistic transformation to bound the NRC between 0 and 1, resulting in the following model structure:

$$NRC = \text{logit}^{-1}\left(\theta_{s,1} + \theta_{s,2} \cdot \frac{t - 31.138}{20.121} + \theta_{s,6} \cdot \frac{\rho - 302.617}{246.568} + \varepsilon\right) \quad \text{with } \varepsilon \sim \mathcal{N}(0, \sigma_s^2). \tag{17}$$

Here, $\text{logit}^{-1}(x) = 1/(1+\exp(-x))$ is the inverse logit function. $\theta_{s,1}$, $\theta_{s,2}$, and $\theta_{s,6}$ are coefficients determined via Bayesian calibration (Section 2.4), and ε is the Normally distributed error term with variance σ_s^2. The definition of NRC and related acoustic metrics are detailed in Methods (Section 2.3.2). The calibration database is provided in the Appendix (Table A.9).

The posterior distributions for the parameters of the NRC model are presented in Table 6. The well-defined parameters (low standard deviations relative to means) indicate successful model calibration and highlight the significant influence of both thickness

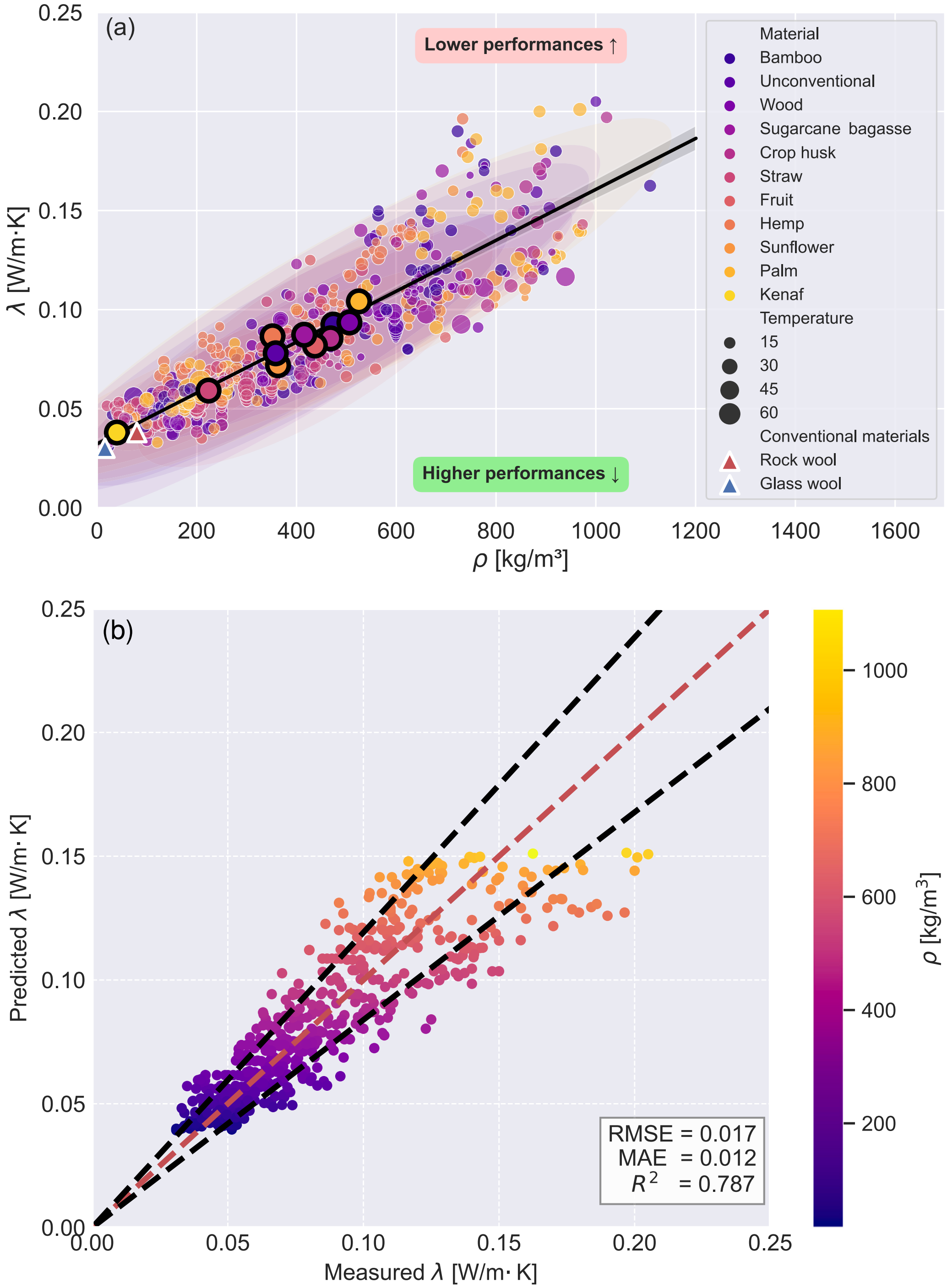

Fig. 6. Comparative analysis of thermal properties for bio-based insulation. (a) Measured thermal conductivity (λ) versus density (ρ) for various materials, size-coded by temperature (T). Solid line shows linear regression with 95% confidence intervals (shaded). Ellipses represent 95% confidence intervals for material group means. Reference points for rock wool [32] and glass wool [60] are shown. (b) Measured λ versus predicted λ using the mean of the probabilistic model (Eq. (16), Table 5). Color indicates density (ρ). The red dashed line is the 1:1 ideal prediction line; black dashed lines represent $\pm\sigma_t$ bounds.

Table 6
Posterior distribution parameters for the Noise Reduction Coefficient (NRC) model (Eq. (17)). Summarizes mean, standard deviation, and 3%–97% HDI for coefficients $\theta_{s,1}$, $\theta_{s,2}$, $\theta_{s,6}$ and error term standard deviation σ_s.

Parameters	Mean	Standard deviation	HDI 3%	HDI 97%	Correlation Coefficient			
					$\theta_{s,1}$	$\theta_{s,2}$	$\theta_{s,6}$	σ_s
$\theta_{s,1}$	−0.525	0.028	−0.580	−0.476	1.000	−0.020	0.017	−0.010
$\theta_{s,2}$	0.563	0.029	0.509	0.616	−0.020	1.000	0.276	0.017
$\theta_{s,6}$	−0.372	0.028	−0.424	−0.319	0.017	0.276	1.000	0.041
σ_s	0.590	0.020	0.553	0.627	−0.010	0.017	0.041	1.000

(positive correlation, $\theta_{s,2} > 0$) and density (negative correlation, $\theta_{s,6} < 0$) on sound absorption, consistent with physical expectations for porous materials.

Fig. 7 evaluates the NRC model's performance. Fig. 7(a) plots measured NRC against density, grouped by material and thickness. While a general linear trend might be inferred, significant scatter exists, emphasizing the need for considering thickness and the inherent variability captured by the probabilistic model. Compared to conventional materials like rock wool and glass wool at similar thickness, some bio-based materials exhibit comparable NRC values, while others underperform, highlighting material-specific differences. Fig. 7(b) compares predicted NRC values (using mean posterior parameters) against measured data. The points cluster around the 1:1 line, mostly within the $\pm\sigma_s$ bounds, confirming the model's predictive capability. The lack of systematic bias across the density range indicates that the chosen non-linear (logit-transformed) model effectively captures the relationship between NRC, density, and thickness.

3.3. Probabilistic model for carbon footprint

In contrast to the thermal and acoustic models — where performance can be linked to physically meaningful predictors (e.g., density and thickness) — the carbon footprint (CF) of bio-based insulation materials is driven by a broader set of exogenous and methodological factors (e.g., agricultural practice, processing energy mix, transport, system boundaries, allocation rules, end-of-life assumptions, and biogenic carbon accounting). Constructing a single process-resolved parametric model from secondary literature would therefore require consistently reported covariates that are not available across the compiled studies. We therefore adopt a screening-level probabilistic characterization: for each material class, CF is represented by a moment-matched distribution capturing the central tendency and dispersion observed in the literature. This representation does not assume that CF is intrinsically Normally distributed; rather, it provides a transparent uncertainty envelope for rapid comparison across material classes and integration into multi-objective workflows. Where project-specific information (e.g., manufacturing route, regional energy mix, and LCA conventions) is available, the class-level distribution can be replaced by refined process-based or non-Gaussian models, while remaining useful as an evidence-based prior for early-stage assessment.

To quantify environmental impact, we develop generalized probabilistic CF models by material class. The compiled dataset intentionally includes studies that both credit and exclude biogenic carbon storage, as LCA conventions differ in whether sequestration is included in Global Warming Potential (GWP). This choice avoids bias towards a single convention and allows the model to reflect the aggregated epistemic uncertainty across heterogeneous sources. Accordingly, for each material class, we model CF using two different types of probabilistic distribution. The first one considers a very low level of knowledge and is a bounded uniform distribution where the bounds are the minimum and maximum of the available data:

$$CF \sim \mathcal{U}(CF_{min}, CF_{max}) \tag{18}$$

where CF_{min} and CF_{max} are the minimum and maximum of the CF values for a specific material type. The second one is a moment-matched normal distribution:

$$CF \sim \mathcal{N}(\mu_c, \sigma_c^2) \tag{19}$$

where μ_c is the mean of the CF values for a specific material type and σ_c^2 is their variance. The methods for calculating CF are outlined in Section 2.3.3.

Because the CF dataset is limited and heterogeneous, when richer, process-resolved LCA data are available, non-normal families or process-based uncertainty propagation should be used to refine CF predictions. The functional unit for the carbon footprint (CF) values compiled in this study is per kilogram of material. The system boundaries are predominantly 'cradle-to-gate', encompassing processes from raw material extraction ('cradle') up to the factory gate. This scope was chosen for consistency, as it is the commonly reported boundary in the literature. While standards like ISO 14067 [62] and EN 15804 [63] provide comprehensive frameworks for LCA, the heterogeneity in the source studies precludes a perfectly harmonized dataset.

Table 7 presents the estimated posterior distributions (mean μ_c and standard deviation σ_c) for the CF of various bio-based materials for normal distribution. The results reveal substantial differences between material types. For instance, kenaf-based materials exhibit the largest mean CF and the highest variability (σ_c), likely reflecting diverse processing pathways and energy inputs across studies. Conversely, fruit-based residues show lower mean CF and less variability. Critically, materials like wood, bamboo, and hemp demonstrate negative mean CF values ($\mu_c < 0$), indicating their potential for net carbon sequestration within the system boundaries considered (often cradle-to-gate).

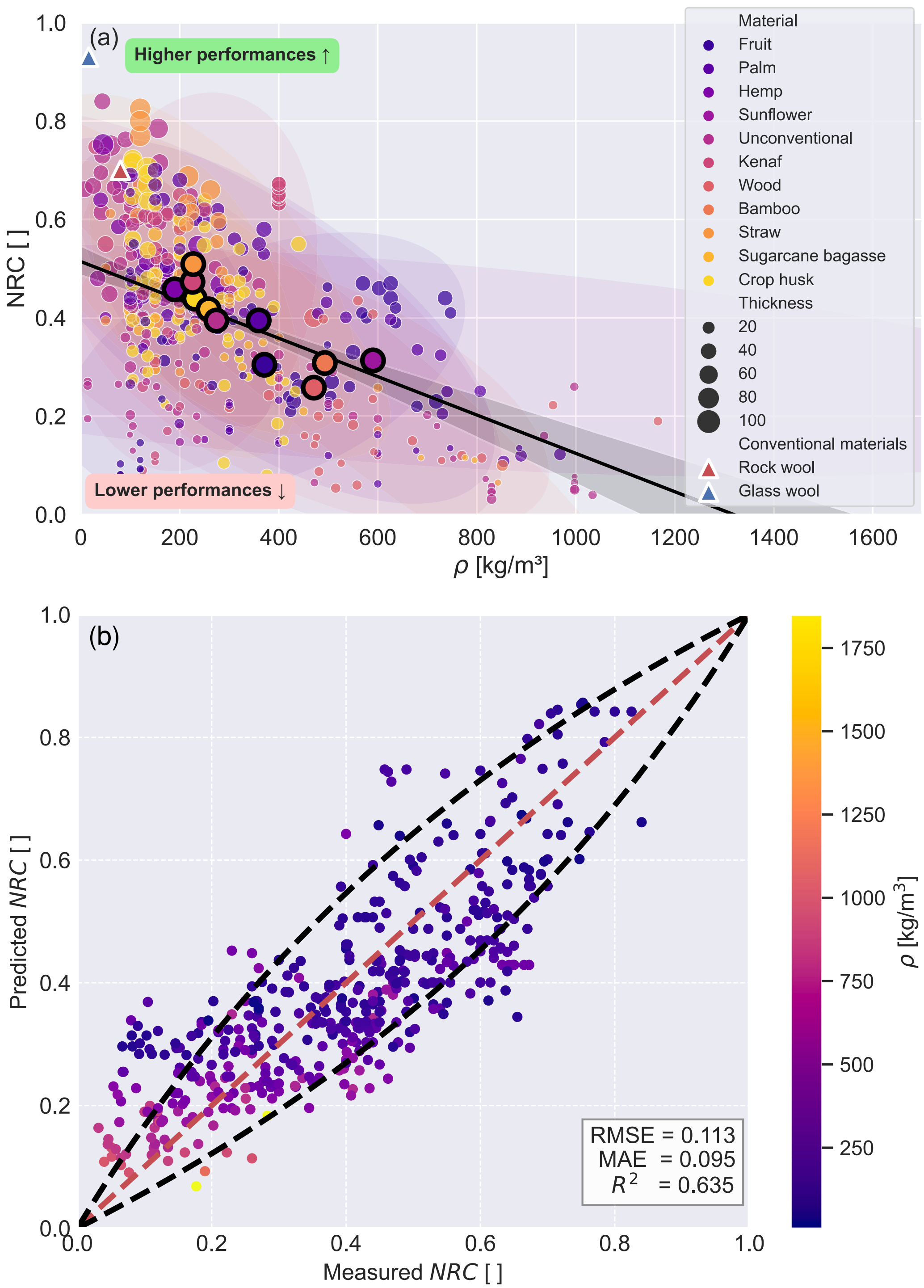

Fig. 7. Comparative analysis of sound absorption properties for bio-based insulation. (a) Measured Noise Reduction Coefficient (NRC) versus density (ρ) for various materials, size-coded by thickness (t). Solid line shows linear regression with 95% confidence intervals (shaded). Ellipses represent 95% confidence intervals for material group means. Reference points for rock wool and glass wool (at $t = 50$ mm) are shown [61]. (b) Measured NRC versus predicted NRC using the mean of the probabilistic model (Eq. (17), Table 6). Color indicates density (ρ). Red dashed line is the 1:1 ideal prediction; black dashed lines represent $\pm\sigma_s$ bounds.

Table 7
Posterior distribution parameters (mean μ_c and standard deviation σ_c) for the Carbon Footprint (CF, in kg $CO_{2,eq}$/kg) model (Eq. (19)) for different bio-based materials. Includes mean, standard deviation, and 3%–97% Highest Density Interval (HDI).

Materials	Mean		Standard deviation		HDI 3%		HDI 97%	
	μ_c	σ_c	μ_c	σ_c	μ_c	σ_c	μ_c	σ_c
Wood	−0.52	0.17	1.17	0.13	−0.83	0.92	−0.18	1.39
Sunflower	0.35	0.07	0.50	0.05	0.22	0.41	0.48	0.59
Sugarcane bagasse	0.15	0.08	0.45	0.07	−0.02	0.34	0.30	0.58
Straw	0.62	0.15	0.79	0.11	0.34	0.61	0.88	1.01
Palm	0.44	0.15	0.75	0.12	0.16	0.54	0.72	0.97
Kenaf	0.62	0.29	1.23	0.24	0.07	0.84	1.19	1.67
Hemp	−0.91	0.15	0.88	0.11	−1.18	0.69	−0.63	1.08
Fruit	0.20	0.04	0.23	0.03	0.11	0.17	0.28	0.29
Crop husk	0.57	0.11	0.53	0.09	0.37	0.38	0.80	0.70
Bamboo	−0.48	0.09	0.62	0.07	−0.64	0.50	−0.30	0.74

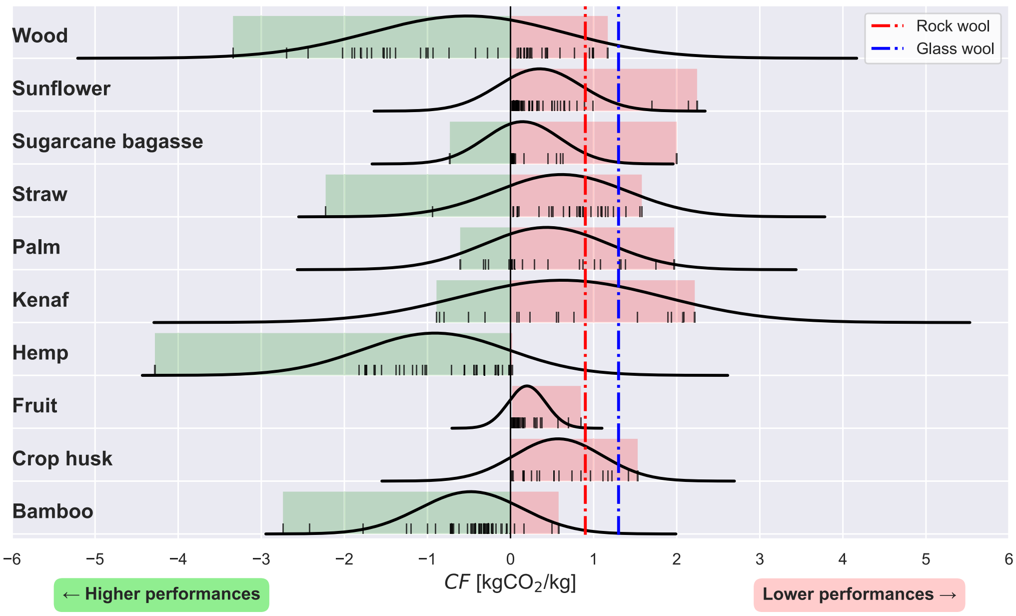

Fig. 8. Posterior probability distributions of carbon footprint (CF) for various bio-based materials (Eq. (19), Table 7). Thick lines represent Normalized probability density functions. Thin vertical lines show individual data points from the literature database. Hatched areas indicate the range of database values, distinguishing potential sequestration (green) from emissions (red). Vertical dash-dotted lines show reference CF values for rock wool and glass wool [28].

Fig. 8 visualizes these posterior probability distributions, offering a clear comparison across materials. The distributions highlight the significant environmental advantage of several bio-based options compared to conventional insulation such as rock wool and glass wool (indicated by vertical lines). The inherent variability (σ_c) captured by the model is also evident, emphasizing that CF assessments require careful consideration of specific production contexts. This material-specific probabilistic approach provides a more nuanced understanding of the environmental implications than single-point estimates.

4. Applications

This section demonstrates the practical utility of the developed probabilistic models through case studies representing common building applications. We assess the performance of bio-based insulation materials in an insulation wall, a sound-absorbing ceiling, and a prefabricated temporary house. Details regarding the design parameters and material compositions for these case studies are provided in the Appendix B.

4.1. Application to thermal performance assessment of bio-based insulation walls

To illustrate the practical use of the thermal conductivity model, this section examines the predicted thermal performance of a prototype bio-based insulation wall assembly, designed for a residential building in China. Details of the wall construction

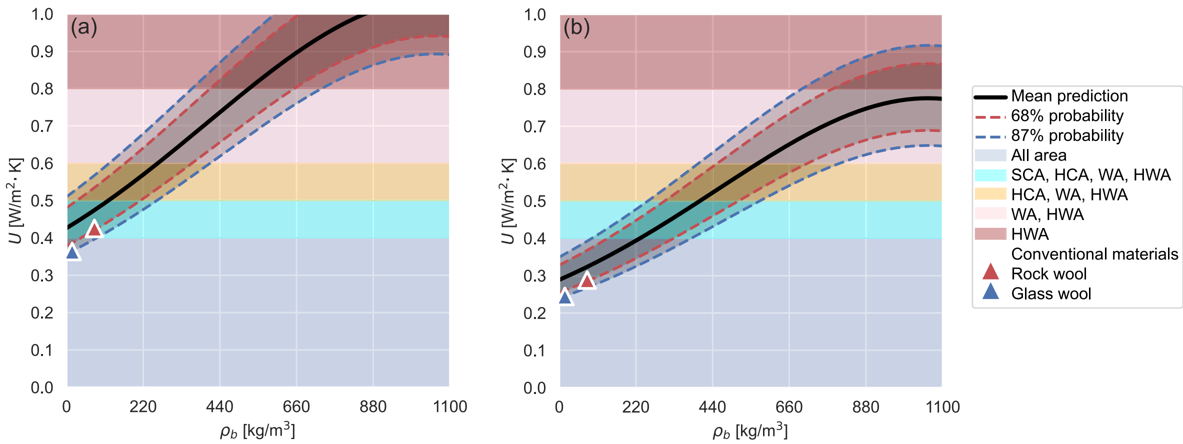

Fig. 9. Predicted thermal transmittance (U) versus bio-based insulation density (ρ_b) for the archetype wall. Results shown for insulation layer thicknesses of (a) 89 mm and (b) 140 mm. Solid lines represent mean predictions; dashed lines show 68% (red) and 87% (blue) probability boundaries. Background colors denote maximum permissible U-values for different Chinese thermal regions [46]. Upward triangles indicate performance with conventional insulation for reference. Model predictions are shown up to $\rho_b = 1100\ \mathrm{kg/m^3}$, the approximate upper limit of the calibration database.

are provided in the Appendix B.1. We calculate the overall thermal transmittance (U) of the wall, incorporating the probabilistic prediction for the bio-based insulation layer (λ_b from Eq. (16)) and considering a standard indoor/outdoor temperature difference (assuming $T = 20$ °C for material property evaluation, although U-value itself is independent of operating temperature). The calculation procedure follows ISO 6946 [45], as described in Methods (Section 2.3).

Fig. 9 plots the predicted thermal transmittance (U) as a function of the bio-based insulation density (ρ_b) for two common insulation layer thicknesses: (a) 89 mm and (b) 140 mm. The background colors indicate the maximum allowable U-values (U_{max}, reciprocal of minimum required R-value) for different climatic regions in China (GB/50176 [46], see Table 1), ranging from Severe Cold Areas (SCA) requiring low U-values to Hot Summer Warm Winter Areas (HWA) with less stringent requirements. The results clearly show that the wall's thermal transmittance (U) increases as the density of the bio-based insulation (ρ_b) increases, consistent with the underlying λ-ρ relationship established in Eq. (16). This highlights the critical impact of material density selection on overall thermal performance. As expected, the thicker insulation layer of 140 mm (Fig. 9(b)) results in lower U-values across all densities compared to the 89 mm layer (Fig. 9(a)), demonstrating improved insulation effectiveness with increased thickness. This probabilistic representation enables designers to evaluate the likelihood that a given combination of bio-based material density and thickness will satisfy regional thermal requirements ($U \leq U_{max}$). By explicitly accounting for material variability, the approach supports informed decision-making that balances thermal performance, material selection, and regulatory compliance. Rather than relying on a single nominal thermal conductivity value reported in product data sheets, the probabilistic model links thermal performance directly to bulk density, allowing designers to rapidly assess compliance across a range of realistic material conditions. The plot includes reference points for walls using conventional insulation, providing context for the performance of the bio-based alternatives.

To illustrate a practical workflow, consider the case of selecting hemp insulation for a 140 mm thick wall in a Cold Area (CA), where the maximum allowable U-value is 0.5 W/(m^2 K) (Fig. 9b). To ensure a high probability of regulatory compliance, the designer refers not to the mean prediction but to the 87th percentile boundary, thereby adopting a conservative approach. By locating the $U_{\mathrm{max}} = 0.5$ W/(m^2 K) line on the plot, the designer identifies the range of densities for which the entire 87% probability curve remains below the regulatory threshold. From the figure, this corresponds to bulk densities (ρ_b) of approximately 250 kg/m^3 or lower. A product with a target density below this value can therefore be specified with high confidence, ensuring compliance even when accounting for material variability.

4.2. Application to sound performance assessment of ceilings

This section demonstrates the application of the probabilistic NRC model (Eq. (17)) to assess the acoustic performance of a sound-absorbing ceiling configuration suitable for spaces like offices or schools. The ceiling design, detailed in the Appendix B.2, involves filling the cavity between ceiling joists/studs with bio-based insulation. We predict the NRC of the bio-based material itself using Eq. (17), which serves as a primary indicator of the ceiling system's potential absorption.

Fig. 10 presents the predicted NRC as a function of the bio-based material density (ρ_b) for two insulation thicknesses: (a) 50 mm and (b) 100 mm. The plots reveal a consistent inverse relationship: NRC generally decreases as the density (ρ_b) of the bio-based material increases, which is typical for porous absorbers where higher density can reduce effective porosity or increase flow resistivity beyond optimal levels. Increasing the thickness from 50 mm (Fig. 10(a)) to 100 mm (Fig. 10(b)) significantly boosts the predicted NRC across all densities, shifting the performance into higher absorption classes. For instance, at lower densities, a 100 mm thick layer is likely to achieve Class II or even Class I performance, whereas a 50 mm layer might predominantly fall

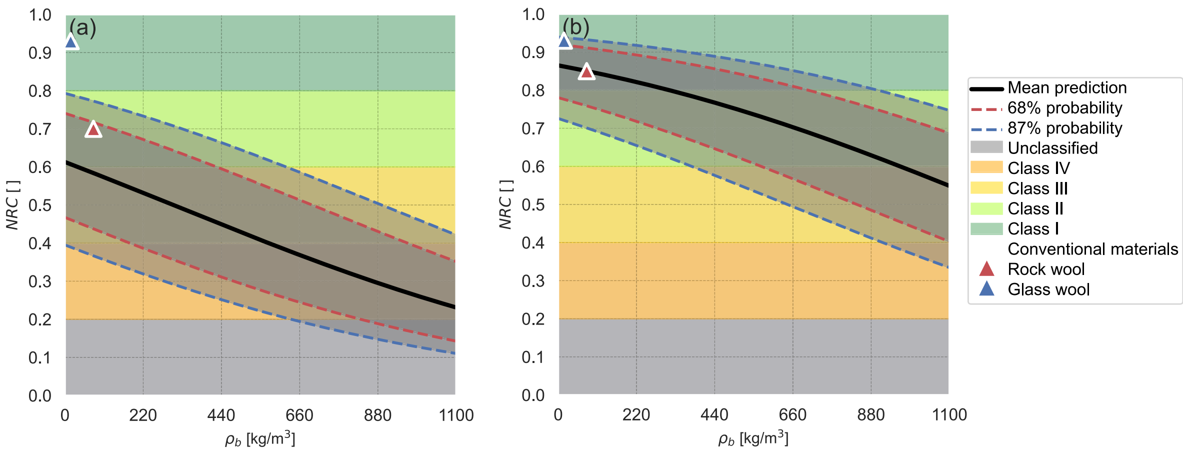

Fig. 10. Predicted Noise Reduction Coefficient (NRC) versus bio-based material density (ρ_b) for ceiling application. Results shown for insulation thicknesses of (a) 50 mm and (b) 100 mm. Solid lines are mean predictions; dashed lines show 68% (red) and 87% (blue) probability boundaries. Background colors represent approximate acoustic absorption classes related to ISO 11654:1997 [47]. Upward triangles indicate reference NRC values for conventional materials. Predictions shown up to $\rho_b = 1100$ kg/m^3.

into Class III or IV. The probabilistic boundaries widen at higher densities and for thicker samples, reflecting greater uncertainty or variability in performance under these conditions. This probabilistic classification aids designers in selecting materials with a specific density and thickness to achieve a target acoustic class with a quantified level of confidence, accounting for material variability. Compared to reference points for traditional rock wool and glass wool, many bio-based materials, especially at lower densities and sufficient thickness, offer competitive sound absorption, although performance varies significantly by material type.

The inverse relationship between NRC and density is explained by the physics of porous absorbers: lower-density materials typically have higher open porosity, allowing sound waves to penetrate and dissipate energy via friction and viscous losses [64]. As density increases beyond an optimal point, the material can become too resistive to airflow, reflecting more sound energy. It is important to note that while lower densities may offer better acoustic performance, practical applications must also consider other constraints such as mechanical stability, durability, and fire resistance, which may impose a lower bound on acceptable density. The probabilistic intervals presented here can be directly translated into design decisions. For example, suppose a project targets acoustic Class C ($NRC \geq 0.60$). The current generation of building codes is not formulated in terms of compliance at a prescribed statistical confidence level, so designers are not required to choose, for instance, between 67% or 87% confidence. Nevertheless, probabilistic characterization can be used — as a conservative internal check — to select density and thickness such that the lower bound of a chosen interval (e.g., 87%) exceeds 0.60, explicitly accounting for material variability. While not mandated today, future code generations could incorporate confidence-based verification to formalize risk-informed design options.

4.3. Application to multi-performance assessment of prefabricated temporary houses

This section integrates the probabilistic models for thermal conductivity (Eq. (16)), NRC (Eq. (17)), and carbon footprint (Eq. (18) and (19)) to conduct a multi-performance assessment of a prefabricated temporary house utilizing various bio-based materials for insulation. The house design details are provided in the Appendix B.3. We evaluate three key performance indicators as a function of the bio-based insulation density (ρ_b): overall thermal conductance (C), average room reverberation time (T_{60}), and total cradle-to-gate carbon footprint (CF_t and $CF_{Building}$). Calculation methods for these metrics are described in Section 2, using Eq. (5) for thermal conductance, Eq. (7) for reverberation time, and Eq. (9) and (10) for CF_t and $CF_{Building}$, with all material properties for the house components detailed in Appendix B.3. Thermal conductance calculations assume T = 20 °C for material property evaluation. Reverberation time calculations consider absorption from walls and ceiling, excluding windows, and use the NRC predicted for the bio-based insulation layer.

Fig. 11(a) shows that thermal conductance (C) generally increases with insulation density (ρ_b), indicating lower thermal resistance, consistent with the λ-ρ relationship. Lower-density bio-based materials offer better thermal insulation for the house envelope. Fig. 11(b) illustrates that reverberation time (T_{60}) also tends to increase with ρ_b. This occurs because higher density generally correlates with lower NRC (as seen in Eq. (17) and Fig. 10), leading to less sound absorption within the room and thus longer reverberation. This suggests that lower-density bio-based materials are generally preferable for achieving better room acoustics (lower T_{60}) in this application. Compared to conventional insulation, bio-based materials offer competitive thermal performance (Fig. 11(a)) but may lead to slightly higher reverberation times depending on density (Fig. 11(b)).

Fig. 11(c) and (d) plots the building-level and total carbon footprint ($CF_{Building}$ and CF_t) of the house (attributable to the insulation choice) against ρ_b for different bio-based material types. The results consistently demonstrate that the majority of bio-based insulation materials substantially outperform conventional insulation systems in terms of carbon performance across the investigated density range. In both modeling approaches, several bio-based materials — most notably wood, bamboo, and hemp — exhibit negative mean values of $CF_{Building}$ and CF_t. These negative values indicate a net carbon sequestration effect associated with the insulation component, whereby biogenic carbon storage outweighs the emissions generated during material production and processing. Consequently, the use of such materials has the potential not only to reduce the embodied carbon of the insulation system itself but also to partially offset emissions arising from other building components. This highlights the dual functional and environmental benefits of selected bio-based insulations, which combine adequate thermal performance with a tangible contribution to climate change mitigation.

A clear distinction is observed in the uncertainty envelopes implied by the two formulations. In Fig. 11(c), the uniform distribution model (Eq. (18)) yields a markedly wider spread, particularly towards highly negative carbon footprints, which is consistent with its weak-information character because bounds set by the observed minimum and maximum of a limited, methodologically heterogeneous database distribute probability mass across the full range, including tails supported by relatively few observations. In contrast, in Fig. 11(d), the moment-matched normal formulation produces a more compact, approximately symmetric envelope by representing variability through the first two moments rather than hard bounds. This serves as a pragmatic screening-level summary of central tendency and dispersion without implying that CF is intrinsically Gaussian, and it may not capture skewness, multi-modality, or heavy tails driven by class- and route-specific effects. Given the limited evidence base, particularly in the tails that drive extreme negative or positive outcomes, there is currently insufficient statistical support to justify a uniquely appropriate parametric form. Therefore, the normal distribution model serves as a pragmatic approximation of central tendency and dispersion, while the uniform distribution model provides a transparent, minimally assumptive bound on epistemic uncertainty. Presenting both envelopes enables a direct sensitivity assessment to distributional choice, while finer class- and route-specific characterization and improved tail modeling are deferred until the database expands.

In summary, our models provide the quantitative inputs for a structured decision-support framework, which includes the following steps:

1. Establish performance targets based on building codes, project goals, and safety requirements (e.g., maximum U-value, minimum NRC class).
2. Use probabilistic models to identify a range of materials (with specific properties like density and thickness) that meet thermal and acoustic targets with the desired confidence level.
3. Evaluate candidates based on their carbon footprint (CF), regional availability, and life cycle costs.
4. Select the optimal material that balances thermal, acoustic, and environmental performance, tailored to the project's climatic, economic, and regulatory context.

The probabilistic nature of the models ensures compliance with building codes and green certifications, offering a robust margin of safety through probability intervals. For example, to meet stringent energy codes, a designer can select insulation properties where the upper 87% probability bound for the U-value stays below the legal limit. Lower-density materials typically offer superior performance, reducing thermal conductance, improving acoustics, and lowering the carbon footprint. However, these advantages must be balanced against essential constraints like mechanical integrity and fire resistance, which may require choosing denser materials with slightly higher thermal, acoustic, or carbon costs.

5. Discussion

5.1. Probabilistic framework and general applicability

This study introduces a robust probabilistic framework, underpinned by an extensive literature review and Bayesian statistical modeling, to assess the performance of bio-based insulation materials across thermal, acoustic, and environmental dimensions. By developing generalized predictive models that explicitly account for the inherent variability of these natural materials, we provide valuable tools to support their effective integration into sustainable construction practices. A key characteristic of the proposed models lies in their general validity, as they are independent of the specific raw materials, the production process, or both. This approach simplifies decision-making during the early stages of design, where a general performance estimate is most valuable. It is acknowledged, however, that for detailed design phases, more specific models tailored to a particular material and manufacturing process could provide refined predictions. Our analysis demonstrates that they offer viable, eco-friendly alternatives to traditional synthetic insulators. The application of our probabilistic models to representative case studies confirms their utility in guiding design decisions for building insulation systems, ultimately fostering the use of renewable resources and contributing to a more circular economy in the built environment [65].

5.2. Performance of bio-based materials

Our findings confirm that bio-based materials possess competitive thermal insulation properties, with thermal conductivity (λ) exhibiting a strong, non-linear dependence on density (ρ). Lower density materials generally provide better insulation, effectively reducing reliance on mechanical heating and cooling and contributing to operational energy savings and CO_2 emission reductions. Acoustically, these materials demonstrate significant sound absorption potential, quantified by the Noise Reduction Coefficient (NRC), which our model shows depends nonlinearly on both density (ρ) and thickness (t). Proper selection based on these

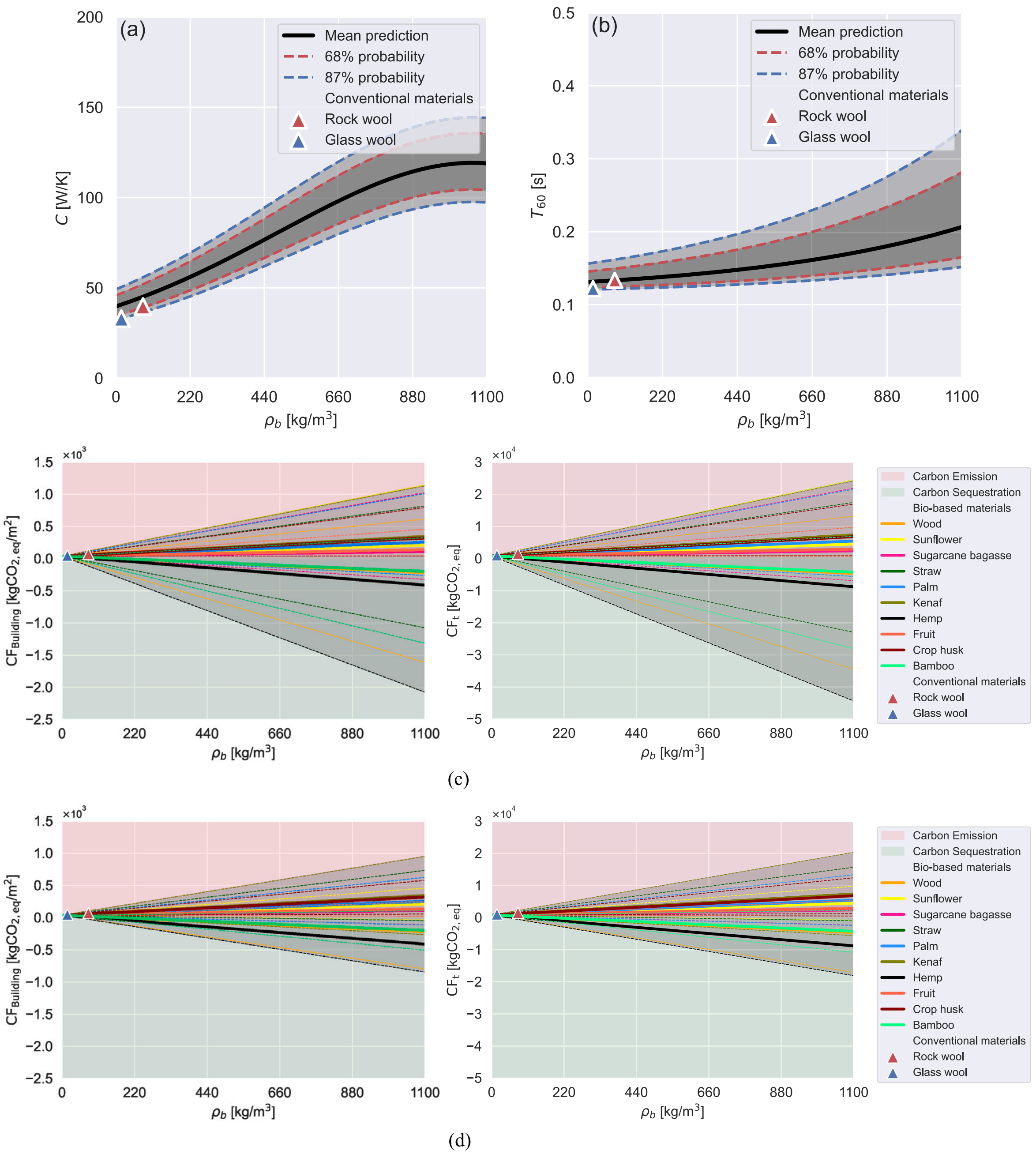

Fig. 11. Multi-performance assessment of bio-based insulation in a prefabricated house. (a) Predicted overall thermal conductance (C) versus insulation density (ρ_b). (b) Predicted room reverberation time (T_{60}) versus ρ_b. In (a) and (b), solid black lines are mean predictions with 68% (dark gray) and 87% (light gray) probability intervals. Reference points for rock wool and glass wool are shown. (c) Predicted building carbon footprint of the insulation component (CF_{Building}) and total building carbon footprint (CF_t) versus ρ_b using the uniform distribution model (Eq. (18)); and (d) using the normal distribution model (Eq. (19)), both grouped by material type for $A_{\text{Building}} = 21.36$ m^2. Thick lines show mean $CF_{Building}$ and CF_t; thin dashed lines represent ±1 standard deviation based on material CF variability (Table 7). Gray shaded area shows overall 68% confidence interval around the generic trend.

parameters can enhance indoor acoustic comfort while avoiding potential indoor air quality issues associated with some synthetic alternatives. Environmentally, the carbon footprint (CF) analysis highlights a key advantage: many bio-based materials not only have lower embodied energy compared to conventional options but also actively sequester atmospheric CO_2 during growth, offering pathways to carbon-neutral or even carbon-negative building components.

The non-linear relationship between thermal conductivity (λ) and density (ρ) can be attributed to several physical factors [59]. At very low densities (typically below approximately 20–30 kg/m^3), heat transfer is governed not only by conduction through the air trapped in the pores, but also by natural convection within larger, interconnected pore spaces [66]. In addition, the presence of moisture in the pore air can significantly enhance heat transfer through combined air–water conduction, an effect that is particularly pronounced in hygroscopic bio-based insulation materials. This moisture-related heat transfer differs substantially from that in conventional insulation materials such as mineral wool, which generally exhibit lower moisture sorption capacity, and represents a fundamental distinction between these two material groups. As density increases, solid-phase conduction through the material matrix becomes more significant, while changes in pore geometry (such as reduced pore size, decreased pore connectivity, or partial closure of pores due to densification) can occur [67]. The inclusion of a cubic term (ρ^3) in our model, as selected by our parsimonious model selection process, empirically captures this complex, non-linear behavior, which aligns with recent overviews suggesting that simple linear models are insufficient. Similarly, the inverse relationship between the Noise Reduction Coefficient (NRC) and density is well-founded in acoustics. Low-density porous materials typically exhibit high porosity and interconnected pores, which allow sound waves to penetrate and dissipate energy through viscous and thermal losses. As density increases, tortuosity may increase, but excessive density can reduce the open-pore content and increase flow resistivity beyond the optimal range, thus reducing sound absorption.

Compared directly to traditional insulation like rock wool and glass wool, bio-based materials present a compelling multi-criteria profile. Thermally, many can match or exceed conventional performance, especially at optimized densities. Acoustically, while performance varies, options like thick, low-density hemp or straw can achieve high NRC values comparable to mineral wool. Environmentally, the advantage is often pronounced, with significantly lower and potentially negative carbon footprints due to biogenic carbon storage.

5.3. Implications for practical applications and future research

Bridging the gap between experimental research and practical application is crucial for leveraging the full potential of bio-based materials in mitigating the environmental impact of the building sector. The probabilistic design tools developed here represent a significant step in this direction, enabling engineers and architects to make informed decisions that account for performance variability. Looking ahead, extending this probabilistic approach to include mechanical properties is essential, particularly for applications where insulation might be integrated with structural elements, such as in prefabricated systems or load-bearing walls. This would enable a truly holistic, multi-performance-based design and retrofitting methodology for sustainable buildings.

6. Conclusions

This study successfully developed and validated probabilistic models for assessing the thermal, acoustic, and environmental performance of bio-based insulation. By synthesizing data from a comprehensive literature review and employing Bayesian statistical methods, we quantified the inherent variability in thermal conductivity, Noise Reduction Coefficient (NRC), and carbon footprint, linking performance to key material properties like density and thickness. The derived models provide a data-driven, statistically robust basis for predicting performance under uncertainty, a critical advancement for the wider adoption of bio-based materials. Application through case studies demonstrated the practical utility of these models in design scenarios, highlighting the potential of bio-based materials to deliver competitive thermal and acoustic performance while offering significant environmental advantages, including net carbon sequestration for certain material types. This probabilistic framework represents a valuable tool for designers and policymakers, facilitating informed material selection and contributing to the transition towards a more sustainable and low-carbon built environment.

6.1. Recommendations

Building upon the insights gained from developing and applying probabilistic models for bio-based insulation, this study offers the following recommendations to accelerate the transition towards more sustainable construction practices.

1. Design Screening via Proxies: Our probabilistic models provide a foundation for utilizing material density (and thickness, for acoustic properties) as practical proxies for the early-stage evaluation of thermal and acoustic performance under conditions of uncertainty. These proxies enable designers to assess material performance across a range of possible scenarios, helping to inform initial design choices with respect to energy efficiency and acoustic properties.
2. Thickness as a Key Performance Lever: The increase in insulation thickness leads to a direct improvement in thermal resistance (i.e., a reduction in U-value) and, within the studied range, typically enhances the Noise Reduction Coefficient (NRC) for acoustic performance. However, this relationship is not infinite. The benefit of increased thickness plateaus beyond certain limits, where further increases provide diminishing returns in both thermal and acoustic performance. Thus, the optimal thickness must be determined in accordance with performance targets, material properties, and design constraints, with particular attention to ensuring that increased thickness remains within a cost-effective and resource-efficient range.

3. Carbon-Performance Trade-offs: The environmental impact of adding insulation thickness is not uniform across materials and is contingent upon the carbon footprint (CF) associated with the material class. For materials with a net-negative CF (i.e., where embodied carbon is less than the carbon sequestered by the material), additional thickness can reduce the overall carbon footprint, as the embodied carbon of the material may be offset by its carbon sequestration potential. Conversely, for materials with a positive CF, increasing insulation thickness will result in higher embodied carbon emissions due to the increased material mass. Therefore, insulation thickness should not be maximized arbitrarily, but rather optimized by balancing the material's thermal performance, embodied carbon, and the broader environmental impact. Material-specific carbon footprints must be carefully evaluated to determine the most sustainable thickness for each application.
4. Broader Implications: The successful, widespread adoption of bio-based materials in building construction requires supportive policies and frameworks that incentivize their use. Policymakers should consider tax credits or subsidies for low-carbon materials and integrate life-cycle carbon assessments into building codes to encourage environmentally responsible material selection [68–70]. Additionally, research should be prioritized to better understand the long-term performance, durability, and carbon footprint of bio-based materials, as their environmental impacts can vary significantly across different types and sources [71]. To maximize the environmental benefits of bio-based materials, their selection should be regionally optimized, considering local resource availability (e.g., agricultural residues, forestry by-products) and the specific climatic and building needs of the region [72].

By actively pursuing these recommendations, the construction sector can more effectively leverage the potential of bio-based insulation materials, contributing significantly to reducing its environmental footprint, promoting resource circularity, and advancing global decarbonization goals through optimized, context-specific sustainable building solutions.

6.2. Limitations and future work

It is important to acknowledge the limitations of this study. The predictive models are based on a limited set of easily measurable predictors (density and thickness) to ensure broad applicability. Factors such as fiber orientation, porosity distribution, and moisture content, while influential, were not explicitly included as predictors and are instead captured within the model's uncertainty term. The models are therefore best suited for preliminary design under typical dry, room-temperature conditions. Future work could focus on developing more complex models that incorporate these additional variables, potentially through machine learning techniques, to provide more refined predictions for detailed engineering. Furthermore, extending this probabilistic approach to include mechanical properties is essential for creating a truly holistic design framework.

CRediT authorship contribution statement

Fengyang Ye: Writing – original draft, Investigation, Formal analysis, Data curation. **Hanlin Wei:** Writing – original draft, Software, Investigation, Data curation, Conceptualization. **Junsong Wang:** Writing – review & editing, Software, Investigation. **Yan Xiao:** Writing – review & editing, Supervision, Conceptualization. **Giuseppe Quaranta:** Writing – review & editing, Supervision, Software, Methodology, Conceptualization. **Paolo Gardoni:** Writing – review & editing, Validation, Supervision, Methodology, Formal analysis, Conceptualization. **Cristoforo Demartino:** Writing – review & editing, Supervision, Resources, Project administration, Investigation, Conceptualization.

Declaration of competing interest

The authors declare that they have no known competing financial interests or personal relationships that could have appeared to influence the work reported in this paper.

Acknowledgments

This study was carried out within the framework of the ≪Artificial Intelligence for ENVIronmental impact minimization of SEismic Retrofitting of Structures (AI-ENVISERS)≫ project, funded by the European Union – NextGenerationEU under the PRIN 2022 PNRR program (D.D. 1409 of 14/09/2022, Ministero dell'Università e della Ricerca). This manuscript reflects only the authors' views; the Ministry cannot be held responsible for any use which may be made of the information contained herein. This work was also partially supported by the Zhejiang University, China and the University of Hong Kong, Hong Kong Institute.

Appendix A. Supplementary data

This appendix contains supplementary data compiled from the literature review.

A.1. Thermal conductivity database

Table A.8 presents the consolidated database of thermal conductivity (λ) for various bio-based materials used in this study.

Table A.8
Consolidated database of thermal conductivity (λ) for various bio-based materials. Data includes density (ρ), average test temperature (T), λ, and source references. Room temperature is assumed to be 20 °C if unspecified in the source.

Materials	ρ [kg/m^3]	T [°C]	λ [W/(m K)]	Ref
Wood	77–925	10–40	0.040–0.173	[73–79]
Bamboo	24–920	20–25	0.031–0.190	[32,80–86]
Hemp	64–924	10–27	0.048–0.196	[87–98]
Straw	20–973	10–60	0.034–0.143	[34,99–112]
Sunflower	36–858	10–40	0.038–0.160	[113–122]
Sugarcane bagasse	16–939	20-57.5	0.031–0.174	[123–134]
Crop husk	53–1022	10–40	0.038–0.197	[78,108,109,123,135–142]
Palm	100–972	18–70	0.033–0.201	[124,143–150]
Fruit	170–907	20–25	0.035–0.159	[151–156]
Cotton	150–450	20	0.059–0.089	[77,157]
Cork	98–195	20–36	0.046–0.055	[98,158]
Grass	60–1000	20	0.045–0.205	[98,159]
Reed	110–150	20	0.052–0.066	[33]
Beet pulp	271–360	20	0.070–0.076	[160]
Eucalyptus globulus leave	74–153	10–60	0.047–0.060	[34]
Corn stalk	280–380	20	0.075–0.108	[161]
Cattail	200–400	24	0.044–0.061	[162]
Pecan shell	599–681	7.2–40.5	0.085–0.112	[163]
Rice hull	154–168	7.2–40.5	0.044–0.056	[163]
Coffee chaff	350	36	0.076	[158]
Rubber	550	36	0.135	[158]
Kenaf	40	23	0.038	[164]
Jute	152–250	25	0.037–0.042	[165]

Table A.9
Consolidated database of Noise Reduction Coefficient (NRC) for various bio-based materials. Data includes density range (ρ), thickness (t), NRC, and source references, illustrating acoustic performance across different materials and configurations.

Materials	ρ [kg/m^3]	t [mm]	NRC	Ref
Wood	100–1166	14–80	0.05–0.60	[31,166–172]
Bamboo	120–852	12–50	0.10–0.67	[173–175]
Hemp	40–400	10–84	0.15–0.75	[31,91,176–182]
Straw	50–825	6–100	0.07–0.83	[57,178,183–190]
Sunflower	34–1850	13–80	0.15–0.48	[116,178,191–193]
Sugarcane bagasse	100–796	5–50	0.11–0.68	[132,194–200]
Crop Husk	105–450	13–100	0.08–0.72	[136,141,183,195,197,201–205]
Palm	100–968	6.5-55	0.06–0.70	[147,206–216]
Fruit	60–747	7–100	0.07–0.75	[31,153,156,193,195,216–219]
Cork	100–195	17.1-30	0.21–0.30	[31,202]
Grass	156–400	20–90	0.33–0.79	[35,220]
Cotton	41	50	0.70	[176,221]
Ramie	96	50	0.69	[176]
Reed	720–818	6.7	0.07–0.18	[222]
Beet pulp	271–360	40	0.45–0.50	[160]
Coffee chaff	350	9.4	0.33	[202]
Rubber	550	16.8	0.20	[202]
Kenaf	30–600	10–60	0.09–0.75	[31,36,174,205,223–226]
Jute	43–250	5.6-60	0.16–0.73	[165,184,227]
Poplar seed	76–178	10–30	0.22–0.53	[228]
Nut leaf	105	6–60	0.13–0.72	[229]
Ground nut shell	234	10–30	0.20–0.42	[230]
Olive	235	15	0.15	[187]
Denim shoddy	43	60	0.84	[227]
Flax	78–115	50–56	0.60–0.65	[176,178,180]
Water hyacinth stem	464–1034	14	0.04–0.30	[231]
Luffa scrap	80–100	20–60	0.36–0.76	[232]
Kapok	8–58	60	0.45–0.67	[233]
Coir	130–198	10–45	0.27–0.61	[211,218,234,235]
Rice hull	400–700	14	0.20–0.28	[236]
Eucalyptus globulus leave	153	40	0.63	[34]
Bark cane	145	40–80	0.45–0.60	[31]

Table A.10
Summary of carbon footprint (CF) data ranges ([CF_{min}, CF_{max}]) for various bio-based materials, expressed as kg $CO_{2,eq}$ per kg of material.

Materials	CF Range [kg $CO_{2,eq}$/kg]	Ref
Wood	[−3.340, 1.170]	[237–242]
Bamboo	[−2.739, 0.579]	[23,242–254]
Hemp	[−4.280, 0.020]	[23,95,255–261]
Straw	[−2.255, 1.580]	[23,242,262–266]
Sunflower	[0.000, 2.245]	[267–277]
Sugarcane bagasse	[−0.730, 2.000]	[277–282]
Crop husk	[0.001, 1.530]	[158,283–291]
Palm	[−0.606, 1.970]	[292–303]
Kenaf	[−0.891, 2.217]	[164,259,304–308]
Fruit	[0.020, 0.846]	[274,309–317]

Table B.11
Layer composition, material properties (density ρ, thickness t, thermal conductivity λ), for the bio-based shear wall design (Fig. B.12), following Wang et al. [32]. ρ_b and λ_b refer to the variable bio-based insulation material.

Layer	Material	ρ [kg/m^3]	t [mm]	λ [W/(m K)]
1	Ferro-cement jacket	2032	19	0.452
2	Damp-proof paper	/	0.17	/
3	Bamboo panel	688	9.5	0.103
4a	Bio-based material	ρ_b	89 or 140	λ_b
4b	Bamboo studs	688	89 or 140	0.103
5	PolyEthylene (PE) sheet	/	0.2	/
6	Gypsum board	684	12	0.148

A.2. Sound absorption database

Table A.9 presents the consolidated database of Noise Reduction Coefficient (NRC) for various bio-based materials.

A.3. Carbon footprint database

Table A.10 presents a summary of the carbon footprint (CF) data ranges ([CF_{min}, CF_{max}]) for various bio-based materials, compiled from life cycle assessment studies.

Appendix B. Case study inputs and details

This section provides the specific inputs, assumptions, and design configurations used in the case studies presented in the main article, illustrating the application of the developed probabilistic models in representative building scenarios.

B.1. Thermal performance assessment of bio-based insulation walls

This subsection details the design of the bio-based insulation wall used in the thermal performance assessment case study (main article), based on Wang et al. [32]. Fig. B.12 illustrates the wall's elements and layers. Structural studs (cross-section 38 × 89 mm or 38 × 140 mm) are spaced at $s = 600$ mm. The overall wall dimensions are 1.22 m (L) × 2.44 m (H). Table B.11 lists the specific material properties and layer thicknesses.

The wall construction, from exterior to interior, is detailed as follows. Layer 1: exterior ferro-cement jacket (19 mm thick) as cladding and primary moisture barrier [243]. Layer 2: air-weather retarder (damp-proof paper, 0.17 mm thick), permeable to vapor but resistant to liquid water and air infiltration [318]. Layer 3: bamboo panel sheathing (9.5 mm thick). Layer 4: framing layer consisting of bamboo studs (Layer 4b) and bio-based insulation material filling the cavities (Layer 4a). The thickness is either 89 mm or 140 mm. Layer 5: polyethylene (PE) vapor retarder sheet (0.2 mm thick) adhered to the framing to control inward vapor diffusion and air movement. Layer 6: interior gypsum board finish (12 mm thick).

B.2. Sound-absorbing performance assessment of ceilings

This subsection describes the sound-absorbing ceiling configuration used in the acoustic performance assessment case study (main article), following the design principles of GJBT-1041-08J931 [61]. Fig. B.13 shows a schematic cross-section. Steel studs, spaced at $d = 400$ mm, support the assembly beneath a concrete slab. The cavity is filled with a bio-based insulation panel (thickness t, typically 50–100 mm in the case study), replacing conventional materials like rock wool or glass wool. A fiberglass cloth is stretched and secured over the studs, followed by protective layers of barbed wire (above the insulation) and an aluminum plate mesh (below the insulation) to maintain structural integrity and contain the insulation material.

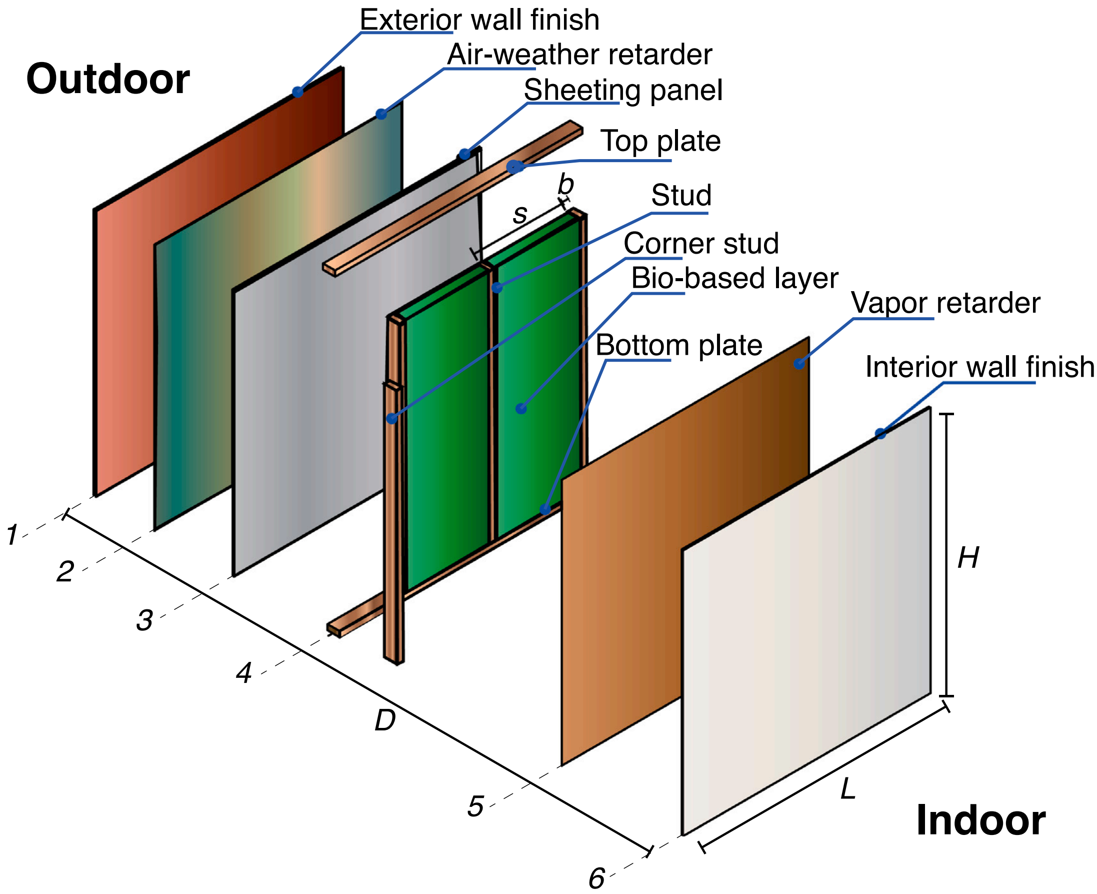

Fig. B.12. Schematic of the multi-layer archetype insulation wall adapted from Wang et al. [32]. Layers include exterior finish, air-weather retarder, sheathing panel, bio-based insulation within stud cavities, interior vapor retarder, and interior finish. Dimensions D (depth), L (width), and H (height) are indicated.

B.3. Carbon footprint assessment of prefabricated temporary houses

This subsection outlines the design of the prefabricated temporary house used for the carbon footprint assessment case study based on Ye et al. [319] and designed according to JGJ/T 188-2009 [320]. This case study adopts a prefabricated temporary house (PTH) archetype that is widely used in China for rapid deployment (e.g., emergency accommodation, temporary worker housing, and field facilities) due to its modularity and fast assembly/disassembly. The steel sheets in the reference configuration represent thin-gauge protective skins (typical ‘steel sheet–insulation–steel sheet’ sandwich panels) primarily used for durability and moisture protection during repeated transport and deployment; the analysis focuses on the insulation layer substitution to quantify the marginal benefits of bio-based insulation within a realistic baseline envelope. Fig. B.14 provides schematic views and key dimensions. The model house features standard components (door: 0.90 × 2.10 m; window: 1.20 × 1.50 m).

Table B.12 specifies the layer composition for the roof, wall, door, window, and floor in the bio-based variant analyzed. A key feature of the bio-based design is the replacement of traditional insulation materials (e.g., rock wool, glass wool) with a 100 mm layer of bio-based insulator (BB). Additionally, Glubam (GB), a laminated bamboo product, is used as the flooring material [32]. The assemblies typically involve sandwiching the insulation between steel sheets (SS). Windows are double-glazed units with glass (G) and an air layer (A).

Appendix C. PRISMA literature screening

This appendix presents the PRISMA 2020 flow diagram used to document the systematic review process, as shown in Fig. C.15.

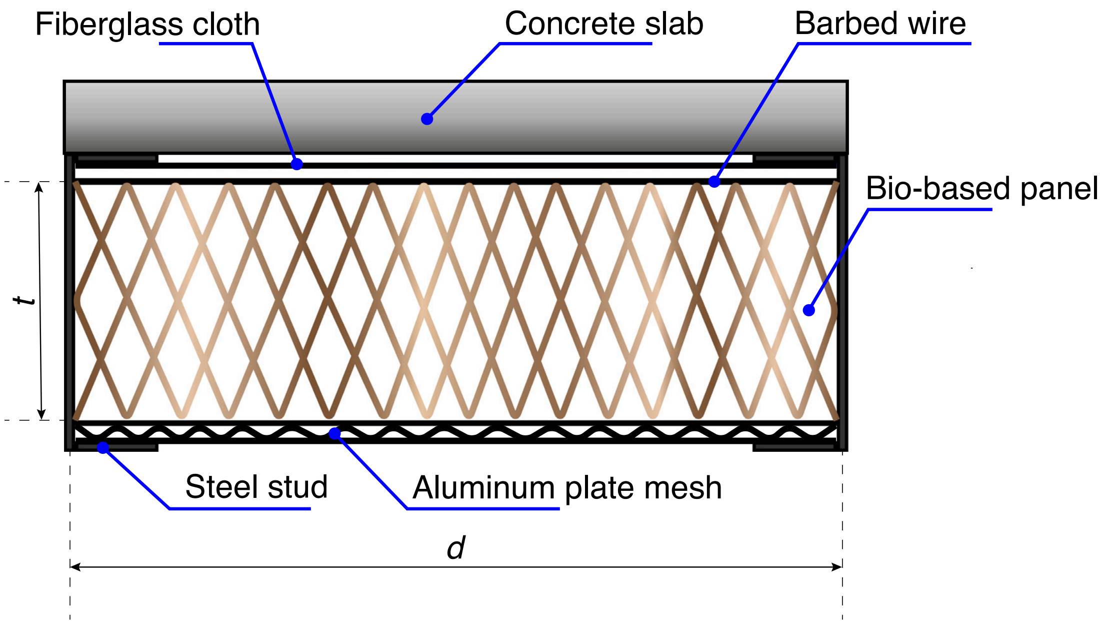

Fig. B.13. Cross-section schematic of the sound-absorbing ceiling assembly. Key components include the concrete slab, steel support studs (spaced at distance d), bio-based insulation panel (thickness t), fiberglass cloth, barbed wire, and aluminum plate mesh.

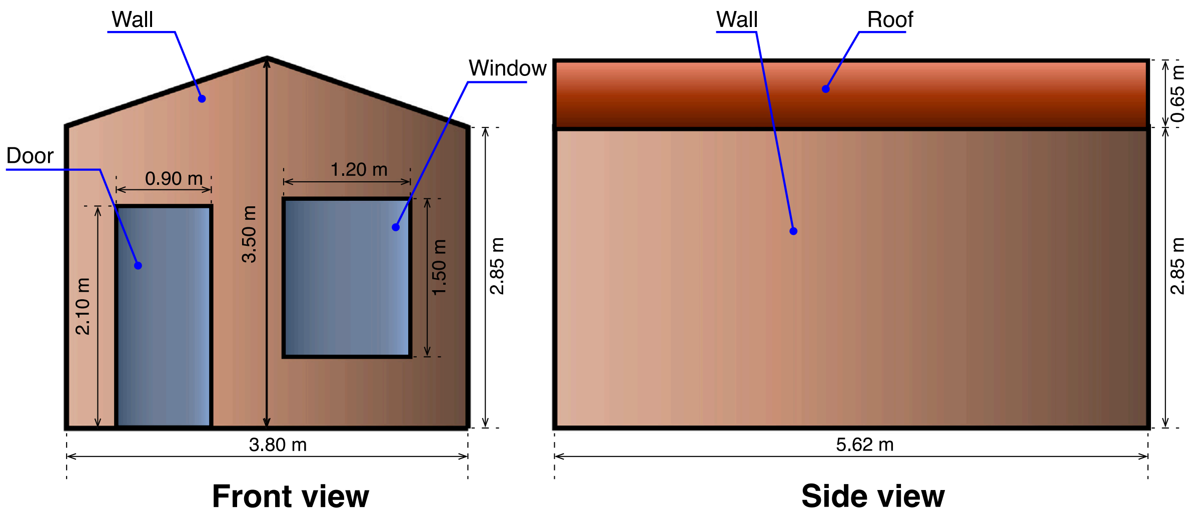

Fig. B.14. Schematic views and dimensions of the prefabricated temporary house model from Ye et al. [319], used in the carbon footprint assessment. Dimensions for walls, roof, door (0.90 × 2.10 m), and window (1.20 × 1.50 m) are shown.

Data availability

The extracted and cleaned datasets compiled from the 266 literature sources (thermal conductivity, NRC, and carbon footprint databases) are publicly available on Zenodo (DOI: 10.5281/zenodo.18061591) and are cited in the manuscript. The deposited files include the processed tabular datasets used for Bayesian calibration and the associated metadata describing variables, units, and inclusion criteria.

Table B.12
Layer design specifications for components of the bio-based prefabricated temporary house. Materials are abbreviated: SS (steel sheet), BB (bio-based material), G (glass), A (air layer), GB (Glubam). Density (ρ) is in kg/m^3 and Carbon Footprint (CF) is in kg $CO_{2,eq}$/kg. ρ_b indicates the density of the variable bio-based material used for insulation.

Components	Bio-based design of the different layers (from outside to inside)								
	Layer 1	ρ	CF	Layer 2	ρ	CF	Layer 3	ρ	CF
Roof Wall Door	0.5 mm SS	7800 [32]	2.19 [242,321]	100 mm BB	ρ_b	See Table A.10	0.5 mm SS	7800 [32]	2.19 [242,321]
Window	6 mm G	2500 [29]	0.84 [29,242]	12 mm A	1.25	0	6 mm G	2500 [29]	0.84 [29,242]
Floor	0.5 mm SS	7800 [32]	2.19 [242,321]	100 mm BB	ρ_b	See Table A.10	10 mm GB	855 [32]	−1.27 [242,252]

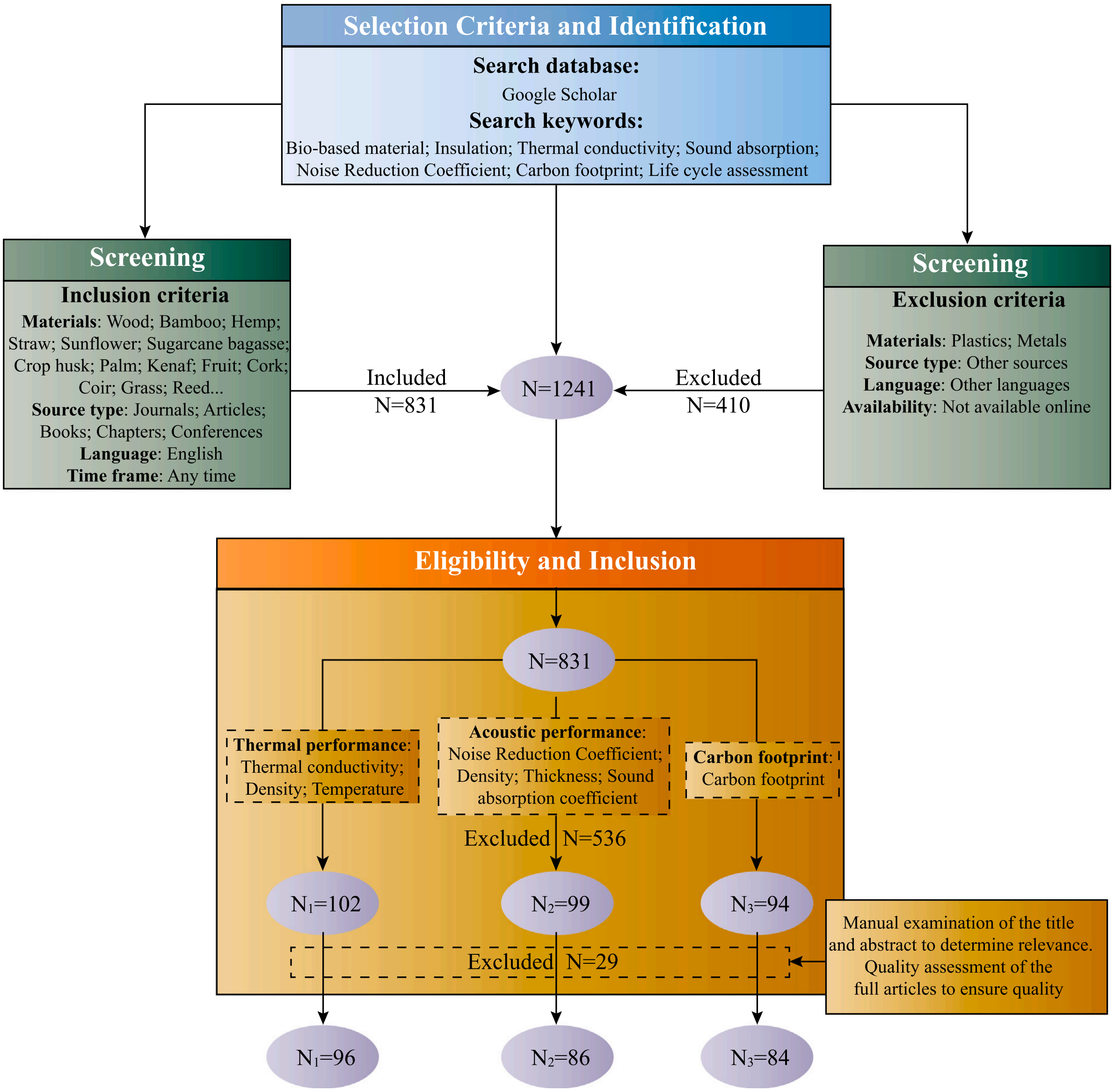

Fig. C.15. PRISMA 2020 flow diagram for the systematic literature review. The diagram details the process of identification, screening, and inclusion of studies for the databases.

References

[1] Saint-Gobain, Constructing a sustainable future, 2023, GlobalABC. URL: https://globalabc.org/resources/publications/constructing-sustainable-future. (Accessed 29 August 2023).

[2] O. Cavalett, M.D. Watanabe, M. Voldsund, S. Roussanaly, F. Cherubini, Paving the way for sustainable decarbonization of the European cement industry, Nat. Sustain. 7 (5) (2024) 568–580, http://dx.doi.org/10.1038/s41893-024-01320-y.

[3] N.P. Gillett, V.K. Arora, K. Zickfeld, S.J. Marshall, W.J. Merryfield, Ongoing climate change following a complete cessation of carbon dioxide emissions, Nat. Geosci. 4 (2) (2011) 83–87, http://dx.doi.org/10.1038/ngeo1047.

[4] C. Wang, Y. Xiong, B. Fan, Q. Yao, H. Wang, C. Jin, Q. Sun, Cellulose as an adhesion agent for the synthesis of lignin aerogel with strong mechanical performance, Sound-absorption and thermal insulation, Sci. Rep. 6 (1) (2016) 32383, http://dx.doi.org/10.1038/srep32383.

[5] X. Zhao, Y. Liu, L. Zhao, A. Yazdkhasti, Y. Mao, A.P. Siciliano, J. Dai, S. Jing, H. Xie, Z. Li, et al., A scalable high-porosity wood for sound absorption and thermal insulation, Nat. Sustain. 6 (3) (2023) 306–315, http://dx.doi.org/10.1038/s41893-022-01035-y.

[6] Y. Huang, C. Xu, L. Wang, A study of thermal performance enhancement of building envelopes by using corncob as construction material, Sci. Rep. 13 (1) (2023) 17891, http://dx.doi.org/10.1038/s41598-023-44206-3.

[7] L. Huang, G. Krigsvoll, F. Johansen, Y. Liu, X. Zhang, Carbon emission of global construction sector, Renew. Sustain. Energy Rev. 81 (2018) 1906–1916, http://dx.doi.org/10.1016/j.rser.2017.06.001.

[8] UNFCCC, Paris agreement, 2015, Adopted at COP 21, Paris, 12 December 2015. URL: https://unfccc.int/documents/37107.

[9] Z. Zhang, M. Chen, T. Zhong, R. Zhu, Z. Qian, F. Zhang, Y. Yang, K. Zhang, P. Santi, K. Wang, et al., Carbon mitigation potential afforded by rooftop photovoltaic in China, Nat. Commun. 14 (1) (2023) 2347, http://dx.doi.org/10.1038/s41467-023-38079-3.

[10] European Parliament and the Council of the European Union, Regulation (EU) 2021/1119 of the European parliament and of the council of 30 june 2021 establishing the framework for achieving climate neutrality and amending regulations (EC) no 401/2009 and (EU) 2018/1999 ('European climate law'), 2021, Official Journal of the European Union, L 243, 9 July 2021, pp. 1–17. URL: https://eur-lex.europa.eu/eli/reg/2021/1119/oj/eng.

[11] United States of America, The long-term strategy of the United States: Pathways to net-zero greenhouse gas emissions by 2050, 2021, UNFCCC submission (LT-LEDS), publication date 01 Nov 2021. URL: https://unfccc.int/documents/308100.

[12] G. Habert, S.A. Miller, V.M. John, J.L. Provis, A. Favier, A. Horvath, K.L. Scrivener, Environmental impacts and decarbonization strategies in the cement and concrete industries, Nat. Rev. Earth Environ. 1 (11) (2020) 559–573, http://dx.doi.org/10.1038/s43017-020-0093-3.

[13] K. Bataineh, A. Al Rabee, A cost effective approach to design of energy efficient residential buildings, Front. Archit. Res. 11 (2) (2022) 297–307, http://dx.doi.org/10.1016/j.foar.2021.10.004.

[14] F. Asdrubali, F. D'Alessandro, S. Schiavoni, A review of unconventional sustainable building insulation materials, Sustain. Mater. Technol. 4 (2015) 1–17, http://dx.doi.org/10.1016/j.susmat.2015.05.002.

[15] S. Schiavoni, F. Bianchi, F. Asdrubali, et al., Insulation materials for the building sector: A review and comparative analysis, Renew. Sustain. Energy Rev. 62 (2016) 988–1011, http://dx.doi.org/10.1016/j.rser.2016.05.045.

[16] Polaris market research, Building Thermal Insulation Market Share, Size, Trends, Industry Analysis Report, By Product (Glass Wool, Mineral Wool, EPS, XPS, Cellulose); By Application (Roof, Walls, Floor); By Region; Segment Forecast, 2024 - 2032, Technical Report, Polaris market research, 2023.

[17] E.A. Zuiderveen, K.J. Kuipers, C. Caldeira, S.V. Hanssen, M.K. van der Hulst, M.M. de Jonge, A. Vlysidis, R. van Zelm, S. Sala, M.A. Huijbregts, The potential of emerging bio-based products to reduce environmental impacts, Nat. Commun. 14 (1) (2023) 8521, http://dx.doi.org/10.1038/s41467-023-43797-9.

[18] F. Pittau, F. Krause, G. Lumia, G. Habert, Fast-growing bio-based materials as an opportunity for storing carbon in exterior walls, Build. Environ. 129 (2018) 117–129, http://dx.doi.org/10.1016/j.buildenv.2017.12.006.

[19] F. Ye, H. Wei, Y. Xiao, U. Berardi, G. Quaranta, C. Demartino, Bio-based insulation materials in sustainable constructions: A review of environmental, thermal and acoustic insulation, durability, and mechanical performances, Renew. Sustain. Energy Rev. 223 (2025) 115872, http://dx.doi.org/10.1016/j.rser.2025.115872.

[20] F. Abik, C. Palasingh, M. Bhattarai, S. Leivers, A. Strom, B. Westereng, K.S. Mikkonen, T. Nypelo, Potential of wood hemicelluloses and their derivates as food ingredients, J. Agricult. Food Chem. 71 (6) (2023) 2667–2683, http://dx.doi.org/10.1021/acs.jafc.2c06449.

[21] X. Cao, F. Li, T. Zheng, G. Li, W. Wang, Y. Li, S. Chen, X. Li, Y. Lu, Cellulose-based functional hydrogels derived from bamboo for product design, Front. Plant Sci. 13 (2022) 958066, http://dx.doi.org/10.3389/fpls.2022.958066.

[22] C. Ingrao, A.L. Giudice, J. Bacenetti, C. Tricase, G. Dotelli, M. Fiala, V. Siracusa, C. Mbohwa, Energy and environmental assessment of industrial hemp for building applications: A review, Renew. Sustain. Energy Rev. 51 (2015) 29–42, http://dx.doi.org/10.1016/j.rser.2015.06.002.

[23] F. Pomponi, J. Hart, J.H. Arehart, B. D'Amico, Buildings as a global carbon sink? A reality check on feasibility limits, One Earth 3 (2) (2020) 157–161, http://dx.doi.org/10.1016/j.oneear.2020.07.018.

[24] Q. Rodriguez Mendez, S. Fuss, S. Lück, F. Creutzig, Assessing global urban CO2 removal, Nat. Cities (2024) 1–11, http://dx.doi.org/10.1038/s44284-024-00069-x.

[25] A. Galimshina, M. Moustapha, A. Hollberg, S. Lasvaux, B. Sudret, G. Habert, Strategies for robust renovation of residential buildings in Switzerland, Nat. Commun. 15 (1) (2024) 2227, http://dx.doi.org/10.1038/s41467-024-46305-9.

[26] B. Dams, D. Maskell, A. Shea, S. Allen, V. Cascione, P. Walker, Upscaling bio-based construction: challenges and opportunities, Build. Res. Inf. 51 (7) (2023) 764–782, http://dx.doi.org/10.1080/09613218.2023.2204414.

[27] G. Tlaiji, S. Ouldboukhitine, F. Pennec, P. Biwole, Thermal and mechanical behavior of straw-based construction: A review, Constr. Build. Mater. 316 (2022) 125915, http://dx.doi.org/10.1016/j.conbuildmat.2021.125915.

[28] R. Kunič, Carbon footprint of thermal insulation materials in building envelopes, Energy Effic. 10 (6) (2017) 1511–1528, http://dx.doi.org/10.1007/s12053-017-9536-1.

[29] Y. Zhang, S. Hu, F. Guo, A. Mastrucci, S. Zhang, Z. Yang, D. Yan, Assessing the potential of decarbonizing China's building construction by 2060 and synergy with industry sector, J. Clean. Prod. 359 (2022) 132086, http://dx.doi.org/10.1016/j.jclepro.2022.132086.

[30] A.F. Ahmed, M.Z. Islam, M.S. Mahmud, M.E. Sarker, M.R. Islam, Hemp as a potential raw material toward a sustainable world: A review, Heliyon 8 (1) (2022) http://dx.doi.org/10.1016/j.heliyon.2022.e08753.

[31] U. Berardi, G. Iannace, Acoustic characterization of natural fibers for sound absorption applications, Build. Environ. 94 (2015) 840–852, http://dx.doi.org/10.1016/j.buildenv.2015.05.029.

[32] J. Wang, C. Demartino, Y. Xiao, Y. Li, Thermal insulation performance of bamboo- and wood-based shear walls in light-frame buildings, Energy Build. 168 (2018) 167–179, http://dx.doi.org/10.1016/j.enbuild.2018.03.017.

[33] F. Asdrubali, F. Bianchi, F. Cotana, F. D'Alessandro, M. Pertosa, A. Pisello, S. Schiavoni, Experimental thermo-acoustic characterization of innovative common reed bio-based panels for building envelope, Build. Environ. 102 (2016) 217–229, http://dx.doi.org/10.1016/j.buildenv.2016.03.022.

[34] M. Ali, A. Alabdulkarem, A. Nuhait, K. Al-Salem, G. Iannace, R. Almuzaiqer, A. Al-turki, F. Al-Ajlan, Y. Al-Mosabi, A. Al-Sulaimi, Thermal and acoustic characteristics of novel thermal insulating materials made of Eucalyptus Globulus leaves and wheat straw fibers, J. Build. Eng. 32 (2020) 101452, http://dx.doi.org/10.1016/j.jobe.2020.101452.

[35] K. Meena, M. Singh, K. Soni, Sound absorption behaviour of vetiver grass fibre-based manufactured pine board, MAPAN 38 (1) (2023) 55–62, http://dx.doi.org/10.1007/s12647-022-00550-9.

[36] E. Taban, P. Soltani, U. Berardi, A. Putra, S.M. Mousavi, M. Faridan, S.E. Samaei, A. Khavanin, Measurement, modeling, and optimization of sound absorption performance of kenaf fibers for building applications, Build. Environ. 180 (2020) 107087, http://dx.doi.org/10.1016/j.buildenv.2020.107087.
[37] F. Ye, Y. Xu, Y. Sun, B. Xiong, J. Wang, C. Demartino, Renewable insulation panels made with cynodon dactylon grass for building applications: Physical, mechanical, acoustic, and thermal properties, J. Build. Eng. 97 (2024) 110602, http://dx.doi.org/10.1016/j.jobe.2024.110602.
[38] T. Adamová, J. Hradeckỳ, M. Prajer, VOC emissions from spruce strands and hemp shive: In search for a low emission raw material for bio-based construction materials, Materials 12 (12) (2019) 2026, http://dx.doi.org/10.3390/ma12122026.
[39] L. Liu, H. Li, A. Lazzaretto, G. Manente, C. Tong, Q. Liu, N. Li, The development history and prospects of biomass-based insulation materials for buildings, Renew. Sustain. Energy Rev. 69 (2017) 912–932, http://dx.doi.org/10.1016/j.rser.2016.11.140.
[40] A. Galimshina, M. Moustapha, A. Hollberg, P. Padey, S. Lasvaux, B. Sudret, G. Habert, Bio-based materials as a robust solution for building renovation: A case study, Appl. Energy 316 (2022) 119102, http://dx.doi.org/10.1016/j.apenergy.2022.119102.
[41] M. Ramesh, K. Palanikumar, K.H. Reddy, Plant fibre based bio-composites: Sustainable and renewable green materials, Renew. Sustain. Energy Rev. 79 (2017) 558–584, http://dx.doi.org/10.1016/j.rser.2017.05.094.
[42] Z. Cao, R.J. Myers, R.C. Lupton, H. Duan, R. Sacchi, N. Zhou, T. Reed Miller, J.M. Cullen, Q. Ge, G. Liu, The sponge effect and carbon emission mitigation potentials of the global cement cycle, Nat. Commun. 11 (1) (2020) 3777, http://dx.doi.org/10.1038/s41467-020-17583-w.
[43] A. Mishra, F. Humpenöder, G. Churkina, C.P. Reyer, F. Beier, B.L. Bodirsky, H.J. Schellnhuber, H. Lotze-Campen, A. Popp, Land use change and carbon emissions of a transformation to timber cities, Nat. Commun. 13 (1) (2022) 4889, http://dx.doi.org/10.1038/s41467-022-32244-w.
[44] J.H. Arehart, J. Hart, F. Pomponi, B. D'Amico, Carbon sequestration and storage in the built environment, Sustain. Prod. Consum. 27 (2021) 1047–1063, http://dx.doi.org/10.1016/j.spc.2021.02.028.
[45] E. ISO, 6946: 2017 Building Components and Building Elements—Thermal Resistance and Thermal Transmittance—Calculation Methods, European Committee for Standardization, Brussels, Belgium, 2017.
[46] G. Mohurd, 50176-2016: Thermal Design Code for Civil Building, China Architecture & Building Press, Beijing, 2016.
[47] ISO11654:1997, Acoustics – sound absorbers for use in buildings and in rooms – rating of sound absorption, 1997, http://dx.doi.org/10.3403/30136189.
[48] R. Peters, Acoustics and Noise Control, Routledge, 2013.
[49] D.F. Ciambrone, Environmental Life Cycle Analysis, CRC Press, 2018, http://dx.doi.org/10.1201/9780203757031.
[50] D. Xiang, F. Xu, R.K. Sah, C. Wei, K. Fang, Carbon footprint accounting method based on dynamic allocation of multi-level carbon data from manufacturing organizations to products, J. Clean. Prod. (2024) 142865, http://dx.doi.org/10.1016/j.jclepro.2024.142865.
[51] EN15978:2011, Sustainability of construction works – Assessment of environmental performance of buildings – calculation method, 2011, URL: https://landingpage.bsigroup.com/LandingPage/Standard?UPI=000000000030256638.
[52] P. Gardoni, A. Der Kiureghian, K.M. Mosalam, Probabilistic capacity models and fragility estimates for reinforced concrete columns based on experimental observations, J. Eng. Mech. 128 (10) (2002) 1024–1038, http://dx.doi.org/10.1061/(ASCE)0733-9399(2002)128:10(1024).
[53] F. Nocera, J. Wang, F. Faleschini, C. Demartino, P. Gardoni, Probabilistic models of concrete compressive strength and elastic modulus with rubber aggregates, Constr. Build. Mater. 322 (2022) 126145, http://dx.doi.org/10.1016/j.conbuildmat.2021.126145.
[54] D. Lai, F. Nocera, C. Demartino, Y. Xiao, P. Gardoni, Probabilistic models of dynamic increase factor (DIF) for reinforced concrete structures: A Bayesian approach, Struct. Saf. 108 (2024) 102430, http://dx.doi.org/10.1016/j.strusafe.2024.102430.
[55] O. Abril-Pla, V. Andreani, C. Carroll, L. Dong, C.J. Fonnesbeck, M. Kochurov, R. Kumar, J. Lao, C.C. Luhmann, O.A. Martin, et al., PyMC: a modern, and comprehensive probabilistic programming framework in python, PeerJ Comput. Sci. 9 (2023) e1516, http://dx.doi.org/10.7717/peerj-cs.1516.
[56] N. Sekino, Density dependence in the thermal conductivity of cellulose fiber mats and wood shavings mats: investigation of the apparent thermal conductivity of coarse pores, J. Wood Sci. 62 (2016) 20–26, http://dx.doi.org/10.1007/s10086-015-1523-6.
[57] C.H.A. Koh, D. Kraniotis, A review of material properties and performance of straw bale as building material, Constr. Build. Mater. 259 (2020) 120385, http://dx.doi.org/10.1016/j.conbuildmat.2020.120385.
[58] H. Bui, N. Sebaibi, M. Boutouil, D. Levacher, Determination and review of physical and mechanical properties of raw and treated coconut fibers for their recycling in construction materials, Fibers 8 (6) (2020) 37, http://dx.doi.org/10.3390/fib8060037.
[59] Z. Pásztory, D.H.A. Le, An overview of factors influencing thermal conductivity of building insulation materials, J. Build. Eng. 44 (2021) 102604, http://dx.doi.org/10.1016/j.jobe.2021.102604.
[60] F. Domínguez-Muñoz, B. Anderson, J.M. Cejudo-López, A. Carrillo-Andrés, Uncertainty in the thermal conductivity of insulation materials, Energy Build. 42 (11) (2010) 2159–2168, http://dx.doi.org/10.1016/j.enbuild.2010.07.006.
[61] 08J931, 08J931 Building Sound Insulation and Absorption Construction Method, National Building Standard Design, 2008.
[62] International Organization for Standardization (ISO), ISO 14067:2018, Greenhouse Gases — Carbon Footprint of Products — Requirements and Guidelines for Quantification, Standard, Geneva, Switzerland, 2018.
[63] European Committee for Standardization (CEN), EN 15804:2012+A2:2019, Sustainability of Construction Works — Environmental Product Declarations — Core Rules for the Product Category of Construction Products, Standard, Brussels, Belgium, 2019.
[64] R.K. Dunne, D.A. Desai, R. Sadiku, A review of porous automotive sound absorbers, their environmental impact and the factors that influence sound absorption, Int. J. Veh. Noise Vib. 13 (2) (2017) 137–163, http://dx.doi.org/10.1504/IJVNV.2017.087910.
[65] D.L. Le, R. Salomone, Q.T. Nguyen, Circular bio-based building materials: A literature review of case studies and sustainability assessment methods, Build. Environ. (2023) 110774, http://dx.doi.org/10.1016/j.buildenv.2023.110774.
[66] W. Batty, S. Probert, J. Lane, Convection and radiation in layers of low-density fibrous insulants, Appl. Energy 18 (2) (1984) 143–161, http://dx.doi.org/10.1016/0306-2619(84)90051-5.
[67] S.A. Carvajal, E.J. Garboczi, R.R. Zarr, Comparison of models for heat transfer in high-density fibrous insulation, J. Res. Natl. Inst. Stand. Technol. 124 (2019) 1, http://dx.doi.org/10.6028/jres.124.010.
[68] Z.-Y. Zhao, L. Gao, J. Zuo, How national policies facilitate low carbon city development: A China study, J. Clean. Prod. 234 (2019) 743–754, http://dx.doi.org/10.1016/j.jclepro.2019.06.116.
[69] E. Dace, A. Cascavilla, M. Bianchi, E. Chioatto, E. Zecca, L. Ladu, G. Yilan, Barriers to transitioning to a circular bio-based economy: Findings from an industrial perspective, Sustain. Prod. Consum. 48 (2024) 407–418, http://dx.doi.org/10.1016/j.spc.2024.05.029.
[70] V. Göswein, J. Arehart, C. Phan-Huy, F. Pomponi, G. Habert, Barriers and opportunities of fast-growing biobased material use in buildings, Build. Cities 3 (1) (2022) 745–755, http://dx.doi.org/10.3929/ethz-b-000587227.
[71] Y. Liang, R. Kleijn, A. Tukker, E. van der Voet, Material requirements for low-carbon energy technologies: a quantitative review, Renew. Sustain. Energy Rev. 161 (2022) 112334, http://dx.doi.org/10.1016/j.rser.2022.112334.
[72] A. Veliz Reyes, A. Carr, D. Olmez, D. Avilés, M. Gomaa, The geographies of sustainable bio-based materials for modern methods of construction, in: Sustainable Materials for the Built Environment, Springer, 2025, pp. 39–55, http://dx.doi.org/10.1007/978-3-031-97818-0_3.
[73] W. Sonderegger, P. Niemz, Thermal conductivity and water vapour transmission properties of wood-based materials, Eur. J. Wood Wood Prod. 67 (3) (2009) 313–321, http://dx.doi.org/10.1007/s00107-008-0304-y.
[74] J. Seo, J. Jeon, J.-H. Lee, S. Kim, Thermal performance analysis according to wood flooring structure for energy conservation in radiant floor heating systems, Energy Build. 43 (8) (2011) 2039–2042, http://dx.doi.org/10.1016/j.enbuild.2011.04.019.
[75] O. Vololonirina, M. Coutand, B. Perrin, Characterization of hygrothermal properties of wood-based products–Impact of moisture content and temperature, Constr. Build. Mater. 63 (2014) 223–233, http://dx.doi.org/10.1016/j.conbuildmat.2014.04.014.

[76] I. Cetiner, A.D. Shea, Wood waste as an alternative thermal insulation for buildings, Energy Build. 168 (2018) 374–384, http://dx.doi.org/10.1016/j.enbuild.2018.03.019.
[77] C. Lacoste, R. El Hage, A. Bergeret, S. Corn, P. Lacroix, Sodium alginate adhesives as binders in wood fibers/textile waste fibers biocomposites for building insulation, Carbohydr. Polymers 184 (2018) 1–8, http://dx.doi.org/10.1016/j.carbpol.2017.12.019.
[78] R. Muthuraj, C. Lacoste, P. Lacroix, A. Bergeret, Sustainable thermal insulation biocomposites from rice husk, wheat husk, wood fibers and textile waste fibers: Elaboration and performances evaluation, Ind. Crop. Prod. 135 (2019) 238–245, http://dx.doi.org/10.1016/j.indcrop.2019.04.053.
[79] F. Segovia, P. Blanchet, N. Auclair, G.G. Essoua Essoua, Thermo-mechanical properties of a wood fiber insulation board using a bio-based adhesive as a binder, Buildings 10 (9) (2020) 152, http://dx.doi.org/10.3390/buildings10090152.
[80] E. Foadieng, P. Talla, G. Nkamgang, M. Fogue, et al., Study of the thermal properties of Raffia Bamboo vinifera L. Arecaceae, Adv. Mater. Sci. Eng. 2017 (2017) http://dx.doi.org/10.1155/2017/9868903.
[81] Z. Huang, Y. Sun, F. Musso, Experimental study on bamboo hygrothermal properties and the impact of bamboo-based panel process, Constr. Build. Mater. 155 (2017) 1112–1125, http://dx.doi.org/10.1016/j.conbuildmat.2017.08.133.
[82] D.M. Nguyen, A.-C. Grillet, T.M.H. Diep, C.N. Ha Thuc, M. Woloszyn, Hygrothermal properties of bio-insulation building materials based on bamboo fibers and bio-glues, Constr. Build. Mater. 155 (2017) 852–866, http://dx.doi.org/10.1016/j.conbuildmat.2017.08.075.
[83] P. Huang, Y.J. Chew, W.-S. Chang, M.P. Ansell, M. Lawrence, E. Latif, A. Shea, G. Ormondroyd, H. Du, Heat and moisture transfer behaviour in Phyllostachys edulis (Moso bamboo) based panels, Constr. Build. Mater. 166 (2018) 35–49, http://dx.doi.org/10.1016/j.conbuildmat.2018.01.092.
[84] D.M. Nguyen, A.-C. Grillet, T.M.H. Diep, Q.B. Bui, M. Woloszyn, Influence of thermo-pressing conditions on insulation materials from bamboo fibers and proteins based bone glue, Ind. Crop. Prod. 111 (2018) 834–845, http://dx.doi.org/10.1016/j.indcrop.2017.12.009.
[85] X. Ding, R. Dai, H. Chen, Z. Shan, Gelatin as green adhesive for the preparation of a multifunctional biobased cryogel derived from bamboo industrial waste, Carbohydr. Polymers 255 (2021) 117340, http://dx.doi.org/10.1016/j.carbpol.2020.117340.
[86] Z. Huang, Y. Sun, Hygrothermal performance comparison study on bamboo and timber construction in Asia-Pacific bamboo areas, Constr. Build. Mater. 271 (2021) 121602, http://dx.doi.org/10.1016/j.conbuildmat.2020.121602.
[87] S. Benfratello, C. Capitano, G. Peri, G. Rizzo, G. Scaccianoce, G. Sorrentino, Thermal and structural properties of a hemp–lime biocomposite, Constr. Build. Mater. 48 (2013) 745–754, http://dx.doi.org/10.1016/j.conbuildmat.2013.07.096.
[88] E. Sassoni, S. Manzi, A. Motori, M. Montecchi, M. Canti, Novel sustainable hemp-based composites for application in the building industry: Physical, thermal and mechanical characterization, Energy Build. 77 (2014) 219–226, http://dx.doi.org/10.1016/j.enbuild.2014.03.033.
[89] R. Walker, S. Pavia, Moisture transfer and thermal properties of hemp–lime concretes, Constr. Build. Mater. 64 (2014) 270–276, http://dx.doi.org/10.1016/j.conbuildmat.2014.04.081.
[90] G. Balčiūnas, I. Pundienė, L. Lekūnaitė-Lukošiūnė, S. Vėjelis, A. Korjakins, Impact of hemp shives aggregate mineralization on physical–mechanical properties and structure of composite with cementitious binding material, Ind. Crop. Prod. 77 (2015) 724–734, http://dx.doi.org/10.1016/j.indcrop.2015.09.011.
[91] G. Balčiūnas, J. Žvironaitė, S. Vėjelis, A. Jagniatinskis, S. Gaidučis, Ecological, thermal and acoustical insulating composite from hemp shives and sapropel binder, Ind. Crop. Prod. 91 (2016) 286–294, http://dx.doi.org/10.1016/j.indcrop.2016.06.034.
[92] B. Mazhoud, F. Collet, S. Pretot, J. Chamoin, Hygric and thermal properties of hemp-lime plasters, Build. Environ. 96 (2016) 206–216, http://dx.doi.org/10.1016/j.buildenv.2015.11.013.
[93] D. Barnat-Hunek, P. Smarzewski, P. Brzyski, Properties of hemp–flax composites for use in the building industry, J. Nat. Fibers 14 (3) (2017) 410–425, http://dx.doi.org/10.1080/15440478.2016.1212764.
[94] A. Bourdot, T. Moussa, A. Gacoin, C. Maalouf, P. Vazquez, C. Thomachot-Schneider, C. Bliard, A. Merabtine, M. Lachi, O. Douzane, H. Karaky, G. Polidori, Characterization of a hemp-based agro-material: Influence of starch ratio and hemp shive size on physical, mechanical, and hygrothermal properties, Energy Build. 153 (2017) 501–512, http://dx.doi.org/10.1016/j.enbuild.2017.08.022.
[95] M. Sinka, P. Van den Heede, N. De Belie, D. Bajare, G. Sahmenko, A. Korjakins, Comparative life cycle assessment of magnesium binders as an alternative for hemp concrete, Resour. Conserv. Recycl. 133 (2018) 288–299, http://dx.doi.org/10.1016/j.resconrec.2018.02.024.
[96] M. Viel, F. Collet, C. Lanos, Development and characterization of thermal insulation materials from renewable resources, Constr. Build. Mater. 214 (2019) 685–697, http://dx.doi.org/10.1016/j.conbuildmat.2019.04.139.
[97] A. Kremensas, S. Vaitkus, S. Vėjelis, S. Członka, A. Kairytė, Hemp shivs and corn-starch-based biocomposite boards for furniture industry: Improvement of water resistance and reaction to fire, Ind. Crop. Prod. 166 (2021) 113477, http://dx.doi.org/10.1016/j.indcrop.2021.113477.
[98] C. Koh, F. Gauvin, K. Schollbach, H. Brouwers, Investigation of material characteristics and hygrothermal performances of different bio-based insulation composites, Constr. Build. Mater. 346 (2022) 128440, http://dx.doi.org/10.1016/j.conbuildmat.2022.128440.
[99] N. Belayachi, D. Hoxha, M. Slaimia, Impact of accelerated climatic aging on the behavior of gypsum plaster-straw material for building thermal insulation, Constr. Build. Mater. 125 (2016) 912–918, http://dx.doi.org/10.1016/j.conbuildmat.2016.08.120.
[100] Y. Brouard, N. Belayachi, D. Hoxha, N. Ranganathan, S. Méo, Mechanical and hygrothermal behavior of clay–Sunflower (Helianthus annuus) and rape straw (Brassica napus) plaster bio-composites for building insulation, Constr. Build. Mater. 161 (2018) 196–207, http://dx.doi.org/10.1016/j.conbuildmat.2017.11.140.
[101] S. Cascone, F. Catania, A. Gagliano, G. Sciuto, Energy performance and environmental and economic assessment of the platform frame system with compressed straw, Energy Build. 166 (2018) 83–92, http://dx.doi.org/10.1016/j.enbuild.2018.01.035.
[102] Ł. Czajkowski, R. Kocewicz, J. Weres, W. Olek, Estimation of thermal properties of straw-based insulating panels, Materials 15 (3) (2022) http://dx.doi.org/10.3390/ma15031073.
[103] F. D'Alessandro, F. Bianchi, G. Baldinelli, A. Rotili, S. Schiavoni, Straw bale constructions: Laboratory, in field and numerical assessment of energy and environmental performance, J. Build. Eng. 11 (2017) 56–68, http://dx.doi.org/10.1016/j.jobe.2017.03.012.
[104] B. Ismail, N. Belayachi, D. Hoxha, L. Arbaret, Modelling of thermal conductivity and nonlinear mechanical behavior of straw insulation composite by a numerical homogenization approach, J. Build. Eng. 43 (2021) 103144, http://dx.doi.org/10.1016/j.jobe.2021.103144.
[105] M. Labat, C. Magniont, N. Oudhof, J.-E. Aubert, From the experimental characterization of the hygrothermal properties of straw-clay mixtures to the numerical assessment of their buffering potential, Build. Environ. 97 (2016) 69–81, http://dx.doi.org/10.1016/j.buildenv.2015.12.004.
[106] T.W. Loh, K.T. Nguyen, Durability and fire resistance of compressed wheat-straw (triticum aestivum) panels subjected to real-world aging environments, Ind. Crop. Prod. 203 (2023) 117141, http://dx.doi.org/10.1016/j.indcrop.2023.117141.
[107] I. Mehrez, H. Hachem, A. Jemni, Thermal insulation potential of wood-cereal straws/plaster composite, Case Stud. Constr. Mater. 17 (2022) e01353, http://dx.doi.org/10.1016/j.cscm.2022.e01353.
[108] C. Rojas, M. Cea, A. Iriarte, G. Valdés, R. Navia, J.P. Cárdenas-R, Thermal insulation materials based on agricultural residual wheat straw and corn husk biomass, for application in sustainable buildings, Sustain. Mater. Technol. 20 (2019) e00102, http://dx.doi.org/10.1016/j.susmat.2019.e00102.
[109] S. Wang, H. Li, S. Zou, L. Liu, C. Bai, G. Zhang, L. Fang, Experimental study on durability and acoustic absorption performance of biomass geopolymer-based insulation materials, Constr. Build. Mater. 361 (2022) 129575, http://dx.doi.org/10.1016/j.conbuildmat.2022.129575.
[110] Y. Wang, K. Wu, M. Xiao, S.B. Riffat, Y. Su, F. Jiang, Thermal conductivity, structure and mechanical properties of konjac glucomannan/starch based aerogel strengthened by wheat straw, Carbohydr. Polymers 197 (2018) 284–291, http://dx.doi.org/10.1016/j.carbpol.2018.06.009.

[111] K. Wei, C. Lv, M. Chen, X. Zhou, Z. Dai, D. Shen, Development and performance evaluation of a new thermal insulation material from rice straw using high frequency hot-pressing, Energy Build. 87 (2015) 116–122, http://dx.doi.org/10.1016/j.enbuild.2014.11.026.
[112] Y. Zhou, A. Trabelsi, M. El Mankibi, Hygrothermal properties of insulation materials from rice straw and natural binders for buildings, Constr. Build. Mater. 372 (2023) 130770, http://dx.doi.org/10.1016/j.conbuildmat.2023.130770.
[113] I. Kocaman, C. Sisman, E. Gezer, Investigation the using possibilities of some mineral-bound organic composites as thermal insulation material in rural buildings, Sci. Res. Essays 6 (7) (2011) 1673–1680, http://dx.doi.org/10.5897/SRE11.275.
[114] V. Virginie, R. Luc, S. Redouan, P. Bernard, New agro-materials with thermal insulation properties, in: 18th Conference on Sunflower, Mar Del Plata Argentina, vol. 169, 2012, p. 949À954.
[115] P. Evon, V. Vandenbossche, P.-Y. Pontalier, L. Rigal, New thermal insulation fiberboards from cake generated during biorefinery of sunflower whole plant in a twin-screw extruder, Ind. Crop. Prod. 52 (2014) 354–362, http://dx.doi.org/10.1016/j.indcrop.2013.10.049.
[116] N. Mati-Baouche, H. De Baynast, A. Lebert, S. Sun, C.J.S. Lopez-Mingo, P. Leclaire, P. Michaud, Mechanical, thermal and acoustical characterizations of an insulating bio-based composite made from sunflower stalks particles and chitosan, Ind. Crop. Prod. 58 (2014) 244–250, http://dx.doi.org/10.1016/j.indcrop.2014.04.022.
[117] A. Mahieu, H. Lenormand, N. Leblanc, A. Vivet, 100% biobased particleboards based on new agricultural wastes, Acad. J. Civ. Eng. 33 (2) (2015) 705–710, http://dx.doi.org/10.26168/icbbm2015.110.
[118] Y. Brouard, N. Belayachi, M. Ranganathan, D. Hoxha, S. Méo, Experimental assessment of hygrothermal properties of clay-sunflower (helianthus annuus) and rape straw (brassica napus) bio-composites, in: 2nd International Conference on Bio-Based Building Materials & 1st Conference on ECOlogical Valorisation of GRAnular and FIbrous Materials, 2017.
[119] H. Lenormand, P. Glé, N. Leblanc, Investigation of the acoustical and thermal properties of sunflower particleboards, Acta Acust. United Acust. 103 (1) (2017) 149–157, http://dx.doi.org/10.3813/AAA.919040.
[120] A. Eschenhagen, M. Raj, N. Rodrigo, A. Zamora, L. Labonne, P. Evon, H. Welemane, et al., Investigation of miscanthus and sunflower stalk fiber-reinforced composites for insulation applications, Adv. Civ. Eng. 2019 (2019) http://dx.doi.org/10.1155/2019/9328087.
[121] A. Mahieu, S. Alix, N. Leblanc, Properties of particleboards made of agricultural by-products with a classical binder or self-bound, Ind. Crop. Prod. 130 (2019) 371–379, http://dx.doi.org/10.1016/j.indcrop.2018.12.094.
[122] T. Verdier, L. Balthazard, M. Montibus, C. Magniont, P. Evon, A. Bertron, Using glycerol esters to prevent microbial growth on sunflower-based insulation panels, Proc. Inst. Civ. Engineers-Construction Mater. 174 (3) (2021) 140–149, http://dx.doi.org/10.1680/jcoma.20.00002.
[123] S. Panyakaew, S. Fotios, New thermal insulation boards made from coconut husk and bagasse, Energy Build. 43 (7) (2011) 1732–1739, http://dx.doi.org/10.1016/j.enbuild.2011.03.015.
[124] K. Manohar, Experimental investigation of building thermal insulation from agricultural by-products, Br. J. Appl. Sci. Technol. 2 (3) (2012) 227–239.
[125] R. Liao, J. Xu, K. Umemura, Low density sugarcane bagasse particleboard bonded with citric acid and sucrose: Effect of board density and additive content, BioResources 11 (1) (2016) 2174–2185.
[126] E.Y. Nakanishi, M.R. Cabral, P. de Souza Gonçalves, V. dos Santos, H.S. Junior, Formaldehyde-free particleboards using natural latex as the polymeric binder, J. Clean. Prod. 195 (2018) 1259–1269, http://dx.doi.org/10.1016/j.jclepro.2018.06.019.
[127] J. Fiorelli, S.B. Bueno, M.R. Cabral, Assessment of multilayer particleboards produced with green coconut and sugarcane bagasse fibers, Constr. Build. Mater. 205 (2019) 1–9, http://dx.doi.org/10.1016/j.conbuildmat.2019.02.024.
[128] R.G.d. Mesquita, A.R. Sanadi, J.M. Marconcini, A.C. Correa, A.A.d.S. César, L.M.F. Andrade, T.A. Lopes, J.A. Simão, L.M. Mendes, The effect of cellulose nanocrystals in sugarcane bagasse particleboards of pith and fibers, Cerne 25 (2019) 203–213, http://dx.doi.org/10.1590/01047760201925022621.
[129] Q.B. Thai, S.T. Nguyen, D.K. Ho, T. Du Tran, D.M. Huynh, N.H. Do, T.P. Luu, P.K. Le, D.K. Le, N. Phan-Thien, et al., Cellulose-based aerogels from sugarcane bagasse for oil spill-cleaning and heat insulation applications, Carbohydr. Polymers 228 (2020) 115365, http://dx.doi.org/10.1016/j.carbpol.2019.115365.
[130] N.A. Ramlee, M. Jawaid, A.S. Ismail, E.S. Zainudin, S.A.K. Yamani, Evaluation of thermal and acoustic properties of oil palm empty fruit bunch/sugarcane bagasse fibres based hybrid composites for wall buildings thermal insulation, Fibers Polym. 22 (9) (2021) 2563–2571, http://dx.doi.org/10.1007/s12221-021-0224-6.
[131] U. Bordoloi, D. Das, D. Kashyap, D. Patwa, P. Bora, H.H. Muigai, P. Kalita, Synthesis and comparative analysis of biochar based form-stable phase change materials for thermal management of buildings, J. Energy Storage 55 (2022) 105801, http://dx.doi.org/10.1016/j.est.2022.105801.
[132] S. Mehrzad, E. Taban, P. Soltani, S.E. Samaei, A. Khavanin, Sugarcane bagasse waste fibers as novel thermal insulation and sound-absorbing materials for application in sustainable buildings, Build. Environ. 211 (2022) 108753, http://dx.doi.org/10.1016/j.buildenv.2022.108753.
[133] B. Phoopat, P. Surin, K. Buasri, Influence of Adhesive on Physical, Mechanical, and Thermal Properties of Corrugated Fibers Composite Roofing from Bagasse Fiber in Sugar Industry, Technical Report, EasyChair, 2023, http://dx.doi.org/10.5604/01.3001.0054.8016.
[134] E. Darwish, A.S. Eldeeb, Utilizing agro-industrial wastes panels in developing cost-efficient thermally insulating wall claddings for residential energy retrofitting in Egypt, Energy Built Environ. 5 (5) (2024) 683–703, http://dx.doi.org/10.1016/j.enbenv.2023.05.007.
[135] S.A. Bekalo, H.-W. Reinhardt, Fibers of coffee husk and hulls for the production of particleboard, Mater. Struct. 43 (8) (2010) 1049–1060, http://dx.doi.org/10.1617/s11527-009-9565-0.
[136] J. António, A. Tadeu, B. Marques, J.A. Almeida, V. Pinto, Application of rice husk in the development of new composite boards, Constr. Build. Mater. 176 (2018) 432–439, http://dx.doi.org/10.1016/j.conbuildmat.2018.05.028.
[137] Š. Hysek, M. Podlena, H. Bartsch, C. Wenderdel, M. Böhm, Effect of wheat husk surface pre-treatment on the properties of husk-based composite materials, Ind. Crop. Prod. 125 (2018) 105–113, http://dx.doi.org/10.1016/j.indcrop.2018.08.035.
[138] A. Antunes, P. Faria, V. Silva, A. Brás, Rice husk-earth based composites: A novel bio-based panel for buildings refurbishment, Constr. Build. Mater. 221 (2019) 99–108, http://dx.doi.org/10.1016/j.conbuildmat.2019.06.074.
[139] S. Hossain, P. Roy, Fabrication of sustainable ceramic board using solid-wastes for construction purpose, Constr. Build. Mater. 222 (2019) 26–40, http://dx.doi.org/10.1016/j.conbuildmat.2019.06.126.
[140] Š. Hysek, P. Neuberger, A. Sikora, O. Schönfelder, G. Ditommaso, Waste utilization: Insulation panel from recycled polyurethane particles and wheat husks, Materials 12 (19) (2019) 3075, http://dx.doi.org/10.3390/ma12193075.
[141] M. Fattahi, E. Taban, P. Soltani, U. Berardi, A. Khavanin, V. Zaroushani, Waste corn husk fibers for sound absorption and thermal insulation applications: a step towards sustainable buildings, J. Build. Eng. 77 (2023) 107468, http://dx.doi.org/10.1016/j.jobe.2023.107468.
[142] A. Silva, F. Gaspar, A. Bakatovich, Composite materials of rice husk and reed fibers for thermal insulation plates using sodium silicate as a binder, Sustainability 15 (14) (2023) 11273, http://dx.doi.org/10.3390/su151411273.
[143] B. Agoudjil, A. Benchabane, A. Boudenne, L. Ibos, M. Fois, Renewable materials to reduce building heat loss: Characterization of date palm wood, Energy Build. 43 (2–3) (2011) 491–497, http://dx.doi.org/10.1016/j.enbuild.2010.10.014.
[144] M. Chikhi, B. Agoudjil, A. Boudenne, A. Gherabli, Experimental investigation of new biocomposite with low cost for thermal insulation, Energy Build. 66 (2013) 267–273, http://dx.doi.org/10.1016/j.enbuild.2013.07.019.
[145] M.E. Ali, A. Alabdulkarem, On thermal characteristics and microstructure of a new insulation material extracted from date palm trees surface fibers, Constr. Build. Mater. 138 (2017) 276–284, http://dx.doi.org/10.1016/j.conbuildmat.2017.02.012.
[146] L. Boukhattem, M. Boumhaout, H. Hamdi, B. Benhamou, F.A. Nouh, Moisture content influence on the thermal conductivity of insulating building materials made from date palm fibers mesh, Constr. Build. Mater. 148 (2017) 811–823, http://dx.doi.org/10.1016/j.conbuildmat.2017.05.020.

[147] R. Belakroum, A. Gherfi, M. Kadja, C. Maalouf, M. Lachi, N. El Wakil, T. Mai, Design and properties of a new sustainable construction material based on date palm fibers and lime, Constr. Build. Mater. 184 (2018) 330–343, http://dx.doi.org/10.1016/j.conbuildmat.2018.06.196.
[148] T. Masri, H. Ounis, L. Sedira, A. Kaci, A. Benchabane, Characterization of new composite material based on date palm leaflets and expanded polystyrene wastes, Constr. Build. Mater. 164 (2018) 410–418, http://dx.doi.org/10.1016/j.conbuildmat.2017.12.197.
[149] H.E. Benchouia, B. Guerira, M. Chikhi, H. Boussehel, C. Tedeschi, An experimental evaluation of a new eco-friendly insulating material based on date palm fibers and polystyrene, J. Build. Eng. 65 (2023) 105751, http://dx.doi.org/10.1016/j.jobe.2022.105751.
[150] E. Darwish, A.S. Eldeeb, M. Midani, Housing retrofit for energy efficiency: utilizing modular date palm midribs claddings to enhance indoor thermal comfort, Ain Shams Eng. J. 15 (1) (2024) 102323, http://dx.doi.org/10.1016/j.asej.2023.102323.
[151] J. Khedari, S. Charoenvai, J. Hirunlabh, New insulating particleboards from durian peel and coconut coir, Build. Environ. 38 (3) (2003) 435–441, http://dx.doi.org/10.1016/S0360-1323(02)00030-6.
[152] S. Tangjuank, et al., Thermal insulation and physical properties of particleboards from pineapple leaves, Int. J. Phys. Sci. 6 (19) (2011) 4528–4532, http://dx.doi.org/10.5897/IJPS11.1057.
[153] C. Badouard, F. Bogard, C. Bliard, M. Lachi, B. Abbes, G. Polidori, Development and characterization of viticulture by-products for building applications, Constr. Build. Mater. 302 (2021) 124142, http://dx.doi.org/10.1016/j.conbuildmat.2021.124142.
[154] M. Vitale, M.d.M. Barbero-Barrera, S.M. Cascone, Thermal, physical and mechanical performance of orange peel boards: A new recycled material for building application, Sustainability 13 (14) (2021) 7945, http://dx.doi.org/10.3390/su13147945.
[155] J.A.T. Di Canto, W.J. Malfait, J. Wernery, Turning waste into insulation–a new sustainable thermal insulation board based on wheat bran and banana peels, Build. Environ. 244 (2023) 110740, http://dx.doi.org/10.1016/j.buildenv.2023.110740.
[156] M.J. SheikhMozafari, E. Taban, P. Soltani, M. Faridan, A. Khavanin, Sound absorption and thermal insulation performance of sustainable fruit stone panels, Appl. Acoust. 217 (2024) 109836, http://dx.doi.org/10.1016/j.apacoust.2023.109836.
[157] X.-y. Zhou, F. Zheng, H.-g. Li, C.-l. Lu, An environment-friendly thermal insulation material from cotton stalk fibers, Energy Build. 42 (7) (2010) 1070–1074, http://dx.doi.org/10.1016/j.enbuild.2010.01.020.
[158] C. Buratti, E. Belloni, E. Lascaro, F. Merli, P. Ricciardi, Rice husk panels for building applications: Thermal, acoustic and environmental characterization and comparison with other innovative recycled waste materials, Constr. Build. Mater. 171 (2018) 338–349, http://dx.doi.org/10.1016/j.conbuildmat.2018.03.089.
[159] V. Guna, M. Ilangovan, K. Adithya, C.A. Koushik, C. Srinivas, S. Yogesh, G. Nagananda, K. Venkatesh, N. Reddy, Biofibers and biocomposites from sabai grass: A unique renewable resource, Carbohydr. Polymers 218 (2019) 243–249, http://dx.doi.org/10.1016/j.carbpol.2019.04.085.
[160] H. Karaky, C. Maalouf, C. Bliard, A. Gacoin, M. Lachi, N. El Wakil, G. Polidori, Characterization of beet-pulp fiber reinforced potato starch biopolymer composites for building applications, Constr. Build. Mater. 203 (2019) 711–721, http://dx.doi.org/10.1016/j.conbuildmat.2019.01.127.
[161] H. Binici, O. Aksogan, C. Demirhan, Mechanical, thermal and acoustical characterizations of an insulation composite made of bio-based materials, Sustain. Cities Soc. 20 (2016) 17–26, http://dx.doi.org/10.1016/j.scs.2015.09.004.
[162] T. Luamkanchanaphan, S. Chotikaprakhan, S. Jarusombati, A study of physical, mechanical and thermal properties for thermal insulation from narrow-leaved cattail fibers, Apcbee Procedia 1 (2012) 46–52, http://dx.doi.org/10.1016/j.apcbee.2012.03.009.
[163] D.W. Yarbrough, K.E. Wilkes, P.A. Olivier, R.S. Graves, A. Vohra, Apparent thermal conductivity data and related information for rice hulls and crushed pecan shells, Therm. Conduct. 27 (2005) 222–230.
[164] F. Ardente, M. Beccali, M. Cellura, M. Mistretta, Building energy performance: a LCA case study of kenaf-fibres insulation board, Energy Build. 40 (1) (2008) 1–10, http://dx.doi.org/10.1016/j.enbuild.2006.12.009.
[165] Z. Jin, J. Li, Q. Wang, W. Su, X. Duan, Z. Tang, Characterization of multifunctional panels from jute fibers for interior wall covering, Ind. Crop. Prod. 167 (2021) 113530, http://dx.doi.org/10.1016/j.indcrop.2021.113530.
[166] J. Smardzewski, T. Kamisiński, D. Dziurka, R. Mirski, A. Majewski, A. Flach, A. Pilch, Sound absorption of wood-based materials, Holzforschung 69 (4) (2015) 431–439, http://dx.doi.org/10.1016/0003-682X(96)00013-8.
[167] A. Nandanwar, M. Kiran, K.C. Varadarajulu, et al., Influence of density on sound absorption coefficient of fibre board, Open J. Acoust. 7 (01) (2017) 1, http://dx.doi.org/10.4236/oja.2017.71001.
[168] M. Pedreño-Rojas, M. Morales-Conde, F. Pérez-Gálvez, C. Rodríguez-Liñán, Eco-efficient acoustic and thermal conditioning using false ceiling plates made from plaster and wood waste, J. Clean. Prod. 166 (2017) 690–705, http://dx.doi.org/10.1016/j.jclepro.2017.08.077.
[169] C.W. Kang, S.S. Jang, H.Y. Kang, C. Li, Sound absorption rate and sound transmission loss of CLT wall panels composed of larch square timber core and plywood cross band, J. Korean Wood Sci. Technol. 47 (1) (2019) 33–39, http://dx.doi.org/10.5658/WOOD.2019.47.1.33.
[170] H. Kolya, C.W. Kang, High acoustic absorption properties of hackberry compared to nine different hardwood species: A novel finding for acoustical engineers, Appl. Acoust. 169 (2020) 107475, http://dx.doi.org/10.1016/j.apacoust.2020.107475.
[171] S.-H. Park, M. Lee, P.-N. Seo, E. Kang, C.-W. Kang, Acoustical properties of wood fiberboards prepared with different densities and resin contents, BioResources 15 (3) (2020) 5291.
[172] Y. Cherradi, I.C. Rosca, C. Cerbu, H. Kebir, A. Guendouz, M. Benyoucef, Acoustic properties for composite materials based on alfa and wood fibers, Appl. Acoust. 174 (2021) 107759, http://dx.doi.org/10.1016/j.apacoust.2020.107759.
[173] T. Koizumi, N. Tsujiuchi, A. Adachi, The development of sound absorbing materials using natural bamboo fibers, WIT Trans. Built Environ. 59 (2002) 157–166, http://dx.doi.org/10.2495/HPS020161.
[174] J. Wong, W.S. Yeo, M. Paridah, Sound absorption properties of kenaf bamboo particleboard at various mixing ratio and density, in: AIP Conference Proceedings, vol. 1902, AIP Publishing, 2017, http://dx.doi.org/10.1063/1.5010618.
[175] Y. Kong, J. Wen, A. Huang, L. Zhou, Y. Xiao, Acoustic properties of glued laminated bamboo and spruce-pine-fir, Wood Mater. Sci. Eng. 18 (5) (2023) 1765–1779, http://dx.doi.org/10.1080/17480272.2023.2187318.
[176] D.J. Oldham, C.A. Egan, R.D. Cookson, Sustainable acoustic absorbers from the biomass, Appl. Acoust. 72 (6) (2011) 350–363, http://dx.doi.org/10.1016/j.apacoust.2010.12.009.
[177] A. Le, A. Gacoin, A. Li, T.H. Mai, N. El Wakil, Influence of various starch/hemp mixtures on mechanical and acoustical behavior of starch-hemp composite materials, Compos. Part B: Eng. 75 (2015) 201–211, http://dx.doi.org/10.1016/j.compositesb.2015.01.038.
[178] P.-A. Chabriac, E. Gourdon, P. Gle, A. Fabbri, H. Lenormand, Agricultural by-products for building insulation: Acoustical characterization and modeling to predict micro-structural parameters, Constr. Build. Mater. 112 (2016) 158–167, http://dx.doi.org/10.1016/j.conbuildmat.2016.02.162.
[179] R. Stapulionienė, R. Tupčiauskas, S. Vaitkus, S. Vėjelis, Development and investigation of thermal insulation from hemp-polylactide fibres, Eng. Struct. Technol. 8 (1) (2016) 23–30, http://dx.doi.org/10.3846/2029882X.2016.1158127.
[180] C. Piégay, P. Glé, E. Gourdon, E. Gourlay, S. Marceau, Acoustical model of vegetal wools including two types of fibers, Appl. Acoust. 129 (2018) 36–46, http://dx.doi.org/10.1016/j.apacoust.2017.06.021.
[181] S. Su, Y. Gao, X. Zhou, X. Xiong, Y. Wang, L. Lyu, Structure of waste hemp stalks and their sound absorbing properties, Polymers 14 (22) (2022) 4844, http://dx.doi.org/10.3390/polym14224844.
[182] B. Martínez, V. Mendizabal, M.B. Roncero, E. Bernat-Maso, L. Gil, Towards sustainable building solutions: Development of hemp shiv-based green insulation material, Constr. Build. Mater. 414 (2024) 134987, http://dx.doi.org/10.1016/j.conbuildmat.2024.134987.

[183] S. Sakamoto, Y. Takauchi, K. Yanagimoto, S. Watanabe, Study for sound absorbing materials of biomass tubule etc (measured result for rice straw, rice husks, and buckwheat husks), J. Environ. Eng. 6 (2) (2011) 352–364, http://dx.doi.org/10.1299/jee.6.352.
[184] H.S. Seddeq, N.M. Aly, A. Marwa A, M. Elshakankery, Investigation on sound absorption properties for recycled fibrous materials, J. Ind. Text. 43 (1) (2013) 56–73, http://dx.doi.org/10.1177/1528083712446956.
[185] M. Saadatnia, G. Ebrahimi, M. Tajvidi, Comparing sound absorption characteristic of acoustic boards made of aspen particles and different percentage of wheat and barely straws, in: 17th World Conference on Nondestructive Testing, 2008, pp. 25–28.
[186] C.-W. Kang, E.-S. Jang, S.-S. Jang, H.-Y. Kang, et al., Comparison of transfer function method and reverberation room method in measuring the sound absorption coefficient of rice straw particle mat, J. Korean Wood Sci. Technol. 46 (4) (2018) 362–367, http://dx.doi.org/10.5658/WOOD.2018.46.4.362.
[187] S. Liuzzi, C. Rubino, F. Martellotta, P. Stefanizzi, C. Casavola, G. Pappalettera, Characterization of biomass-based materials for building applications: The case of straw and olive tree waste, Ind. Crop. Prod. 147 (2020) 112229, http://dx.doi.org/10.1016/j.indcrop.2020.112229.
[188] S.T. Nguyen, N.D. Do, N.N.T. Thai, Q.B. Thai, H.K.P. Huynh, A.N. Phan, et al., Green aerogels from rice straw for thermal, acoustic insulation and oil spill cleaning applications, Mater. Chem. Phys. 253 (2020) 123363, http://dx.doi.org/10.1016/j.matchemphys.2020.123363.
[189] M. Lesiecki, J. Kawalerczyk, A. Derkowski, M. Wieruszewski, D. Dziurka, R. Mirski, Properties of lightweight insulating boards produced from triticale straw particles, Materials 16 (15) (2023) 5272, http://dx.doi.org/10.3390/ma16155272.
[190] H. Kolya, C.-W. Kang, Rice straw stems reveal higher sound absorption coefficient than crushed rice straw: a sustainable approach to the recycling of rice straw, Clean Technol. Environ. Policy 25 (10) (2023) 3219–3229, http://dx.doi.org/10.1007/s10098-023-02609-w.
[191] N. Mati-Baouche, H. de Baynast, P. Michaud, T. Dupont, P. Leclaire, Sound absorption properties of a sunflower composite made from crushed stem particles and from chitosan bio-binder, Appl. Acoust. 111 (2016) 179–187, http://dx.doi.org/10.1016/j.apacoust.2016.04.021.
[192] I. Oancea, C. Bujoreanu, M. Budescu, M. Benchea, C.M. Grădinaru, Considerations on sound absorption coefficient of sustainable concrete with different waste replacements, J. Clean. Prod. 203 (2018) 301–312, http://dx.doi.org/10.1016/j.jclepro.2018.08.273.
[193] M. Ali, Z. Al-Suhaibani, R. Almuzaiqer, K. Al-Salem, A. Nuhait, F. Algubllan, M. Al-Howaish, A. Aloraini, I. Alqahtani, Sunflower and watermelon seeds and their hybrids with pineapple leaf fibers as new novel thermal insulation and sound-absorbing materials, Polymers 15 (22) (2023) 4422, http://dx.doi.org/10.3390/polym15224422.
[194] C. Othmani, M. Taktak, A. Zain, T. Hantati, N. Dauchez, T. Elnady, T. Fakhfakh, M. Haddar, Acoustic characterization of a porous absorber based on recycled sugarcane wastes, Appl. Acoust. 120 (2017) 90–97, http://dx.doi.org/10.1016/j.apacoust.2017.01.010.
[195] S. Sharma, S. Shukla, A. Sethy, Acoustical behaviour of natural fibres-based composite boards as sound-absorbing materials, J. Indian Acad. Wood Sci. 17 (2020) 66–72, http://dx.doi.org/10.1007/s13196-020-00255-z.
[196] N.M. Isa, A.Z.A. Wahid, A study of sugarcane bagasse and wood dust as acoustic panel in building, Prog. Eng. Appl. Technol. 2 (1) (2021) 319–327.
[197] E. Taban, S. Amininasab, S. Mehrzad, M. Fattahi, L. Tajik, S.E. Samaei, Comparison of experimental and empirical approaches for determination of sound absorption properties of bagasse and cornhusk fibers, J. Nat. Fibers 19 (14) (2022) 9024–9038, http://dx.doi.org/10.1080/15440478.2021.1982108.
[198] M.H. Beheshti, A. Firoozi, M. Jafarizaveh, A. Tabrizi, Acoustical and thermal characterization of insulating materials made from wool and sugarcane bagasse, J. Nat. Fibers 20 (2) (2023) 2237675, http://dx.doi.org/10.1080/15440478.2023.2237675.
[199] M. Haghighat, S.E. Samaei, S. Amininasab, M. Faridan, S. Mehrzad, M.J. Sheikhmozafari, E. Taban, The impact of fiber size on the sound absorption behavior of composites made from sugarcane bagasse wastes fibers, J. Nat. Fibers 20 (1) (2023) 2175760, http://dx.doi.org/10.1080/15440478.2023.2175760.
[200] V. Puyana-Romero, J.S.A. Chuquín, S.I.M. Chicaiza, G. Ciaburro, Characterization and simulation of acoustic properties of sugarcane bagasse-based composite using artificial neural network model, Fibers 11 (2) (2023) 18, http://dx.doi.org/10.3390/fib11020018.
[201] M. Kaamin, N.F.M. Zaid, M.E. Daud, R. Rahman, H. Mubarak, Analysis on absorption sound acoustic panels from egg tray with corn husk and sugar cane, Int. J. Innov. Technol. Explor. Eng. 8 (2019) 1426–1431, http://dx.doi.org/10.35940/ijitee.I3304.0789S319.
[202] P. Ricciardi, F. Torchia, E. Belloni, E. Lascaro, C. Buratti, Environmental characterisation of coffee chaff, a new recycled material for building applications, Constr. Build. Mater. 147 (2017) 185–193, http://dx.doi.org/10.1016/j.conbuildmat.2017.04.114.
[203] D. Balasubramanian, S. Rajendran, B. Srinivasan, N. Angamuthu, Elucidating the sound absorption characteristics of foxtail millet (setariaitalica) husk, Materials 13 (22) (2020) 5126, http://dx.doi.org/10.3390/ma13225126.
[204] B. Marques, A. Tadeu, J. António, J. Almeida, J. de Brito, Mechanical, thermal and acoustic behaviour of polymer-based composite materials produced with rice husk and expanded cork by-products, Constr. Build. Mater. 239 (2020) 117851, http://dx.doi.org/10.1016/j.conbuildmat.2019.117851.
[205] S. Etemadinezhad, S.E. Samaei, E. Taban, M. Faridan, Experimental and theoretical investigation of the acoustic absorbers fabricated from natural kenaf fibres and rice husk, J. Nat. Fibers 19 (16) (2022) 15045–15057, http://dx.doi.org/10.1080/15440478.2022.2069635.
[206] A.A. Abdullah Alabdulkarem, M.A. Mohamed Ali, G. Iannace, S.S. Shereef Sadek, R.A. Redhwan Almuzaiqer, Thermal analysis, microstructure and acoustic characteristics of some hybrid natural insulating materials, 2018, http://dx.doi.org/10.1016/j.conbuildmat.2018.07.213.
[207] R. Belakroum, A. Gherfi, K. Bouchema, A. Gharbi, Y. Kerboua, M. Kadja, C. Maalouf, T.H. Mai, N. El Wakil, M. Lachi, Hygric buffer and acoustic absorption of new building insulation materials based on date palm fibers, J. Build. Eng. 12 (2017) 132–139, http://dx.doi.org/10.1016/j.jobe.2017.05.011.
[208] C.C. Ferrandez-Garcia, C.E. Ferrandez-Garcia, M. Ferrandez-Villena, M.T. Ferrández-García, T. Garcia-Ortuno, Acoustic and thermal evaluation of palm panels as building material, BioResources 12 (4) (2017) 8047–8057.
[209] E.M. Samsudin, L.H. Ismail, A. Kadir, I.N. Nasidi, Thickness, density and porosity relationship towards sound absorption performance of mixed palm oil fibers, in: Proceedings of the 24th International Congress on Sound and Vibration, ICSV 24, London, UK, 2017, pp. 23–27.
[210] R. Kalaivani, L. Ewe, O. Zaroog, H. Woon, Z. Ibrahim, et al., Acoustic properties of natural fiber of oil palm trunk, Int. J. Adv. Appl. Sci. 5 (6) (2018) 88–92, http://dx.doi.org/10.21833/ijaas.2018.06.013.
[211] E. Taban, A. Khavanin, M. Faridan, S. Samaei, K. Samimi, R. Rashidi, Comparison of acoustic absorption characteristics of coir and date palm fibers: experimental and analytical study of green composites, Int. J. Environ. Sci. Technol. 17 (2020) 39–48, http://dx.doi.org/10.1007/s13762-019-02304-8.
[212] E. Taban, S. Amininasab, P. Soltani, U. Berardi, D.D. Abdi, S.E. Samaei, Use of date palm waste fibers as sound absorption material, J. Build. Eng. 41 (2021) 102752, http://dx.doi.org/10.1016/j.jobe.2021.102752.
[213] P. Chanlert, S. Tongyoo, C. Rordrak, Effects of urea–formaldehyde and polyvinyl acetate adhesive on sound absorption coefficient and sound transmission loss of palmyra palm fruit fiber composites, Appl. Acoust. 198 (2022) 108984, http://dx.doi.org/10.1016/j.apacoust.2022.108984.
[214] E. Darwish, M. Midani, The potential of date palm midribs-based fabric acoustic panels for sustainable interior design, Ain Shams Eng. J. 14 (6) (2023) 102100, http://dx.doi.org/10.1016/j.asej.2022.102100.
[215] B. Istana, I.M.L. Batan, Sutikno, S. Khem, U. Ubaidillah, I. Yahya, Influence of particle size and bulk density on sound absorption performance of oil palm frond-reinforced composites particleboard, Polymers 15 (3) (2023) 510, http://dx.doi.org/10.3390/polym15030510.
[216] M. Ali, Z. Al-Suhaibani, R. Almuzaiqer, A. Albahbooh, K. Al-Salem, A. Nuhait, New composites derived from the natural fiber polymers of discarded date palm surface and pineapple leaf fibers for thermal insulation and sound absorption, Polymers 16 (7) (2024) 1002, http://dx.doi.org/10.3390/polym16071002.
[217] M. Ali, Microstructure, thermal analysis and acoustic characteristics of calotropis procera (apple of sodom) fibers, J. Nat. Fibers 13 (3) (2016) 343–352, http://dx.doi.org/10.1080/15440478.2015.1029198.
[218] M. Rusli, M. Irsyad, H. Dahlan, M. Bur, et al., Sound absorption characteristics of the natural fibrous material from coconut coir, oil palm fruit bunches, and pineapple leaf, in: IOP Conference Series: Materials Science and Engineering, vol. 602, IOP Publishing, 2019, 012067, http://dx.doi.org/10.1088/1757-899X/602/1/012067.

[219] C.O.B. Mendes, M.A. de Araújo Nunes, Acoustic performance of the banana pseudostem fiber, Appl. Acoust. 191 (2022) 108657, http://dx.doi.org/10.1016/j.apacoust.2022.108657.
[220] J.P. Arenas, R. del Rey, J. Alba, R. Oltra, Sound-absorption properties of materials made of esparto grass fibers, Sustainability 12 (14) (2020) 5533, http://dx.doi.org/10.3390/su12145533.
[221] X. Liu, X. Xiong, J. Pang, L. Wu, H. Zhang, Airflow resistivity measurement and sound absorption performance analysis of sound-absorb cotton, Appl. Acoust. 179 (2021) 108060, http://dx.doi.org/10.1016/j.apacoust.2021.108060.
[222] M.T. Ferrandez-García, A. Ferrandez-Garcia, T. Garcia-Ortuño, C.E. Ferrandez-Garcia, M. Ferrandez-Villena, Assessment of the physical, mechanical and acoustic properties of Arundo donax L. biomass in low pressure and temperature particleboards, Polymers 12 (6) (2020) 1361, http://dx.doi.org/10.3390/polym12061361.
[223] F. D'Alessandro, G. Pispola, Sound absorption properties of sustainable fibrous materials in an enhanced reverberation room, in: INTER-NOISE and NOISE-CON Congress and Conference Proceedings, vol. 2005, Institute of Noise Control Engineering, 2005, pp. 2209–2218.
[224] E. Taban, F. Valipour, D. Abdi, S. Amininasab, Mathematical and experimental investigation of sound absorption behavior of sustainable kenaf fiber at low frequency, Int. J. Environ. Sci. Technol. 18 (2021) 2765–2780, http://dx.doi.org/10.1007/s13762-020-03024-0.
[225] I.N. Nasidi, L.H. Ismail, E. Samsudin, M.I. Jaffar, Effects of kenaf fiber strand treatment by sodium hydroxide on sound absorption, J. Nat. Fibers 19 (13) (2022) 6727–6736, http://dx.doi.org/10.1080/15440478.2021.1932670.
[226] S.E. Samaei, E. Taban, U. Berardi, S.M. Mousavi, M. Faridan, A. Hassan, Optimization and modeling of sound-absorption properties of natural fibers for acoustical application, J. Nat. Fibers 19 (13) (2022) 7157–7173, http://dx.doi.org/10.1080/15440478.2021.1944429.
[227] M. Raj, S. Fatima, N. Tandon, Recycled materials as a potential replacement to synthetic sound absorbers: A study on denim shoddy and waste jute fibers, Appl. Acoust. 159 (2020) 107070, http://dx.doi.org/10.1016/j.apacoust.2019.107070.
[228] Y. Liu, L. Lyu, J. Guo, Y. Wang, Sound absorption performance of the poplar seed fiber/PCL composite materials, Materials 13 (6) (2020) 1465, http://dx.doi.org/10.3390/ma13061465.
[229] M. Raj, S. Fatima, N. Tandon, A study of areca nut leaf sheath fibers as a green sound-absorbing material, Appl. Acoust. 169 (2020) 107490, http://dx.doi.org/10.1016/j.apacoust.2020.107490.
[230] U.A. Malawade, V.V. Malgaonkar, A.M. Badadhe, M.G. Jadhav, Utilization and study of raw groundnut shell as a source of sound absorbing material, J. Nat. Fibers 19 (13) (2022) 6335–6347, http://dx.doi.org/10.1080/15440478.2021.1916673.
[231] M. Olivares-Marín, S. Román, V.G. Escobar, C.M. González, A. Chaves-Zapata, B. Ledesma, Thermal performance and sound absorption capability of water hyacinth stems-based materials, J. Clean. Prod. 425 (2023) 138903, http://dx.doi.org/10.1016/j.jclepro.2023.138903.
[232] Y. Chen, F. Yuan, Q. Su, C. Yu, K. Zhang, P. Luo, D. Hu, Y. Guo, A novel sound absorbing material comprising discarded luffa scraps and polyester fibers, J. Clean. Prod. 245 (2020) 118917, http://dx.doi.org/10.1016/j.jclepro.2019.118917.
[233] H.-f. Xiang, D. Wang, H.-c. Liua, N. Zhao, J. Xu, Investigation on sound absorption properties of kapok fibers, Chin. J. Polym. Sci. 31 (3) (2013) 521–529, http://dx.doi.org/10.1007/s10118-013-1241-8.
[234] M.H. Fouladi, M. Ayub, M.J.M. Nor, Analysis of coir fiber acoustical characteristics, Appl. Acoust. 72 (1) (2011) 35–42, http://dx.doi.org/10.1016/j.apacoust.2010.09.007.
[235] E. Taban, A. Tajpoor, M. Faridan, S.E. Samaei, M.H. Beheshti, Acoustic absorption characterization and prediction of natural coir fibers, Acoust. Aust. 47 (2019) 67–77, http://dx.doi.org/10.1007/s40857-019-00151-8.
[236] C.-W. Kang, S.-W. Oh, T.-B. Lee, W. Kang, J. Matsumura, Sound absorption capability and mechanical properties of a composite rice hull and sawdust board, J. Wood Sci. 58 (2012) 273–278, http://dx.doi.org/10.1007/s10086-011-1243-5.
[237] R. Bergman, M. Puettmann, A. Taylor, K.E. Skog, The carbon impacts of wood products, For. Prod. J. 64 (7–8) (2014) 220–231.
[238] C. Martínez-Alonso, L. Berdasco, Carbon footprint of sawn timber products of Castanea sativa Mill. in the north of Spain, J. Clean. Prod. 102 (2015) 127–135, http://dx.doi.org/10.1016/j.jclepro.2015.05.004.
[239] W.-L. Lao, W.-G. Li, Comparative carbon footprint estimation of three types of wooden door: A case study from China, J. Clean. Prod. 433 (2023) 139745, http://dx.doi.org/10.1016/j.jclepro.2023.139745.
[240] C.M. Ouellet-Plamondon, L. Ramseier, M. Balouktsi, L. Delem, G. Foliente, N. Francart, A. Garcia-Martinez, E. Hoxha, T. Lützkendorf, F.N. Rasmussen, et al., Carbon footprint assessment of a wood multi-residential building considering biogenic carbon, J. Clean. Prod. 404 (2023) 136834, http://dx.doi.org/10.1016/j.jclepro.2023.136834.
[241] W.-L. Lao, Y.-m. Han, et al., Carbon footprint as an environmental indicator for wood flooring industry in China, Case Stud. Constr. Mater. (2024) e03594, http://dx.doi.org/10.1016/j.cscm.2024.e03594.
[242] S. Yan, F. Shi, C. Zheng, Y. Ma, J. Huang, Whole biomass material envelope system for nearly-zero energy houses: Carbon footprint and construction cost assessment, J. Build. Eng. 86 (2024) 108757, http://dx.doi.org/10.1016/j.jobe.2024.108757.
[243] Y. Xiao, R. Yang, B. Shan, Production, environmental impact and mechanical properties of glubam, Constr. Build. Mater. 44 (2013) 765–773, http://dx.doi.org/10.1016/j.conbuildmat.2013.03.087.
[244] L.-C. Assessment, The environmental impact of industrial bamboo products, 2015.
[245] P. van der Lugt, J. Vogtländer, J. Van Der Vegte, J. Brezet, Environmental assessment of industrial bamboo products—life cycle assessment and carbon sequestration, in: 10th World Bamboo Congress, World Bamboo Organization, 2015, pp. 1–16.
[246] Á. Restrepo, R. Becerra, et al., Energetic and carbon footprint analysis in manufacturing process of bamboo boards in Colombia, J. Clean. Prod. 126 (2016) 563–571, http://dx.doi.org/10.1016/j.jclepro.2016.02.144.
[247] P. van der Lugt, D.E. Hebel, F. Heisel, in: D. Hebel, F. Heisel (Eds.), 'Engineered Bamboo Products-A Sustainable Choice?', 2017, pp. 86–95.
[248] F.-C. Chang, K.-S. Chen, P.-Y. Yang, C.-H. Ko, Environmental benefit of utilizing bamboo material based on life cycle assessment, J. Clean. Prod. 204 (2018) 60–69, http://dx.doi.org/10.1016/j.jclepro.2018.08.248.
[249] V.T. Phuong, N.V. Xuan, Life Cycle Assessment for Key Bamboo Products inViet Nam, International Network for Bamboo and Rattan (INBAR), Beijing, 2020.
[250] J. Gan, M. Chen, K. Semple, X. Liu, C. Dai, Q. Tu, Life cycle assessment of bamboo products: Review and harmonization, Sci. Total Environ. 849 (2022) 157937, http://dx.doi.org/10.1016/j.scitotenv.2022.157937.
[251] A. Ibrahim, S. Withaningsih, et al., Life cycle analysis of carbon footprint and carbon stored on tali bamboo (gigantochloa apus (JA & JH schultes) kurz) products using life cycle assessment approach, in: IOP Conference Series: Earth and Environmental Science, vol. 1211, IOP Publishing, 2023, 012011, http://dx.doi.org/10.1088/1755-1315/1211/1/012011.
[252] Y. Zhao, Z. Lou, Q. Wang, T. Yuan, M. Chen, H. Han, X. Wu, L. Xu, Y. Li, Fabrication of a bamboo-based glulam based on reconstitution unit innovation: mechanical property investigation and carbon footprint evaluation, Ind. Crop. Prod. 202 (2023) 117046, http://dx.doi.org/10.1016/j.indcrop.2023.117046.
[253] Y. Zhao, L. Liu, M. Yu, Comparison and analysis of carbon emissions of traditional, prefabricated, and green material buildings in materialization stage, J. Clean. Prod. 406 (2023) 137152, http://dx.doi.org/10.1016/j.jclepro.2023.137152.
[254] M. Zhang, G. Zhou, L. Gu, W. Wang, Grading of products utilizing bamboo as a substitute for plastic based on environmental effects, Sci. China Earth Sci. (2024) 1–10, http://dx.doi.org/10.1007/s11430-023-1387-x.
[255] K. Ip, A. Miller, Life cycle greenhouse gas emissions of hemp–lime wall constructions in the UK, Resour. Conserv. Recycl. 69 (2012) 1–9, http://dx.doi.org/10.1016/j.resconrec.2012.09.001.

[256] L. Zampori, G. Dotelli, V. Vernelli, Life cycle assessment of hemp cultivation and use of hemp-based thermal insulator materials in buildings, Environ. Sci. Technol. 47 (13) (2013) 7413–7420, http://dx.doi.org/10.1021/es401326a.

[257] S. Pretot, F. Collet, C. Garnier, Life cycle assessment of a hemp concrete wall: Impact of thickness and coating, Build. Environ. 72 (2014) 223–231, http://dx.doi.org/10.1016/j.buildenv.2013.11.010.

[258] A. Arrigoni, R. Pelosato, P. Melià, G. Ruggieri, S. Sabbadini, G. Dotelli, Life cycle assessment of natural building materials: the role of carbonation, mixture components and transport in the environmental impacts of hempcrete blocks, J. Clean. Prod. 149 (2017) 1051–1061, http://dx.doi.org/10.1016/j.jclepro.2017.02.161.

[259] N. de Beus, M. Carus, M. Barth, Carbon footprint and sustainability of different natural fibres for biocomposites and insulation material, 2019, Study providing data for the automotive and insulation industry.

[260] F. Scrucca, C. Ingrao, C. Maalouf, T. Moussa, G. Polidori, A. Messineo, C. Arcidiacono, F. Asdrubali, Energy and carbon footprint assessment of production of hemp hurds for application in buildings, Environ. Impact Assess. Rev. 84 (2020) 106417, http://dx.doi.org/10.1016/j.eiar.2020.106417.

[261] D. Rivas-Aybar, M. John, W. Biswas, Environmental life cycle assessment of a novel hemp-based building material, Materials 16 (22) (2023) 7208, http://dx.doi.org/10.3390/ma16227208.

[262] J. Boonniteewanich, S. Pitivut, S. Tongjoy, S. Lapnonkawow, S. Suttiruengwong, Evaluation of carbon footprint of bioplastic straw compared to petroleum based straw products, Energy Procedia 56 (2014) 518–524, http://dx.doi.org/10.1016/j.egypro.2014.07.187.

[263] A.D. González, Energy and carbon embodied in straw and clay wall blocks produced locally in the Andean Patagonia, Energy Build. 70 (2014) 15–22, http://dx.doi.org/10.1016/j.enbuild.2013.11.003.

[264] N. Sun, C. Gao, Y. Ding, Y. Bi, P.A. Seglah, Y. Wang, Five-dimensional straw utilization model and its impact on carbon emission reduction in China, Sustainability 14 (24) (2022) 16722, http://dx.doi.org/10.3390/su142416722.

[265] Y. Sun, B. Yang, Y. Wang, Z. Zheng, J. Wang, Y. Yue, W. Mu, Carbon footprint analysis of straw collection, transportation, and storage system for power generation in China based on emergy evaluation, Environ. Sci. Pollut. Res. 29 (44) (2022) 66922–66934, http://dx.doi.org/10.1007/s11356-022-20525-2.

[266] R. Guo, R. Qian, M.A. Naseer, F. Han, P. Zhang, Z. Jia, X. Chen, X. Ren, Integrated straw-derived biochar utilization to increase net ecosystem carbon budget and economic benefit and reduce the environmental footprint, Field Crop. Res. 307 (2024) 109247, http://dx.doi.org/10.1016/j.fcr.2023.109247.

[267] D. Chiaramonti, L. Recchia, Is life cycle assessment (LCA) a suitable method for quantitative CO2 saving estimations? The impact of field input on the LCA results for a pure vegetable oil chain, Biomass Bioenergy 34 (5) (2010) 787–797, http://dx.doi.org/10.1016/j.biombioe.2010.01.022.

[268] A. Iriarte, J. Rieradevall, X. Gabarrell, Life cycle assessment of sunflower and rapeseed as energy crops under Chilean conditions, J. Clean. Prod. 18 (4) (2010) 336–345, http://dx.doi.org/10.1016/j.jclepro.2009.11.004.

[269] S. Eady, P. Sanguansri, R. Bektash, B. Ridoutt, L. Simons, P. Swiergon, Carbon foot-print for Australian agricultural products and downstream food products in the supermarket, in: 7th Australian Conf. on Life Cycle Assessment, Melbourne, Australia, 9–10 March 2011, 2011.

[270] P. Goglio, E. Bonari, M. Mazzoncini, LCA of cropping systems with different external input levels for energetic purposes, Biomass Bioenergy 42 (2012) 33–42, http://dx.doi.org/10.1016/j.biombioe.2012.03.021.

[271] P. Spugnoli, R. Dainelli, L. D'Avino, M. Mazzoncini, L. Lazzeri, Sustainability of sunflower cultivation for biodiesel production in tuscany within the EU renewable energy directive, Biosyst. Eng. 112 (1) (2012) 49–55, http://dx.doi.org/10.1016/j.biosystemseng.2012.02.004.

[272] D. Spinelli, S. Jez, R. Pogni, R. Basosi, Environmental and life cycle analysis of a biodiesel production line from sunflower in the province of siena (Italy), Energy Policy 59 (2013) 492–506, http://dx.doi.org/10.1016/j.enpol.2013.04.009.

[273] F. Al-Mansour, V. Jejcic, Carbon footprint of conventional and organic crops production on family farms in Slovenia, in: Book of Abstracts of the 1st South East European Conference on Sustainable Development of Energy, Water and Environment Systems, Ohrid, Republic of Macedonia, vol. 29, 2014.

[274] F. Al-Mansour, V. Jejcic, A model calculation of the carbon footprint of agricultural products: The case of Slovenia, Energy 136 (2017) 7–15, http://dx.doi.org/10.1016/j.energy.2016.10.099.

[275] F. Figueiredo, É.G. Castanheira, F. Freire, Life-cycle assessment of irrigated and rainfed sunflower addressing uncertainty and land use change scenarios, J. Clean. Prod. 140 (2017) 436–444, http://dx.doi.org/10.1016/j.jclepro.2016.06.151.

[276] M.B. Forleo, N. Palmieri, A. Suardi, D. Coaloa, L. Pari, The eco-efficiency of rapeseed and sunflower cultivation in Italy. joining environmental and economic assessment, J. Clean. Prod. 172 (2018) 3138–3153, http://dx.doi.org/10.1016/j.jclepro.2017.11.094.

[277] W. Liu, G. Zhang, X. Wang, F. Lu, Z. Ouyang, Carbon footprint of main crop production in China: Magnitude, spatial-temporal pattern and attribution, Sci. Total Environ. 645 (2018) 1296–1308, http://dx.doi.org/10.1016/j.scitotenv.2018.07.104.

[278] M. Yuttitham, S.H. Gheewala, A. Chidthaisong, Carbon footprint of sugar produced from sugarcane in eastern Thailand, J. Clean. Prod. 19 (17–18) (2011) 2119–2127, http://dx.doi.org/10.1016/j.jclepro.2011.07.017.

[279] C.A. García, E.S. García-Treviño, N. Aguilar-Rivera, C. Armendáriz, Carbon footprint of sugar production in Mexico, J. Clean. Prod. 112 (2016) 2632–2641, http://dx.doi.org/10.1016/j.jclepro.2015.09.113.

[280] F. Mohammadi, A. Roedl, M.A. Abdoli, M. Amidpour, H. Vahidi, Life cycle assessment (LCA) of the energetic use of bagasse in Iranian sugar industry, Renew. Energy 145 (2020) 1870–1882, http://dx.doi.org/10.1016/j.renene.2019.06.023.

[281] M. Hiloidhari, V. Vijay, R. Banerjee, D. Baruah, A.B. Rao, Energy-carbon-water footprint of sugarcane bioenergy: A district-level life cycle assessment in the state of maharashtra, India, Renew. Sustain. Energy Rev. 151 (2021) 111583, http://dx.doi.org/10.1016/j.rser.2021.111583.

[282] P. Khatri, A.B. Pandit, Systematic review of life cycle assessments applied to sugarcane bagasse utilization alternatives, Biomass Bioenergy 158 (2022) 106365, http://dx.doi.org/10.1016/j.biombioe.2022.106365.

[283] P.T.M. Thao, K.H. Kurisu, K. Hanaki, Greenhouse gas emission mitigation potential of rice husks for An Giang province, Vietnam, Biomass Bioenergy 35 (8) (2011) 3656–3666, http://dx.doi.org/10.1016/j.biombioe.2011.05.023.

[284] A. Mellado, C. Catalán, N. Bouzón, M. Borrachero, J. Monzó, J. Payá, Carbon footprint of geopolymeric mortar: study of the contribution of the alkaline activating solution and assessment of an alternative route, RSC Adv. 4 (45) (2014) 23846–23852, http://dx.doi.org/10.1039/C4RA03375B.

[285] E.A. Christoforou, P.A. Fokaides, Life cycle assessment (LCA) of olive husk torrefaction, Renew. Energy 90 (2016) 257–266, http://dx.doi.org/10.1016/j.renene.2016.01.022.

[286] L. Caldas, M. da Gloria, D. Santos, V. Andreola, M. Pepe, R. Toledo Filho, Carbon footprint of bamboo particles, rice husk and wood shavings-cement composites, Acad. J. Civ. Eng. 35 (2) (2017) 499–506, http://dx.doi.org/10.26168/iccbm2017.76.

[287] M.Á. Hidalgo-Salazar, J.P. Correa-Aguirre, J.M. Montalvo-Navarrete, D.F. Lopez-Rodriguez, A.F. Rojas-González, Recycled polypropylene-coffee husk and coir coconut biocomposites: morphological, mechanical, thermal and environmental studies, Thermosoftening Plast. (2018) http://dx.doi.org/10.5772/intechopen.81635.

[288] L. Hu, Z. He, S. Zhang, Sustainable use of rice husk ash in cement-based materials: Environmental evaluation and performance improvement, J. Clean. Prod. 264 (2020) 121744, http://dx.doi.org/10.1016/j.jclepro.2020.121744.

[289] D. Shoji, Z. He, D. Zhang, V.C. Li, The greening of engineered cementitious composites (ECC): A review, Constr. Build. Mater. 327 (2022) 126701, http://dx.doi.org/10.1016/j.conbuildmat.2022.126701.

[290] M. Zheng, K. Zhang, J. Zhang, L. Zhu, G. Du, R. Zheng, Cheap, high yield, and strong corn husk-based textile bio-fibers with low carbon footprint via green alkali retting-splicing-twisting strategy, Ind. Crop. Prod. 188 (2022) 115699, http://dx.doi.org/10.1016/j.indcrop.2022.115699.

[291] M.A. Thomas-Vallejo, L.R. Conde-Rivera, A.F. Suárez-Escobar, Influence of cocoa bean husk and coffee husk composition on bio-oil yield and life cycle assessment in fast pyrolysis, in: Contributions of Chemical Engineering To Sustainability, Springer, 2024, pp. 221–257, http://dx.doi.org/10.1007/978-3-031-55594-7_8.

[292] C. Bessou, L.D. Chase, I.E. Henson, A.F. Abdul-Manan, L.M. i Canals, F. Agus, M. Sharma, M. Chin, Pilot application of palmghg, the roundtable on sustainable palm oil greenhouse gas calculator for oil palm products, J. Clean. Prod. 73 (2014) 136–145, http://dx.doi.org/10.1016/j.jclepro.2013.12.008.

[293] Y.D. Rivera-Méndez, D.T. Rodríguez, H.M. Romero, Carbon footprint of the production of oil palm (Elaeis guineensis) fresh fruit bunches in Colombia, J. Clean. Prod. 149 (2017) 743–750, http://dx.doi.org/10.1016/j.jclepro.2017.02.149.

[294] Z. Hashim, V. Subramaniam, M.H. Harun, N. Kamarudin, Carbon footprint of oil palm planted on peat in Malaysia, Int. J. Life Cycle Assess. 23 (2018) 1201–1217, http://dx.doi.org/10.1007/s11367-017-1367-y.

[295] F. Farizal, T. Amanda, M. Dachyar, Z.Z. Noor, 2030 oil palm plantation carbon footprint estimation using O-LCA and forecasting, J. Clean. Prod. 463 (2024) 142646, http://dx.doi.org/10.1016/j.jclepro.2024.142646.

[296] A. Islam, U.J. Alengaram, M.Z. Jumaat, I.I. Bashar, S.A. Kabir, Engineering properties and carbon footprint of ground granulated blast-furnace slag-palm oil fuel ash-based structural geopolymer concrete, Constr. Build. Mater. 101 (2015) 503–521, http://dx.doi.org/10.1016/j.conbuildmat.2015.10.026.

[297] J. Saleem, F. Tahir, M.Z.K. Baig, G. McKay, Environmental impacts of activated carbon flakes from palm fiber and polyolefin wastes using life cycle assessment, Mater. Today: Proc. (2024) http://dx.doi.org/10.1016/j.matpr.2024.05.146.

[298] L. Laasri, H. Naim, Evaluation of environmental impact of palm-fiber based geotextile using a life cycle method, Key Eng. Mater. 925 (2022) 9–16, http://dx.doi.org/10.4028/p-s4qw4k.

[299] D.A. Munar, N. Ramírez-Contreras, Y. Rivera-Méndez, J.A. Garcia-Nuñez, H.M. Romero, Carbon footprint management for a sustainable oil palm crop, in: Advances of Footprint Family for Sustainable Energy and Industrial Systems, Springer, 2021, pp. 93–110, http://dx.doi.org/10.1007/978-3-030-76441-8_5.

[300] C. Skinner, M. Jawaid, B. Singh, A. Alzahri, R. Elias, H. Fouad, M. Hashem, Life cycle assessment of pulp-moulded and thermoformed oil palm fibre-based food tray, Discov. Appl. Sci. 6 (12) (2024) 632, http://dx.doi.org/10.1007/s42452-024-06335-w.

[301] A.S. Muntohar, M.E. Rahman, Lightweight masonry block from oil palm kernel shell, Constr. Build. Mater. 54 (2014) 477–484, http://dx.doi.org/10.1016/j.conbuildmat.2013.12.087.

[302] S.S. Sinoh, Z. Ibrahim, F. Othman, Life cycle assessment of palm oil clinker as a binder and aggregate replacement in concrete, J. Oil Palm Res. 33 (1) (2021) 151–170, http://dx.doi.org/10.21894/jopr.2020.0081.

[303] A.Y.Y. Chow, A.M.N. Aman, A. Selvarajoo, Life cycle assessment of palm oil waste biochar as a partial cement replacement in concrete production in Malaysia, IEM J. 86 (2) (2025) http://dx.doi.org/10.54552/v86i2.272.

[304] S. Schiavoni, F. Bianchi, F. Asdrubali, et al., Insulation materials for the building sector: A review and comparative analysis, Renew. Sustain. Energy Rev. 62 (2016) 988–1011, http://dx.doi.org/10.1016/j.rser.2016.05.045.

[305] J. Korol, A. Hejna, D. Burchart-Korol, J. Wachowicz, Comparative analysis of carbon, ecological, and water footprints of polypropylene-based composites filled with cotton, jute and kenaf fibers, Materials 13 (16) (2020) 3541, http://dx.doi.org/10.3390/ma13163541.

[306] L. Operato, L. Vitiello, P. Aprea, V. Ambrogi, M.S. de Luna, G. Filippone, Life cycle assessment of poly (lactic acid)-based green composites filled with pine needles or kenaf fibers, J. Clean. Prod. 387 (2023) 135901, http://dx.doi.org/10.1016/j.jclepro.2023.135901.

[307] M. Shadhin, M. Rahman, R. Jayaraman, Y. Chen, D. Mann, W. Zhong, Natural biomass & waste biomass fibers–structures, environmental footprints, sustainability, degumming methods, & surface modifications, Ind. Crop. Prod. 204 (2023) 117252, http://dx.doi.org/10.1016/j.indcrop.2023.117252.

[308] A.K. Singh, S. Aboo, T. Goswami, G. Kar, Jute and kenaf carrier bags: an eco-friendly alternative to plastic bags in India, Environ. Sci. Pollut. Res. 30 (22) (2023) 61904–61912, http://dx.doi.org/10.1007/s11356-023-26436-0.

[309] L.M. i Canals, G. Burnip, S. Cowell, Evaluation of the environmental impacts of apple production using life cycle assessment (LCA): case study in New Zealand, Agric. Ecosyst. Environ. 114 (2–4) (2006) 226–238, http://dx.doi.org/10.1016/j.agee.2005.10.023.

[310] Y. Liu, V. Langer, H. Høgh-Jensen, H. Egelyng, Life cycle assessment of fossil energy use and greenhouse gas emissions in Chinese pear production, J. Clean. Prod. 18 (14) (2010) 1423–1430, http://dx.doi.org/10.1016/j.jclepro.2010.05.025.

[311] S. Bosco, C. Di Bene, M. Galli, D. Remorini, R. Massai, E. Bonari, et al., Greenhouse gas emissions in the agricultural phase of wine production in the maremma rural district (tuscany, Italy), Ital. J. Agron. 6 (2011) 93–100, http://dx.doi.org/10.4081/ija.2011.e15.

[312] W.W. Ingwersen, Life cycle assessment of fresh pineapple from costa rica, J. Clean. Prod. 35 (2012) 152–163, http://dx.doi.org/10.1016/j.jclepro.2012.05.035.

[313] F. Stoessel, R. Juraske, S. Pfister, S. Hellweg, Life cycle inventory and carbon and water foodprint of fruits and vegetables: application to a Swiss retailer, Environ. Sci. Technol. 46 (6) (2012) 3253–3262, http://dx.doi.org/10.1021/es2030577.

[314] V.D. Litskas, C.S. Karaolis, G.C. Menexes, A.P. Mamolos, T.M. Koutsos, K.L. Kalburtji, Variation of energy flow and greenhouse gas emissions in vineyards located in Natura 2000 sites, Ecol. Indic. 27 (2013) 1–7, http://dx.doi.org/10.1016/j.ecolind.2012.11.016.

[315] M. Yan, K. Cheng, Q. Yue, Y. Yan, R.M. Rees, G. Pan, Farm and product carbon footprints of China's fruit production—life cycle inventory of representative orchards of five major fruits, Environ. Sci. Pollut. Res. 23 (2016) 4681–4691, http://dx.doi.org/10.1007/s11356-015-5670-5.

[316] V.D. Litskas, T. Irakleous, N. Tzortzakis, M.C. Stavrinides, Determining the carbon footprint of indigenous and introduced grape varieties through life cycle assessment using the island of cyprus as a case study, J. Clean. Prod. 156 (2017) 418–425, http://dx.doi.org/10.1016/j.jclepro.2017.04.057.

[317] A. Iriarte, P. Yáñez, P. Villalobos, C. Huenchuleo, R. Rebolledo-Leiva, Carbon footprint of southern hemisphere fruit exported to Europe: The case of Chilean apple to the UK, J. Clean. Prod. 293 (2021) 126118, http://dx.doi.org/10.1016/j.jclepro.2021.126118.

[318] G.E. Sherwood, R.C. Stroh, Wood-Frame House Construction, Courier Corporation, 1990.

[319] R. Ye, J. Wang, H. Jiang, N. Xie, Numerical study on thermal comfort and energy-saving potential of a prefabricated temporary house integrated with composite phase change materials, Energy Build. 268 (2022) 112169, http://dx.doi.org/10.1016/j.enbuild.2022.112169.

[320] JGJ/T 188-2009, Technical code of temporary building of construction site, Build. Constr. Ind. Stand. (2009).

[321] X. Song, S. Du, C. Deng, P. Shen, M. Xie, C. Zhao, C. Chen, X. Liu, Carbon emissions in China's steel industry from a life cycle perspective: Carbon footprint insights, J. Environ. Sci. 148 (2025) 650–664, http://dx.doi.org/10.1016/j.jes.2023.04.027.